ORNL/CON-175

Energy Division

THE OAK RIDGE HEAT PUMP MODELS: III. DESIGN TOOLS FOR HEAT PUMP DEVELOPMENT

S. K. Fischer
C. K. Rice
C. J. Emerson

Date Published—April 1987

OAK RIDGE NATIONAL LABORATORY
Oak Ridge, Tennessee 37831
operated by
MARTIN MARIETTA ENERGY SYSTEMS, INC.
for the
U.S. DEPARTMENT OF ENERGY
under contract DE-AC05-84OR21400

Publications Staff

Editor:
S. H. McConathy
Graphic Artist:
L. D. Gilliam
Compositor:
K. M. Dobbs
Word Processors:
P. J. Lewis
T. J. Simmons
Makeup Artist:
G. G. Ross

CONTENTS

LIST OF EXHIBITS vi

LIST OF FIGURES vii

ACKNOWLEDGMENTS viii

EXECUTIVE SUMMARY ix

ABSTRACT x

1. INTRODUCTION 1

2. APF MODEL WITH STEADY-STATE CALCULATIONS 3

   2.1 INTRODUCTION 3
   2.2 PROGRAM MODIFICATIONS 3
   2.3 MODIFICATIONS TO INPUT DATA 4
   2.4 CALCULATING STEADY-STATE PERFORMANCE AT SEVERAL AMBIENT CONDITIONS 4
   2.5 APF MODEL AS A SUBROUTINE 5
   2.6 FURTHER CHANGES IN COMPONENT DATA AND HPDM 5
   2.7 CONCLUSION 6

3. SYSTEM PERFORMANCE COMPARISONS 7

   3.1 INTERMEDIATE DATA FILES 7
   3.2 STEADY-STATE COMPARISONS 7
   3.3 COMPARISON OF POWER CONSUMPTIONS INCLUDING DYNAMIC LOSSES 9
   3.4 CONCLUSION 13

4. PLOTS OF STEADY-STATE AND DYNAMIC PERFORMANCE 14

   4.1 INTRODUCTION 14
   4.2 DESCRIPTION 14

5. DIGITIZATION AND CURVE FITTING FOR COMPRESSOR MAP DATA 16

   5.1 INTRODUCTION 16
   5.2 DATA ENTRY 16
   5.3 ENTRY OF REMAINING DATA 17
      5.3.1 Tabular Input 17
      5.3.2 Digitized Input 18
   5.4 WEIGHTING FACTORS FOR DIGITIZED DATA 19
   5.5 FITTING THE DATA 19

5.6 PLOTS OF THE CURVE FITS 21
5.7 CALCULATION AND PLOTS OF COMPRESSOR EFFICIENCIES 21

6. CONVERSION OF THE APF MODEL TO SUBROUTINE FUNCT1 27

6.1 INTRODUCTION 27
6.2 THE SUBROUTINE FUNCT1 27
6.3 THE TRANSFORMATION ROUTINE TRNSFM 28
6.4 THE SUBROUTINE SETVAR 30
6.5 CONCLUSION 30

7. CONTOUR PLOTS 31

7.1 INTRODUCTION 31
7.2 MULTIPLE FUNCTIONS OF COMMON VARIABLES 34
7.3 DATA GENERATION 35
7.4 ID HEADER BLOCK 36
7.5 DATA BLOCKS FOR CONTOURS 39
7.6 CONTOUR PLOTTING 40
7.6.1 The Routine CONPLT 40
7.6.2 The Routine BLOCK DATA 40
7.6.3 The Routine FRSTRT 42
7.6.4 The Routines XSTEP and XSTP2 42
7.6.5 The Routine PARAM 42
7.6.6 The Routine PLTCAP 42
7.6.7 The Routine TRIANG 43
7.6.8 The Routines PLTCON and CONSTP 44
7.7 OPTIONAL CALL TO PLTCON 44
7.8 CONCLUSION 45

8. NUMERICAL OPTIMIZATION OF HEAT PUMP DESIGN 46

8.1 INTRODUCTION 46
8.2 UNCONSTRAINED VS CONSTRAINED OPTIMIZATION 47
8.3 SEQUENTIAL AUGMENTED LAGRANGIANS 47
8.4 GRADIENTS 48
8.5 MINIMIZATION ALONG A SEARCH DIRECTION 50
8.6 SCALING 51
8.6.1 Objective Functions and Independent Variables 51
8.6.2 Objective Functions and Constraints 53
8.7 THE MAIN PROGRAM GRADIE 54
8.8 UNFINISHED BUSINESS 55

9. CHANGES TO THE STEADY-STATE DESIGN MODEL SINCE ORNL/CON-80 56

REFERENCES 58

Appendix A: INPUT DATA DEFINING AMBIENT CONDITIONS FOR STEADY-STATE CALCULATIONS 59

Appendix B: INPUT DATA FOR COMPRESSOR MAP MODEL TO DO HEATING AND COOLING CALCULATIONS 61

Appendix C: LISTINGS OF NEW SUBROUTINES FOR THE COMBINED APF/STEADY-STATE MODEL 63

Appendix D: SAMPLES OF SYSTEM COMPARISONS 65

Appendix E: LISTINGS OF PROGRAMS TO GENERATE SYSTEM COMPARISONS 77

Appendix F: LISTING OF PROGRAM TO PLOT STEADY-STATE AND DYNAMIC HEAT PUMP PERFORMANCE 79

Appendix G: DESCRIPTION OF GRAPHICS SUBROUTINES 81

Appendix H: LISTING OF COMPRESSOR MAP-FITTING ROUTINES 85

Appendix I: TRANSFORMATION OF COORDINATES FROM DIGITIZING TABLET 87

Appendix J: SOLUTION OF LEAST SQUARES PROBLEM IN COMPRESSOR CURVE FITTING 93

Appendix K: PLOTTING VERSION OF SUBROUTINE FIT 97

Appendix L: LISTING OF SUBROUTINE FUNCT1 99

Appendix M: LISTING OF DATA GENERATION PROGRAM DRIVER 101

Appendix N: LISTING OF CONTOUR PLOTTING PROGRAM CONPLT 103

Appendix O: LISTING OF SUBROUTINES FOR OPTIMIZATION AND PROGRAM GRADIE 105

Appendix P: DESCRIPTION OF REVISED INPUT DATA FORMAT FOR HEAT PUMP DESIGN MODEL 107

LIST OF EXHIBITS

3.1 Example of tabulated system comparisons from program TABULA 8
3.2 Example of tabulated component steady-state performance from program TABULA 10
3.3 Comparison of heating season power consumption by temperature bins for compressors and fans printed by COMPAR 11
3.4 Comparison of heating season dynamic losses by temperature bins printed by COMPAR 12
5.1 Tabulated comparison of calculated and specified compressor map data 20
7.1 Sample data file for contour plots 37

LIST OF FIGURES

4.1 Sample plot generated by PLOTHP 15
5.1 Graphical output from compressor map-fitting routine showing compressor power consumption data and curve fit 22
5.2 Graphical output from compressor map-fitting routine showing refrigerant flow data and curve fit 23
5.3 Graphical output from compressor map-fitting routine showing derived isentropic efficiency data and curve fit 24
5.4 Graphical output from compressor map-fitting routine showing derived volumetric efficiency data and curve fit 25
7.1 Dependence of annual performance factor on indoor and outdoor air flow rates of 710, 850, and 1275 L/s (1500, 1800, and 2700 ft^3/min) 31
7.2 Dependence of annual performance factor on indoor and outdoor air flow rates of 710, 850, 1275, and 1415 L/s (1500, 1800, 2700, and 3000 ft^3/min) 32
7.3 Dependence of design cooling capacity and annual performance factor on indoor and outdoor air flow rates 32
7.4 Perspective drawing of the relationship between annual performance factor and indoor and outdoor flow rates 33
7.5 Contour plot showing dependence of annual performance factor on indoor and outdoor air flow rates 34
7.6 Contour plot showing dependence of annual performance factor and design cooling capacity on indoor and outdoor flow rates 35
7.7 Rectangular grid of data points for contour plots 36
7.8 Hierarchy of subroutine calls in contour plotting package CONPLT 41
7.9 Identification of nodes and mesh elements in triangulation of input data for contour plots 43
8.1 Graph showing a minimum of a function of a single variable 50
8.2 Sample contour plot of a well-scaled function 51
8.3 Sample contour plot of a poorly scaled function 52
8.4 Example of a contour plot with a superimposed constraint line 53
I.1 Layout on digitizing tablet showing coordinates of two points with exagerated variation from true horizontal 87
I.2 Layout on digitizing tablet identifying points and distances in "tablet" and "graph" units 89
I.3 Layout on digitizing tablet showing points and distances used in the transformation of coordinates 89
I.4 Layout on digitizing tablet showing points and distances used in the transformation of the vertical coordinates 90

ACKNOWLEDGMENTS

This report would never have been published if it had consisted solely of contributions of the authors. Many other people participated with us in developing the programs described here and in assembling this documentation of those programs. Foremost among these are our sponsors at the Department of Energy, John Ryan, Ron Fiskum, and Terry Statt. Among those at Oak Ridge National Laboratory are Bill Jackson and Kay Zimmerman, who worked with us on code development, and the Publications Staff, who labored long and hard to put our draft report into a useful document. Our greatest debt, however, is to Ray Ellison and Fred Creswick, who brought heat pump modeling to the Laboratory and established a program and atmosphere that provided opportunities for us to establish and pursue research goals. We most sincerely acknowledge their contributions and those made by the many others who have helped us in this work.

EXECUTIVE SUMMARY

Oak Ridge National Laboratory (ORNL) has been a leader in developing analytical tools for the design of electrically driven, air-to-air heat pumps. A user's manual for ORNL's 1980 steady-state heat pump model, ORNL/CON-80/R1, has been published; and a report on the annual performance factor (APF) model is being prepared. These two computer programs have been demonstrated to be accurate, easy-to-use models and have received broad national and international distribution.

The models have been used widely within ORNL in studies investigating opportunities for energy conservation in residential space heating and cooling. During the course of those projects, other computer programs were written to assist in the use of the steady-state and APF models. Although each of the codes in this secondary package performs a small specialized task, taken together they form a valuable enhancement to the steady-state and APF models that fostered them.

The programs that have been developed fall generally into six categories: (1) subroutines to combine the steady-state and APF models to predict annual performance from compressor and heat exchanger specifications, (2) programs to tabulate detailed comparisons of the seasonal performance of two heat pumps, (3) a program to plot the steady-state and dynamic performance (accounting for cycling, frosting/defrosting, and resistance heat) of a heat pump as functions of the outdoor temperature, (4) stand-alone programs to assist in digitizing compressor map data and fitting polynomial approximations to them, (5) contour plotting programs to display performance as functions of two independent design variables, and (6) subroutines to serve as an interface between the steady-state, APF, and combined models and numerical optimization packages. Each of these has been rigorously documented in this report so that individuals can tailor the programs to their own needs and computer equipment.

This package of programs is a valuable addition to the set of design tools for the development of electrically driven heat pumps. Each code contributes to either the preparation of data for the steady-state and APF models or the analysis of results computed by them. This report describes the programs in depth and explains their uses and how to modify and enhance them.

ABSTRACT

This report describes a variety of computer programs that have been written in the course of several projects on heat pump development at Oak Ridge National Laboratory (ORNL). These codes were designed to be used in conjunction with the ORNL steady-state heat pump model and the annual performance factor (APF) model for air-source heat pumps. These design tools, as well as the steady-state and APF models, were developed for the U.S. Department of Energy (DOE) and are available without charge to anyone doing research on heat pump efficiency and design.

The computer programs in the design tool package were developed to relieve engineers of the tedious, mundane tasks associated with preparing data for the steady-state model and analyzing results from the steady-state and APF models. The programs include (1) the subroutines necessary to combine these models into a single code to compute annual energy consumption from design parameters, (2) programs to compare alternative designs, (3) a program to plot steady-state and dynamic performance (coefficient of performance and capacity with and without cycling, frosting, and defrosting losses and resistance heat) against outdoor temperature, (4) a program to generate polynomial fits to compressor data, (5) a program to draw contour plots of parametric design alternatives, and (6) the subroutines required to use the steady-state or APF models with numerical optimization software. Each of these six codes is carefully documented and explained in the report so that each user can apply the codes to his or her tasks or tailor them to individual needs.

These programs have been used extensively at ORNL in the analysis of energy-saving, high-efficiency, air-source heat pumps. Each one is a design tool that can save time and effort; all together they are a valuable addition to the steady-state and APF models. They are written in Fortran IV and can be used with little or no modification.

1. INTRODUCTION

The Building Equipment Research (BER) Program at Oak Ridge National Laboratory (ORNL) has conducted analytical studies of electrically driven, air-source heat pumps for the Department of Energy (DOE). This work included the development of computer models for the simulation of the steady-state operation of a residential-sized heat pump,[1–4] the annual performance of heat pumps,* and optimization of heat pump performance.[5–8] The steady-state heat pump design model (HPDM) has been publicly available since 1978; more than 75 copies of it have been sent out to manufacturers, universities, and research organizations upon their request. The annual performance factor (APF) model will be available for public distribution in 1985.

A number of computer programs have been developed in conjunction with the steady-state and APF models. These codes are also available to the public, and although they are not complex engineering models, they can be generally useful. These include:

- A combined program that uses the HPDM to compute the steady-state data required by the APF model
- Programs to generate tables comparing the annual, steady-state, and dynamic performance of alternative heat pump designs
- A program to plot the house heating and cooling loads and the heat pump steady-state and dynamic COP and capacity vs ambient temperature
- A program to approximate compressor map data with analytical functions of the condensing and evaporating temperatures
- Programs to draw contour plots of heat pump performance as a function of two design variables
- Subroutines necessary to execute the HPDM or APF model under control of numerical optimization programs

Changes made to the steady-state model since the latest version was released in 1981 are also documented.

This report explains each of the programs, or program changes, listed in the previous paragraph in such a way that they can be used outside of ORNL. It does presume a familiarity with previous reports, particularly with regard to the steady-state model[3,4] and to a lesser extent the APF model.[5] The subsequent chapters in this report are also directed to those who would be using these programs on their own computers. There is a brief introduction of what each program does, but primarily the discussion centers on the details of how the programs work and what changes may be necessary to use the codes on other (non-ORNL) computers.

Distribution of these programs as a package is handled free of charge; a request for one program will result in a tape containing all of them. Requests should be sent to one of the authors at

Oak Ridge National Laboratory
P.O. Box Y
Building 9102-1
Oak Ridge, TN 37831

*Documentation for this model is being prepared.

Requests must be accompanied by a nine-track computer tape and a cover letter that specifies

- Tape density (1600 or 6250 bpi)
- Character representation (ASCII or EBCDIC)
- Whether the tape should be labeled or not labeled
- Desired blocksize or the number of records (card images) per block

In the past, computer programs from BER projects have been readily transportable, and no major problems are anticipated in this case.

These computer programs, used in conjunction with this and previous reports, can be valuable tools in the design and analysis of advanced electric heat pumps. They have been directed toward meeting needs in the heating, ventilating, and air-conditioning (HVAC) industry, both expressed and perceived, and it is sincerely hoped that they will prove useful.

2. APF MODEL WITH STEADY-STATE CALCULATIONS

2.1 INTRODUCTION

Computer programs have been developed at ORNL that can model the steady-state, seasonal, and annual performance of electrically driven or thermally activated air-source heat pumps.[1,2] This report describes programs that supplement those two models and enhance their utility. Consequently, it presumes a familiarity with earlier reports on the steady-state and APF models and does not summarize or restate the information in them. The steady-state HPDM was designed to read data describing the heat pump components and indoor and outdoor temperatures and relative humidities. It uses this information to compute the steady-state coefficient of performance (COP) and capacity at the specified ambient conditions, refrigerant state points throughout the circuit, and performance levels for the different components (e.g., heat exchanger effectiveness and compressor efficiencies).

The APF model was designed to

- Read tables of data describing the steady-state performance (i.e., heating or cooling capacity and either power input or COP vs ambient temperatures)
- Combine that information with
  - — degradation factors for the dynamic losses (e.g., frosting, cycling)
  - — residential heating and cooling loads
  - — weather data
- Calculate seasonal and annual power consumption and performance factors

It was a natural extension of this past work to combine these two programs. This resulted in a modified APF model that reads component data and employs the steady-state program to calculate COPs and capacities as an intermediate step in computing seasonal performance factors (SPFs) and an APF.

2.2 PROGRAM MODIFICATIONS

This combination of programs required some modification of existing subroutines and the development of some new ones. The APF model needed to perform several functions with the steady-state HPDM that it was not originally designed to do:

- Run the steady-state model sequentially in both heating and cooling modes
- Invoke the program several times for different ambient conditions
- Keep track of the COPs and capacities for each ambient temperature

The HPDM was thus converted into a subroutine that is called by the APF model (a SUBROUTINE statement was added at the beginning of the stand-alone steady-state model, and the STOP statement was changed to a RETURN). COMMON BLOCKS were added to pass component information to the HPDM and to return the computed COPs and capacities to the APF model.

2.3 MODIFICATIONS TO INPUT DATA

The three tasks identified in the preceding paragraph are performed by a modified version of DATAIN (from the original HPDM) and new subroutines named HX, CONFIG, STEADY, and SUMMAR. The HPDM was set up, internally, to read data for the condenser and the evaporator, with the order depending on the mode of operation. This would not work for a combined program that would need to run the HPDM in both heating and cooling modes. Consequently, DATAIN was modified so that the heat exchanger data were actually assigned to variables for the indoor and the outdoor coils (as opposed to being stored as condenser and evaporator parameters). A new routine, HX, is employed to assign the condenser and evaporator variables from these data based on the mode of operation (NCORH=1 for cooling, NCORH=2 for heating). Because the condenser and evaporator parameters may be changing from one call to HX to the next, HX also calls CALC (from the HPDM) to compute the geometric ratios used by the condenser and evaporator subroutines (see ref. 1 for a description of CALC).

2.4 CALCULATING STEADY-STATE PERFORMANCE AT SEVERAL AMBIENT CONDITIONS

A subroutine named STEADY was developed so that a single call to it from the APF model would return all the information needed to calculate the seasonal and annual performance of a heat pump with the given set of components. It does several things to accomplish this.

1. The very first time it is called (and only the first time), it reads data about the ambient conditions for each of the required steady-state calculations.
2. It calls the HPDM for the specified list of ambient temperatures for both heating and cooling modes.
3. It stores the steady-state COP and capacity for each temperature.
4. It stores the condensing and evaporating temperatures at each ambient condition for use as initial guesses for iterations should STEADY be called again.
5. It calls CONFIG and SUMMAR to print a table of the heat pump component configuration and a summary of the computed steady-state performance.

A part of STEADY is executed only the first time that the subroutine is called. This is used to read a file of data that specifies ambient temperatures for the steady-state calculations. This file contains the number of ambient temperatures to use in each mode of operation, and for each temperature:

- The desired outdoor temperature and relative humidity
- The corresponding desired indoor temperature and humidity
- Estimates of the condensing and evaporating temperatures at those operating conditions

These data are stored internally to STEADY and are used each time it is called (i.e., once for each APF calculation). The data and formats are described in Appendix A.

STEADY is divided into two nearly identical sections; one for heating mode calculations and one for cooling mode. In each case, NCORH is set to its appropriate

value and STEADY calls HX to assign data for the heat exchangers. Each section also contains a loop that sets up input data for the HPDM for each of the specified ambient temperatures. The temperature and relative humidity of the air crossing each heat exchanger are assigned before calling HPDM using the input data that was described earlier. The estimated saturation temperatures at the compressor shell inlet and outlet are also assigned to be used as starting points in heat exchanger iterations (these may be from the input data for the ambient conditions or from previous calculations). This loop calls the HPDM to do the steady-state calculations and stores the results when it finishes.

2.5 APF MODEL AS A SUBROUTINE

Ordinarily the APF model is used to predict the performance of a single heat pump configuration. There are instances, however, in which it is convenient to use this model repetitively. The contour plotting and design optimization described later are examples of applications in which the APF model is called dozens, or even hundreds, of times. (The APF model is converted to a subroutine in the same manner that the HPDM was.)

In these instances it is useful for STEADY to store more than the bare minimum of data after each steady-state calculation. STEADY always stores the COP and capacity at each temperature so they can be used to define steady-state performance curves for the APF model. It also stores the saturation temperatures at the compressor shell inlet and outlet. STEADY can be used to save data for the system performance comparisons or contour plots (as described in Chaps. 3 and 7).

If the APF model is put under the control of a data-generating program for contour plots or an optimization routine, it is called on to compute the annual performance of many systems that have only slight differences in their designs. If these differences are not too great, the calculated refrigerant conditions for one system will provide an excellent estimate to the shell inlet and outlet temperatures for the next. Making use of previous results decreases the computational time for subsequent calls to the APF model and also improves the likelihood that the steady-state computations will converge. Thus, these data are stored and used as input to the HPDM the next time it is called with the corresponding ambient temperature.

2.6 FURTHER CHANGES IN COMPONENT DATA AND HPDM

There was one other modification of the original steady-state program that was dictated by combining it with the APF model. This subroutine employs curve fits of the compressor power and mass flow rate (or capacity) as functions of the saturation temperatures at the shell inlet and outlet.

The manufacturer's literature may present a single set of curves, or tables, that spans the entire range of compressor operating conditions for both heating and cooling. In that event a single set of coefficients for the power and mass flow could be used by the steady-state model. It is also possible, however, that different sets of curves would be given for the heating and the cooling performance of the compressor. In this case, two different curve fits would be required. The steady-state model was modified to accommodate this. It now

requires two sets of coefficients to describe the compressor performance, the first for cooling mode and the second for heating.

2.7 CONCLUSION

The result of this work is a collection of subroutines that can be used together with the steady-state and APF models released earlier.[1,2] These new routines allow the earlier programs to be used together to compute seasonal and annual performance for a single heat pump from component data. It is also possible to use the program to assess the effects of different design changes on the seasonal or annual performance. The code is organized in such a way that it can in turn be modified for use with other "driving" programs for contour plotting and optimization to study effects of component design configurations in a more systematic manner.

3. SYSTEM PERFORMANCE COMPARISONS

The combined APF/steady-state program can give the user detailed information about the steady-state operation of a heat pump along with detailed tables that summarize the net unit performance by temperature bins. These can make for interesting reading, but there is so much information that it is difficult, if not impossible, to compare the performance of one heat pump with another and to conclude why it is a better or poorer system. Some modifications to existing programs and some new programs facilitate the comparison of two systems.

3.1 INTERMEDIATE DATA FILES

The main program and subroutine OUTPUT, both from the combined APF/steady-state model, were changed so that they store information about heat pumps. These data can then be used as input to system comparison programs.

OUTPUT was modified so that it saves information about the steady-state operation of the heat pump on a disk file. (This requires that the variable LPRINT be set to 1 in the input data for the HPDM to get full steady-state output.) The steady-state COP and capacity, compressor and fan power consumptions, refrigerant temperatures, pressures, enthalpies, saturation temperatures throughout the circuit, and many other numbers can be stored for later processing.

The main program was also changed to include WRITE statements to logical unit number 7. These save information on the component dimensions and efficiencies, the seasonal and annual performance, the power consumptions for each of the fans and the compressor for each temperature bin, and the dynamic losses for each bin. These data are stored with the steady-state data mentioned in the preceding paragraph. Listings of these modified routines appear in Appendix C.

3.2 STEADY-STATE COMPARISONS

Two programs, TABULA and COMPAR, have been written to assist in comparing the steady-state and seasonal performance of different heat pumps. Both of these read the data stored by the versions of MAIN and OUTPUT just discussed.

TABULA prints an eight-page tabular summary that deals primarily with the steady-state performance of the heat pumps. This interactive program prompts the user to type the names of two data sets that were generated using the combined APF/steady-state program with these routines. A sample of the first page of tabulated output is shown in Exhibit 3.1. This page gives the descriptive title assigned to each of the heat pumps (as input data to the steady-state routine) and the component descriptions for each system. A summary of the seasonal and annual performance of each system follows, which includes (1) SPFs and APFs, (2) power consumptions for the compressor and fans, (3) cycling losses, (4) frosting and defrosting losses, (5) resistance heat, and (6) the differences in each of the preceding five items (column 1 minus column 2) for each season and for the year.

SYSTEM PERFORMANCE COMPARISONS

SYSTEM #1, FILE NAME: EXAMPLE.DAT
TEST CASE #1: HIGH EFFICIENCY HEAT PUMP

SYSTEM #2, FILE NAME: SAMPLE.DAT
TEST CASE #2: DESIGN OPTIMIZED FOR BEST SEASONAL PERFORMANCE

	#1	#2	
COMPRESSOR			
DISPLACEMENT	2.907	2.678	CU IN
SHELL HEAT LOSS	0.095	0.095	TIMES COMPRESSOR POWER
DIAMETER OF DUCTS	6.000	6.000	INCHES

	INDOOR HEAT EXCHANGER #1	INDOOR HEAT EXCHANGER #2	OUTDOOR HEAT EXCHANGER #1	OUTDOOR HEAT EXCHANGER #2	
AIR FLOW RATE	997.0	848.5	1820.0	2427.0	CFM
FACE VELOCITY	273.9	167.4	363.3	285.2	FT/MIN
FRONTAL AREA	3.640	5.070	5.010	8.510	SQ FT
TUBE ROWS	4.0	2.5	3.0	2.0	
REFRIGERANT CIRCUITS	2.4	3.0	2.4	3.0	
FRACTION OF HX AREA	0.492	0.427	0.508	0.573	
CAPILLARY FLOW FACTOR	3.673	3.530	3.035	2.248	
FIN THICKNESS	0.005	0.005	0.006	0.006	INCHES
VERTICAL TUBE SPACING	1.000	1.000	1.250	1.250	INCHES
HORIZONTAL TUBE SPACING	0.072	0.072	1.080	1.080	INCHES
OUTSIDE DIAMETER OF TUBES	0.395	0.395	0.395	0.395	INCHES
INSIDE DIAMETER OF TUBES	0.371	0.371	0.371	0.371	INCHES

	HEATING SEASON #1	HEATING SEASON #2	HEATING SEASON -	COOLING SEASON #1	COOLING SEASON #2	COOLING SEASON -	ANNUAL #1	ANNUAL #2	ANNUAL -	
PERFORMANCE FACTORS	2.002	2.118	-5.79	2.483	2.750	-10.75	2.186	2.354	-7.69	%
POWER CONSUMPTION										
STEADY-STATE										
COMPRESSOR	3091.	3221.	-130.	2637.	2515.	122.	5727.	5736.	-9.	KWH
INDOOR FAN	484.	265.	219.	368.	187.	181.	852.	452.	400.	KWH
OUTDOOR FAN	322.	224.	98.	120.	132.	-12.	442.	356.	86.	KWH
SUBTOTAL	3897.	3710.	187.	3125.	2834.	291.	7021.	6544.	477.	KWH
RESISTANCE HEAT	830.	744.	86.				830.	744.	86.	KWH
FROSTING/DEFROSTING	608.	577.	31.				608.	577.	31.	KWH
CYCLING LOSSES	619.	598.	21.	591.	520.	71.	1210.	1117.	93.	KWH
TOTAL	5954.	5629.	325.	3716.	3354.	362.	9670.	8983.	687.	KWH

Exhibit 3.1. Example of tabulated system comparisons from program TABULA.

Exhibit 3.2 is a sample of one of the remaining seven pages of output from TABULA. This particular page lists the steady-state capacity of the compressor and each of the heat exchangers, the total system capacity, and the steady-state power consumption rate for the compressor and fans at each of the ambient temperatures used for calculations. It also gives the steady-state COPs and total power consumption rates. The remaining six pages list:

- Refrigerant temperatures, pressures, enthalpies, and saturation temperatures at the inlets and outlets of the compressor, condenser, and evaporator
- Air-side and refrigerant-side pressure drops across the indoor and outdoor heat exchangers and the pressure drop across the expansion device
- Fan and compressor efficiencies
- Refrigerant flow rate, power per unit mass flow, condenser subcooling, and several other miscellaneous things

A complete listing of the output from TABULA is in Appendix D, and the program itself is listed in Appendix E.

3.3 COMPARISON OF POWER CONSUMPTIONS INCLUDING DYNAMIC LOSSES

A second program, COMPAR, can be used to print tables of comparisons of two heat pumps using the calculations in the APF model (TABULA prints data only at the temperatures used for the steady-state calculations while COMPAR prints data for each of the temperature bins used in the APF computations). These tables include the steady-state performance of each component (i.e., the compressor and both fans) and the dynamic losses based on the empirical loss factors in the APF model. Exhibits 3.3 and 3.4 contain excerpts from the tables printed by COMPAR.

Exhibit 3.3 shows some of the component data for a heating season. The ambient temperature bins are listed in the first column. This is followed, from left to right, by blocks of four columns each for the hours of operation and power consumption for the compressor, indoor fan, and outdoor fan. Columns 1 and 2 under "Hours of operation" contain the number of hours each of the heat pumps would operate during the course of the year at that particular temperature (based on the weather data used for the simulation). The third column shows the difference in hours of operation between the two systems. The final column in this block is the cumulative difference in hours of operation, a running sum of the numbers in the preceding column from the lowest ambient temperature up to that one.

The next four columns contain data comparing the compressor operation of the two systems at each temperature. Steady-state power input for each compressor and the differences between them are shown. The difference between this tabulation and the corresponding one in Exhibit 3.2 is that this block also contains the cumulative sum of the differences in energy consumption (steady-state input power times the hours of operation) for the first system less the energy consumption for the second system. Note that while steady-state data are in watts, the cumulative differences in annual power consumption are

SYSTEM PERFORMANCE COMPARISONS

SYSTEM #1, FILE NAME: EXAMPLE.DAT
TEST CASE #1: HIGH EFFICIENCY HEAT PUMP

SYSTEM #2, FILE NAME: SAMPLE.DAT
TEST CASE #2: DESIGN OPTIMIZED FOR BEST SEASONAL PERFORMANCE

COMPRESSOR & HEAT EXCHANGER CAPACITIES:

OUTDOOR TEMPERATURE (F)	COMPRESSOR CAPACITY (BTU/HR)			CONDENSER CAPACITY (BTU/HR)			EVAPORATOR CAPACITY (BTU/HR)			TOTAL CAPACITY (BTU/HR)		
	#1	#2	-	#1	#2	-	#1	#2	-	#1	#2	-
-10.0	3011.	3717.	-706.	4729.	6653.	-1924.	2885.	4134.	-1249.	5698.	7188.	-1490.
0.0	3628.	4163.	-535.	7943.	9852.	-1909.	5497.	6815.	-1318.	8911.	10387.	-1476.
10.0	4208.	4630.	-422.	11615.	13291.	-1676.	8544.	9663.	-1119.	12582.	13825.	-1243.
20.0	4776.	5118.	-342.	15534.	16703.	-1169.	11795.	12542.	-747.	16501.	17237.	-737.
30.0	5393.	5635.	-242.	19702.	20442.	-740.	15269.	15769.	-500.	20668.	20976.	-308.
40.0	5979.	6222.	-243.	23956.	24617.	-661.	18935.	19352.	-417.	24921.	25150.	-230.
50.0	6606.	6902.	-296.	28716.	29131.	-415.	23075.	23187.	-112.	29679.	29664.	15.
60.0	7300.	7757.	-457.	34038.	34095.	-57.	27710.	27285.	425.	34999.	34627.	372.
70.0	7355.	6662.	693.	40381.	37780.	2601.	33981.	32073.	1908.	32771.	31475.	1296.
75.0	7511.	6910.	601.	39569.	37277.	2292.	33027.	31313.	1714.	31818.	30715.	1103.
80.0	7726.	7162.	564.	38844.	36749.	2095.	32040.	30506.	1534.	30830.	29908.	922.
85.0	7921.	7412.	509.	37857.	36123.	1734.	30870.	29664.	1206.	29662.	29066.	596.
90.0	8167.	7666.	501.	37047.	35491.	1556.	29842.	28779.	1063.	28640.	28181.	458.
95.0	8337.	7921.	416.	36186.	34823.	1363.	28801.	27860.	941.	27604.	27263.	341.
100.0	8503.	8170.	333.	35294.	34130.	1164.	27773.	26924.	849.	26582.	26327.	255.

POWER CONSUMPTIONS & COP'S:

OUTDOOR TEMPERATURE (F)	INDOOR FAN (W)			OUTDOOR FAN (W)			COMPRESSOR (W)			COP			TOTAL POWER (W)		
	#1	#2	-	#1	#2	-	#1	#2	-	#1	#2	-	#1	#2	-
-10.0	283.8	156.7	127.1	138.3	127.0	11.3	975.0	1203.3	-228.3	1.195	1.164	0.031	1397.1	1487.0	-89.9
0.0	283.7	156.7	127.0	135.8	126.3	9.5	1174.7	1347.7	-173.0	1.638	1.474	0.164	1594.2	1630.7	-36.5
10.0	283.4	156.6	126.8	133.4	125.7	7.7	1362.3	1499.1	-136.8	2.072	2.068	0.004	1779.1	1781.4	-2.3
20.0	283.2	156.5	126.7	131.2	125.2	6.0	1546.2	1656.9	-110.7	2.466	2.605	-0.139	1960.6	1938.6	22.0
30.0	282.9	156.4	126.5	189.4	128.0	61.4	1745.9	1824.4	-78.5	2.730	2.914	-0.184	2218.2	2108.8	109.4
40.0	282.6	156.3	126.3	206.1	132.7	73.4	1935.7	2014.3	-78.6	3.012	3.199	-0.187	2424.4	2303.3	121.1
50.0	282.2	156.1	126.1	232.6	148.0	84.6	2138.6	2234.6	-96.0	3.277	3.424	-0.147	2653.4	2538.7	114.7
60.0	281.7	155.9	125.8	249.0	158.1	90.9	2363.3	2511.3	-148.0	3.544	3.591	-0.047	2894.0	2825.3	68.7
70.0	354.4	175.2	179.2	117.0	123.6	-6.6	2381.1	2156.9	224.2	3.366	3.755	-0.389	2852.5	2455.7	396.8
75.0	354.1	175.2	178.9	116.3	123.6	-7.3	2431.8	2237.0	194.8	3.212	3.549	-0.337	2902.2	2535.8	366.4
80.0	354.5	175.2	179.3	115.6	123.7	-8.1	2501.4	2318.8	182.6	3.040	3.348	-0.308	2971.5	2617.7	353.8
85.0	353.9	175.1	178.8	114.9	123.7	-8.8	2564.3	2399.7	164.6	2.865	3.156	-0.291	3033.1	2698.5	334.6
90.0	352.3	175.1	177.2	114.3	123.8	-9.5	2644.2	2482.0	162.2	2.698	2.969	-0.271	3110.8	2780.9	329.9
95.0	350.7	175.0	175.7	113.6	123.8	-10.2	2699.1	2564.4	134.7	2.557	2.790	-0.233	3163.4	2863.2	300.2
100.0	348.9	175.0	173.9	112.9	123.9	-11.0	2752.7	2645.0	107.7	2.423	2.620	-0.197	3214.5	2943.9	270.6

Exhibit 3.2. Example of tabulated component steady-state performance from program TABULA.

COMPARISON OF STEADY-STATE
COMPONENT POWER CONSUMPTION
(HEATING SEASON CALCULATIONS)

SYSTEM #1, FILE NAME: EXAMPLE.DAT
TEST CASE #1: HIGH EFFICIENCY HEAT PUMP

SYSTEM #2, FILE NAME: SAMPLE.DAT
TEST CASE #2: DESIGN OPTIMIZED FOR BEST SEASONAL PERFORMANCE

	HOURS OF OPERATION				COMPRESSOR				INDOOR FAN				OUTDOOR FAN			
TEMP (F)	#1 (HR)	#2 (HR)	- (HR)	CUMUL (HR)	#1 (W)	#2 (W)	- (W)	CUMUL (KWH)	#1 (W)	#2 (W)	- (W)	CUMUL (KWH)	#1 (W)	#2 (W)	- (W)	CUMUL (KWH)
-13.	1.0	1.0	0.0	0.0	914.7	1159.5	-244.8	-0.2	283.9	156.7	127.2	0.1	139.1	127.2	11.9	0.0
-8.	1.0	1.0	0.0	0.0	1014.8	1231.9	-217.1	-0.5	283.8	156.7	127.1	0.3	137.8	126.8	11.0	0.0
-3.	4.0	4.0	0.0	0.0	1114.9	1304.3	-189.3	-1.2	283.7	156.7	127.1	0.8	136.6	126.5	10.1	0.1
2.	9.0	9.0	0.0	0.0	1212.3	1377.9	-165.6	-2.7	283.6	156.6	127.0	1.9	135.3	126.2	9.2	0.1
7.	21.0	21.0	0.0	0.0	1305.6	1453.6	-148.0	-5.8	283.5	156.6	126.9	4.6	134.2	125.9	8.3	0.3
12.	41.0	41.0	0.0	0.0	1398.6	1530.7	-132.2	-11.2	283.4	156.6	126.8	9.8	133.0	125.6	7.4	0.6
17.	98.0	98.0	0.0	0.0	1490.8	1609.9	-119.1	-22.9	283.2	156.5	126.7	22.2	131.9	125.3	6.5	1.3
22.	167.0	167.0	0.0	0.0	1586.1	1690.8	-104.7	-40.4	283.1	156.5	126.6	43.3	142.9	125.8	17.1	4.1
27.	277.7	271.6	6.2	6.2	1686.0	1774.3	-88.3	-54.0	283.0	156.4	126.6	79.5	172.0	127.2	44.8	17.3
32.	331.9	327.5	4.4	10.6	1783.9	1862.4	-78.5	-71.8	282.8	156.4	126.5	122.1	192.7	128.9	63.8	39.1
37.	292.7	289.6	3.1	13.7	1878.7	1957.3	-78.6	-88.7	282.7	156.3	126.4	159.6	201.1	131.3	69.8	59.9
42.	212.8	211.3	1.5	15.2	1976.3	2058.3	-82.1	-103.2	282.5	156.3	126.3	186.7	211.4	135.7	75.6	76.2
47.	135.6	135.3	0.3	15.4	2077.7	2168.5	-90.7	-114.9	282.3	156.2	126.1	203.8	224.7	143.4	81.3	87.3
52.	79.1	79.4	-0.2	15.2	2183.6	2289.9	-106.3	-123.8	282.1	156.1	126.0	213.8	235.9	150.0	85.9	94.0
57.	33.8	34.0	-0.3	14.9	2295.9	2428.3	-132.4	-128.9	281.8	156.0	125.8	218.0	244.1	155.1	89.0	97.0
62.	6.1	6.1	-0.1	14.9	2408.3	2566.6	-158.4	-130.1	281.6	155.9	125.7	218.7	252.2	160.1	92.1	97.6

STEADY-STATE COMPONENT	SYSTEM #1	SYSTEM #2	DIFFERENCE
COMPRESSOR POWER	3091.	3221.	-130. KWH
INDOOR FAN POWER	484.	265.	219. KWH
OUTDOOR FAN POWER	322.	224.	98. KWH
TOTAL STEADY STATE	3896.	3710.	186. KWH
RESISTANCE HEAT	830.	744.	86. KWH
FROSTING/DEFROSTING LOSSES	608.	577.	32. KWH
CYCLING LOSSES	619.	598.	22. KWH
TOTAL POWER CONSUMPTION	5954.	5628.	326. KWH

Exhibit 3.3. Comparison of heating season power consumption by temperature bins for compressors and fans printed by COMPAR.

COMPARISON OF DYNAMIC
POWER CONSUMPTION
(HEATING SEASON CALCULATIONS)

SYSTEM #1, FILE NAME: EXAMPLE.DAT
TEST CASE #1: HIGH EFFICIENCY HEAT PUMP

SYSTEM #2, FILE NAME: SAMPLE.DAT
TEST CASE #2: DESIGN OPTIMIZED FOR BEST SEASONAL PERFORMANCE

	HOURS OF OPERATION				CYCLING LOSSES				FROSTING & DEFROSTING LOSSES				RESISTANCE HEAT			
TEMP (F)	#1 (HR)	#2 (HR)	- (HR)	CUMUL (HR)	#1 (W)	#2 (W)	- (W)	CUMUL (KWH)	#1 (W)	#2 (W)	- (W)	CUMUL (KWH)	#1 (KW)	#2 (KW)	- (KW)	CUMUL (KWH)
-13.	1.0	1.0	0.0	0.0	0.0	0.0	0.0	0.0	0.0	0.0	0.0	0.0	10.6	10.2	0.4	0.4
-8.	1.0	1.0	0.0	0.0	0.0	0.0	0.0	0.0	0.0	0.0	0.0	0.0	9.0	8.5	0.4	0.9
-3.	4.0	4.0	0.0	0.0	0.0	0.0	0.0	0.0	0.0	0.0	0.0	0.0	8.1	7.7	0.4	2.6
2.	9.0	9.0	0.0	0.0	0.0	0.0	0.0	0.0	0.0	0.0	0.0	0.0	6.7	6.3	0.4	6.4
7.	21.0	21.0	0.0	0.0	0.0	0.0	0.0	0.0	0.0	0.0	0.0	0.0	5.3	4.9	0.4	14.5
12.	41.0	41.0	0.0	0.0	0.0	0.0	0.0	0.0	74.5	68.9	5.6	0.2	3.9	3.6	0.3	28.4
17.	98.0	98.0	0.0	0.0	0.0	0.0	0.0	0.0	221.8	226.8	-5.0	-0.3	2.6	2.3	0.3	54.2
22.	167.0	167.0	0.0	0.0	0.0	0.0	0.0	0.0	408.6	419.6	-11.0	-2.1	1.2	1.0	0.2	86.5
27.	277.7	271.6	6.2	6.2	34.0	46.1	-12.1	-3.1	443.0	359.5	83.5	23.3	0.0	0.0	0.0	86.5
32.	331.9	327.5	4.4	10.6	203.0	200.4	2.6	-1.3	432.0	427.7	4.3	26.6	0.0	0.0	0.0	86.5
37.	292.7	289.6	3.1	13.7	391.7	377.3	14.4	4.1	618.2	609.4	8.8	31.1	0.0	0.0	0.0	86.5
42.	212.8	211.3	1.5	15.2	624.8	599.0	25.8	10.4	319.3	318.5	0.8	31.8	0.0	0.0	0.0	86.5
47.	135.6	135.3	0.3	15.4	950.4	908.4	42.0	16.4	0.0	0.0	0.0	31.8	0.0	0.0	0.0	86.5
52.	79.1	79.4	-0.2	15.2	1268.4	1217.2	51.2	20.2	0.0	0.0	0.0	31.8	0.0	0.0	0.0	86.5
57.	33.8	34.0	-0.3	14.9	1600.3	1551.0	49.4	21.4	0.0	0.0	0.0	31.8	0.0	0.0	0.0	86.5
62.	6.1	6.1	-0.1	14.9	1863.5	1825.3	38.2	21.5	0.0	0.0	0.0	31.8	0.0	0.0	0.0	86.5

STEADY-STATE COMPONENT	SYSTEM #1	SYSTEM #2	DIFFERENCE
COMPRESSOR POWER	3091.	3221.	-130. KWH
INDOOR FAN POWER	484.	265.	219. KWH
OUTDOOR FAN POWER	322.	224.	98. KWH
TOTAL STEADY STATE	3896.	3710.	186. KWH
RESISTANCE HEAT	830.	744.	86. KWH
FROSTING/DEFROSTING LOSSES	608.	577.	32. KWH
CYCLING LOSSES	619.	598.	22. KWH
TOTAL POWER CONSUMPTION	5954.	5628.	326. KWH

Exhibit 3.4. Comparison of heating season dynamic losses by temperature bins printed by COMPAR.

in kilowatthours. The blocks for each of the two fans are similar to the one for the compressor. A comparable table is printed for the cooling mode calculations. In each case, summary information on seasonal energy use breakdown of the two heat pumps is printed at the bottom.

COMPAR also prints a second set of tables that lists the cycling losses, frosting and defrosting losses, and resistance heat requirements by each temperature bin. A sample is given in Exhibit 3.4. These are also repeated for the cooling mode. Full listings of the output from COMPAR are given in Appendix D, and the program is listed in Appendix E.

3.4 CONCLUSION

The APF/steady-state model is useful in predicting if one particular set of components will make a heat pump perform better than another set. The reasons for the improved performance are not necessarily obvious, although the energy breakdowns can help in deciphering why one system performs better than the other. Alternate versions of the MAIN program and OUTPUT can be used, however, to store detailed data for use by system comparison programs. Two such programs have been written and are given in the appendixes. These codes, together with the comparison codes TABULA and COMPAR, are useful in identifying why one simulation predicts lower power consumptions or dynamic losses than another. In effect, they are useful tools for handling the enormous amounts of data available from the APF and steady-state calculations.

4. PLOTS OF STEADY-STATE AND DYNAMIC PERFORMANCE

4.1 INTRODUCTION

It is often useful to examine graphs of the steady-state COP and capacity of a heat pump vs the outdoor ambient temperature. Placing graphs side by side, or overlaying them, can provide a visual, qualitative comparison of two alternative systems. It is even more revealing to look at graphs of the COP and capacity after the dynamic losses have been included (i.e., frosting and defrosting, cycling, and resistance heat).

4.2 DESCRIPTION

All of the information needed to produce such a graph is available in the APF model, and it is only a minor extension of the program to get a computer-generated plot from it. This capability was added in such a way that no changes were made to the main program. The APF model *always* calls a subroutine named PLOTHP. The "default" version of that subroutine has only three statements: SUBROUTINE, RETURN, and END. If that version of PLOTHP is used, the APF model does not generate a plot.

An alternate version of PLOTHP was written that can be used in place of the default version for those times when a plot is desired. A sample of the plots generated by this subroutine (Fig. 4.1) shows two graphs on a single page (capacity vs temperature at the top and COP vs temperature at the bottom) and several tables along the right margin that list the heat pump component data. The graph of heat pump capacity, at the top of the page, has the house heating and cooling loads for each bin (small squares and triangles, respectively) with linear fits to them. The steady-state heating and cooling capacity curves are bold, solid lines, and the degraded heating capacity in the frosting range is a bold, dashed line.

The lower graph in Fig. 4.1 shows the steady-state COPs for the heating and cooling seasons and also the COPs after performance has been degraded for frosting/defrosting, cycling, and resistance heat. Identifying data are placed along the right margin of the plot by a subroutine named PARAM. Subroutines PLOTHP and PARAM are listed in Appendix F.

PLOTHP and PARAM use a proprietary graphics software package named DISSPLA. It should not be difficult, however, to convert them to use a different subroutine library. A description of the DISSPLA routines is given in Appendix G to facilitate a one-for-one substitution.

ORNL–DWG 86–8033

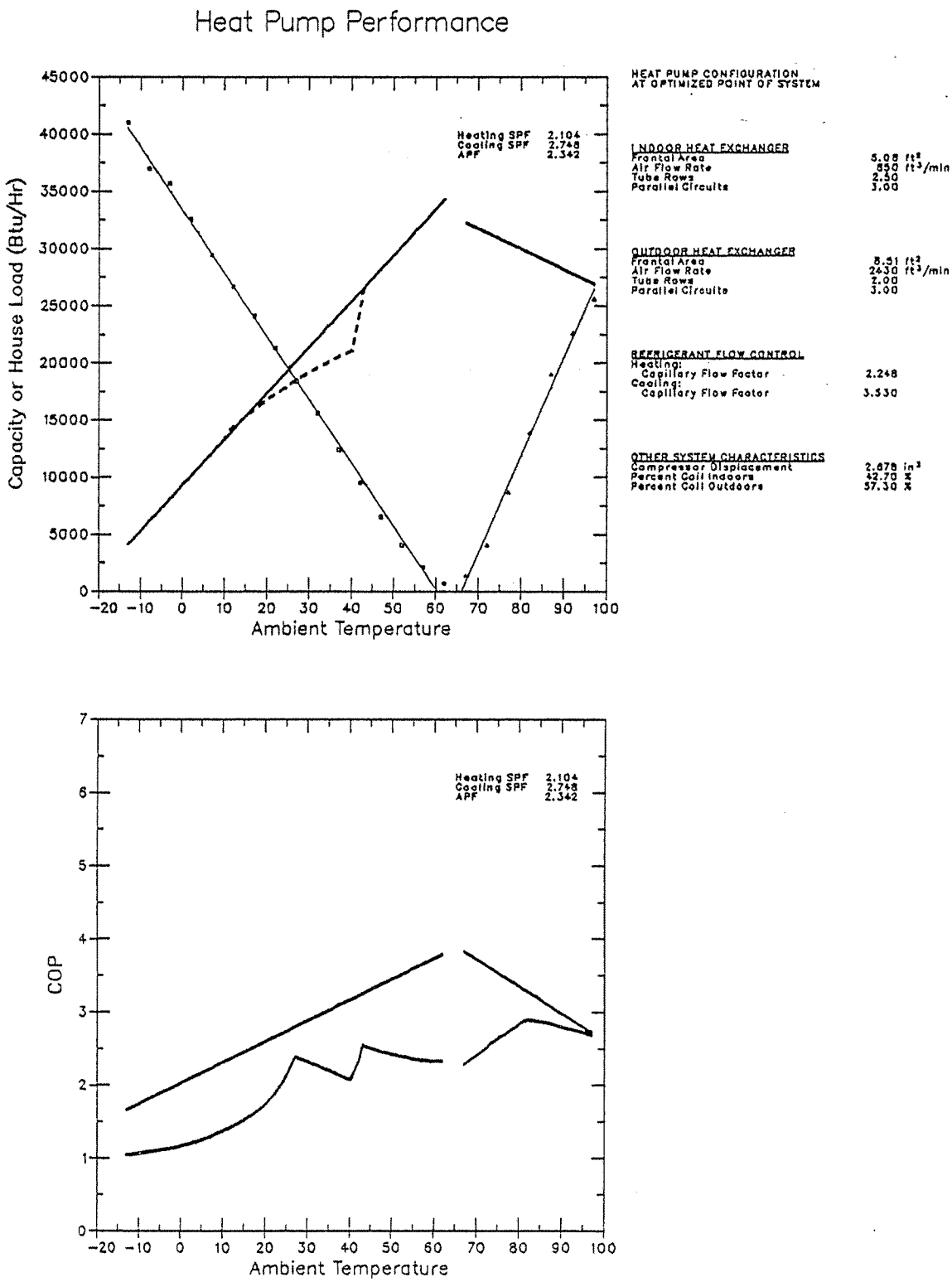

Fig. 4.1. Sample plot generated by PLOTHP.

5. DIGITIZATION AND CURVE FITTING FOR COMPRESSOR MAP DATA

5.1 INTRODUCTION

The HPDM has two different subroutines that can be used to model compressor performance: a model based on loss and efficiency parameters and a model that employs power and either mass flow or capacity data from a compressor map. The latter compressor routine requires the user to supply coefficients for curve fits to the map data. Although these fits are not performed frequently, it can be an onerous chore each time it is done.

The map fitting program distributed with the HPDM can be used to alleviate some of the burden in computing the necessary coefficients. This program is set up to perform electronic entry of data from published curves using a digitizing tablet or to prompt the user to type entries for tabular compressor data and compute the weighted least squares fits for compressor power consumption and mass flow rate as functions of the condensing and evaporating temperatures. The code will also print tables summarizing the calculated values at each point, the input data (either typed in or digitized), and the percent of difference between the two. The input data can be either power and mass flow rate or power and compressor capacity. The map fitting program also prints tables of the isentropic and volumetric efficiencies at each combination of condensing and evaporating temperatures. Graphs of any of the tabulated quantities can also be produced as an optional form of output.

5.2 DATA ENTRY

Data entry is an interactive program that was written for our own use on a Digital Equipment Corporation PDP-10 with graphics terminals and tablets produced by Tektronix, Inc. As such, it is likely to require some modification for use on other computers (although we hope that only minor changes will be required). READ and WRITE statements have been used throughout for interactive input and prompting messages instead of the less conventional TYPE and ACCEPT statements available in DEC FORTRAN-10. The input/output (I/O) to and from the terminal uses variables for the logical unit numbers that correspond to the TYPE and ACCEPT statements. These are assigned values in the main program, and changing them there should take care of the interactive I/O for the entire program. Printed output of the calculated data is routed to logical unit number 6.

The program has made use of the "free formats" available in FORTRAN-10. These permit the entry of several floating point or integer variables by separating them with a space or comma instead of requiring that they be right adjusted in a particular field. The only other known portions of the program that are not readily transportable pertain to the digitization and plotting of data. These are necessarily linked to the hardware and software libraries available and cannot be made much more portable than they already are.

The user is prompted to type the appropriate superheat and subcooling for the compressor, the compressor displacement, and the rated speed of the compressor (in revolutions per minute). The superheat and subcooling are used to compute refrigerant mass flow rate (if the capacity is given), and the superheat is also used to derive an isentropic efficiency at each combination of condensing and evaporating temperatures. The displacement and speed are used to calculate standardized volumetric efficiencies. The user is also prompted to type the number of condensing and evaporating temperatures used for the input data and those temperatures.

This program uses English units of measure for both its input and output data. It was written to help prepare data for the HPDM, which uses English units, and thus the code must also use English units. This is a necessary departure from the ORNL policy of using the International System of Units on all new programs.

5.3 ENTRY OF REMAINING DATA

The user has a choice between entering the remaining data using a digitizing tablet or typing the data at the terminal in response to prompting messages from the program. Because the second option is the easiest to explain, it is discussed first.

5.3.1 Tabular Input

Typing of data at the terminal is performed by a subroutine named TABLE. The loops for all of the calculations and I/O in the program are set up based on a rectangular grid of input data.

There can be more evaporating temperatures than condensing temperatures, but there must be a data value (i.e., power, mass flow rate, or capacity) for each combination of condensing and evaporating temperatures. If data are "missing" on the map, the algorithms used require that a dummy value be supplied by the user. Because the program is doing a weighted least squares fit, the dummy value will not affect the fit if it is matched with a zero weight (note that this is not the same as using zero for the data value and a nonzero weight). The user is prompted to type all the data values and weighting factors for either the power consumption (in kilowatts) and mass flow rate (in pound meters per hour) or the power consumption and capacity (in 1000 Btu/h).

The user also specifies whether the second set of data is for refrigerant mass flow rate (by typing "1" in response to the appropriate question) or capacity (by typing "2"). If the data are for capacity, they are fit with a biquadratic function (as described later) and converted to mass flow rates. The conversion is performed using Eq. 5.1,

$$\dot{m}_r = \frac{1000\ \dot{Q}_{ss}}{h_{\text{outlet}} - h_{\text{inlet}}}, \tag{5.1}$$

where the steady-state capacity $\dot{Q}_{ss}$ is in 1000 Btu/h and the enthalpies at the shell inlet h_{inlet} and outlet h_{outlet} are computed from the two saturation temperatures, the superheat, and the subcooling for which the map was generated. These calculations employ refrigerant property routines that are described in ref. 1.

5.3.2 Digitized Input

Digitized data are handled in much the same way as the tabular input of data. A rectangular grid of data is required. The first set of data must be the power consumption, and the second set can be either mass flow rate or capacity. This form of input is handled by the subroutine TABLET.

TABLET performs the same functions for both sets of data (i.e., power and mass flow rate or power and refrigerating capacity). These operations are

- Digitizing the end points of each axis
- Digitizing the coordinates of each of the performance curves
- Transforming the data as they are digitized from the tablet units to the graph units
- Calculating the weighting factors for each point

The user is prompted to type the values at the upper and lower limits of each axis and to digitize those points. These data are used to transform the data on each curve from the integer coordinates of the tablet (from the 1024 by 1024 grid) to the real coordinates of the plot.

The actual digitization of the data is performed using some FORTRAN and MACRO-10 subroutines that were designed for Tektronix terminals and tablets. These are unlikely to work with other equipment, and most assuredly the MACRO-10 routines will only work on a PDP-10. These subroutines are listed with the rest of the map-fitting program in Appendix H. They were not written (nor understood) by the authors. We have convinced ourselves that they work and have left it at that.

The transformation of variables, from tablet units to graph units, is described in Appendix I. As long as one is satisfied with the results, the user does not need to delve too deeply into what these subroutines are doing. For the curious, or dubious, we relied on basic geometry to compute the transformed coordinates. These are corrected for any slight misalignments of the paper on the tablet from true horizontal and vertical, and they are transformed from the integer coordinates of the tablet to the real units of the axes.

The digitization is performed so that data for each condensing temperature at one evaporating temperature is input before proceeding to the next evaporating temperature. The calculated horizontal coordinate is checked to see if it is within 0.10°F of the specified evaporating temperature. If it is, the "bell" on the terminal is sounded once, the calculated vertical coordinate is printed on the terminal screen, and the user is prompted to digitize the next point. If the calculated evaporating temperature is not within 0.10°F of the specified temperature, the bell is sounded three times in quick succession, the computed and specified evaporating temperatures are printed on the screen, and the user is prompted to digitize that point again. This process is repeated until a good data point is digitized.

The input of data from the tablet continues until the entire plot has been digitized. Data should always be digitized in the same order by *condensing temperature*: not from the top curve to the bottom one or from bottom to top, but rather from low condensing temperature to high or vice versa. Also, the order of digitization for the second set of curves, either the mass flow rate or the capacity, should be the same as for the first. If it is different, the derived compressor efficiencies will be meaningless.

5.4 WEIGHTING FACTORS FOR DIGITIZED DATA

The weighting factors are computed so that each *evaporating temperature* has the same influence on the curve fit as any other. If there is actually a rectangular grid of input data from the map (no dummy values), then each point will be weighted equally. If there are only three "real" data points at one evaporating temperature and four at another, it is assumed to be just as important that the function fit as well at that first evaporating temperature as at the second (the extreme case of this would be when there are data for only one condensing temperature at a particular evaporating temperature). Points with dummy values are digitized by placing the cross-hair cursor above the upper limit or below the lower limit of the plot. These will be given a value and a weight of 0. The other weights at each evaporator temperature are assigned so they add up to the number of condensing temperatures for the plot.

5.5 FITTING THE DATA

The data are fit using linear least squares techniques by a function of the form shown in Eq. 5.2.

$$f(x,y) = a_1x^2 + a_2x + a_3y^2 + a_4y + a_5xy + a_6 \ . \tag{5.2}$$

This has been used with the condensing temperature as the first variable and the evaporating temperature as the second variable. For lack of a better term, it is referred to as a biquadratic form. It is certainly possible to fit the data with more or fewer terms. We have had good results with this function and have stayed with it. Should other users wish to try something else, they need only to make consistent changes to subroutine FIT in this program and subroutines DATAIN and CMPMAP in the HPDM.

The implementation of the least squares and the subroutines used to solve the linear system of equations are described in Appendix J. Subroutine FIT prints a table that lists the coefficients of the best fit to the data as functions of the condensing temperature X and the evaporating temperature Y and also gives a table of the input and output. An example of this tabulated output (Exhibit 5.1) gives

- Calculated value (e.g., power consumption, mass flow rate) of the fit using the condensing and evaporating temperatures
- Input or map data, either typed in or digitized by the user
- Weighting factor used for the fit
- Percent deviation of the computed, fit value from the specified map value

These tables are printed for the compressor power consumption, the refrigerant mass flow rate, the isentropic efficiency of the compressor, and the volumetric efficiency of the compressor.

If the input data include the compressor capacity instead of the mass flow rate, a table of these data is also printed. The weights for the efficiency fits are the products of the weights for the power and mass flow fits. This way if either the power or mass flow is a dummy value, then the efficiency at that point will not enter into the curve fitting.

SAMPLE MASS FLOW RATE DATA FOR HEATING MODE OPERATION

ISENTROPIC EFFICIENCY

COEFFICIENTS FOR BI-QUADRATIC FIT:

```
F(X,Y)=-5.2443E-05*X*X +  1.0878E-02*X   + -6.7760E-05*Y*Y +
       -1.8764E-03*Y   +  6.3813E-05*X*Y + -9.0261E-02
```

EVAPORATING TEMPERATURE		CONDENSING TEMPERATURE 80.00	90.00	100.00	110.00
-20.0	I FIT	0.3527	0.3596	0.3559	0.3418
	I MAP	0.3632	0.3642	0.3541	0.3348
	I %	-2.8984	-1.2607	0.5321	2.0938
-15.0	I FIT	0.3807	0.3908	0.3903	0.3794
	I MAP	0.3846	0.3883	0.3866	0.3795
	I %	-1.0096	0.6296	0.9606	-0.0374
-10.0	I FIT	0.4053	0.4186	0.4213	0.4136
	I MAP	0.4048	0.4155	0.4182	0.4143
	I %	0.1260	0.7315	0.7512	-0.1595
-5.0	I FIT	0.4265	0.4430	0.4489	0.4444
	I MAP	0.4246	0.4428	0.4485	0.4508
	I %	0.4498	0.0310	0.0851	-1.4147
0.0	I FIT	0.4444	0.4640	0.4731	0.4718
	I MAP	0.4369	0.4615	0.4703	0.4757
	I %	1.7042	0.5520	0.6006	-0.8134
5.0	I FIT	0.4588	0.4816	0.4940	0.4958
	I MAP	0.4530	0.4826	0.4934	0.5010
	I %	1.2880	-0.1971	0.1093	-1.0333
10.0	I FIT	0.4699	0.4959	0.5114	0.5165
	I MAP	0.4659	0.4972	0.5122	0.5226
	I %	0.8525	-0.2634	-0.1602	-1.1677
15.0	I FIT	0.4776	0.5068	0.5255	0.5337
	I MAP	0.4747	0.5072	0.5255	0.5339
	I %	0.5944	-0.0823	0.0006	-0.0352
20.0	I FIT	0.4818	0.5142	0.5361	0.5476
	I MAP	0.4823	0.5174	0.5375	0.5477
	I %	-0.0958	-0.6055	-0.2597	-0.0242
25.0	I FIT	0.4827	0.5183	0.5434	0.5580
	I MAP	0.4858	0.5217	0.5463	0.5559
	I %	-0.6312	-0.6464	-0.5267	0.3827
30.0	I FIT	0.4802	0.5190	0.5473	0.5651
	I MAP	0.4818	0.5189	0.5494	0.5591
	I %	-0.3212	0.0289	-0.3890	1.0782
35.0	I FIT	0.4744	0.5163	0.5478	0.5688
	I MAP	0.4760	0.5151	0.5489	0.5627
	I %	-0.3386	0.2460	-0.1947	1.0816

THE MAXIMUM % VARIATION FROM THE MAP VALUE	2.8984
THE WEIGHTED AVERAGE OF THE ABSOLUTE VALUES OF THE % VARIATIONS	0.6141
THE WEIGHTED AVERAGE OF THE % VARIATIONS	0.0072
THE STANDARD DEVIATION FROM THE AVERAGE % VARIATION	0.8554

Exhibit 5.1. Tabulated comparison of calculated and specified compressor map data.

A brief summary of the percent errors is also printed below the table of input and output data. This summary shows

- The maximum magnitude of the variation from the map data
- The average magnitude of the errors (the sum of the weights times the absolute value of the corresponding error divided by the sum of the weights)
- The weighted average of the errors (this should be close to 0 for the fit to be about evenly distributed between positive and negative variations from the data)
- The standard deviation of the absolute errors (about 66% of the fit data will be within one standard deviation of the map data and 95% within two standard deviations)

These are useful statistics in assessing the quality of the fit.

5.6 PLOTS OF THE CURVE FITS

An alternate version of subroutine FIT contains plotting calls to draw graphs of the input data and the curve fits using the computed coefficients. Some examples of these plots are shown in Figs. 5.1–5.4. The typed or digitized map data (e.g., power consumptions) or the derived efficiencies are plotted with small markers (e.g., squares, triangles). The solid lines are plots of the biquadratic fits to the data. The calculated coefficients are used with the specified condensing temperatures across the range of evaporating temperatures. These, like the performance plots described in Chap. 3, are generated using the DISSPLA graphics package. The plotting version of FIT is listed in Appendix K, and the graphics subroutines are described in Appendix G.

5.7 CALCULATION AND PLOTS OF COMPRESSOR EFFICIENCIES

As mentioned earlier, the isentropic and volumetric efficiencies of the compressor are computed at each combination of saturation temperatures for which there are data for both the power and mass flow rate. The volumetric efficiency is computed using Eq. 5.3:

$$\eta_{vol} = \frac{1728 \ \dot{m}_r \ v_{inlet}}{60 \ DS} , \tag{5.3}$$

where

$\dot{m}_r$ = refrigerant mass flow rate (lbm/h),
v_{inlet} = specific volume of refrigerant at the shell inlet (ft^3/lbm),
S = rated speed (revolutions/min),
D = compressor displacement ($in.^3$/revolution),

The factors 1728 and 60 are used to convert from cubic feet to cubic inches and from hours to minutes, respectively.

The calculation of the isentropic efficiency uses Eq. 5.4:

$$\eta_{isen} = \frac{\dot{m}_r \ \Delta h_{isen}}{\dot{w}_{input}} , \tag{5.4}$$

ORNL–DWG 86–8034

SAMPLE COMPRESSOR DATA
POWER CONSUMPTION (KW)

Superheat 20.00 F Displacement 3.640 in^3
Subcooling 15.00 F Motor Speed 3450.0 rpm

Maximum Error 1.2167 %
Average Error 0.3249 %
Standard Deviation 0.4233 %

$$F(T_c,T_e) = 7.2450*10^{-5}T_c^2 - 1.0564*10^{-2}T_c - 1.2533*10^{-4}T_e^2 + 1.1462*10^{-3}T_e + 2.6824*10^{-4}T_cT_e + 2.3688*10^{0}$$

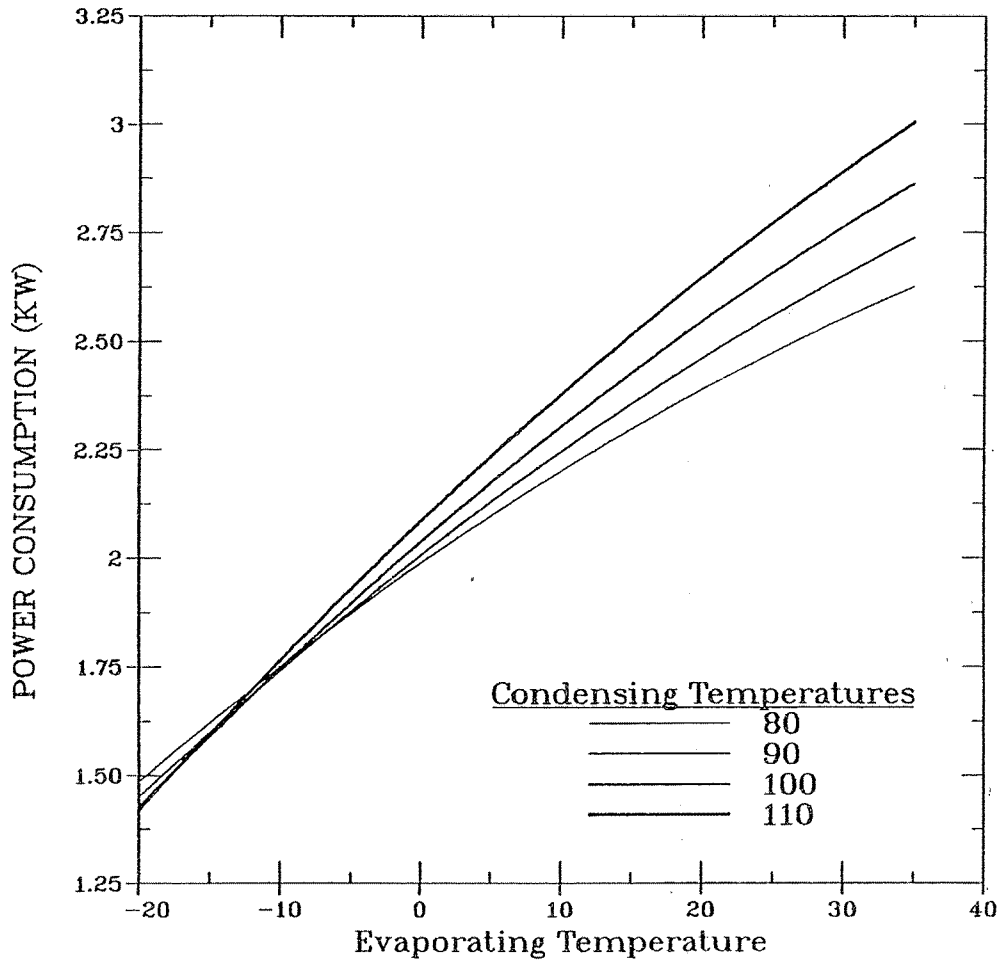

Fig. 5.1. Graphical output from compressor map-fitting routine showing compressor power consumption data and curve fit.

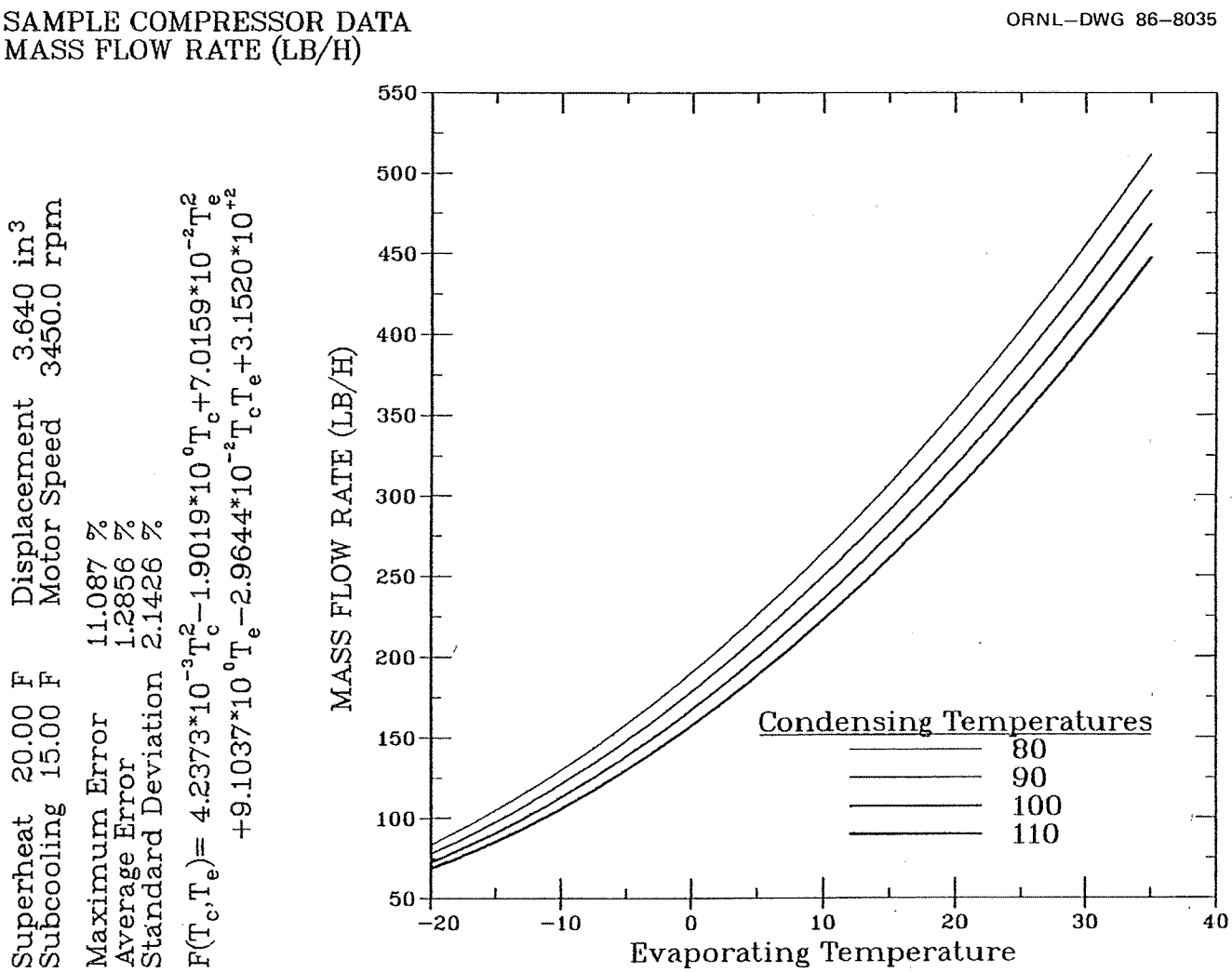

Fig. 5.2. Graphical output from compressor map-fitting routine showing refrigerant flow data and curve fit.

ORNL–DWG 86–8036

SAMPLE COMPRESSOR DATA
ISENTROPIC EFFICIENCY

Superheat 20.00 F Displacement 3.640 in^3
Subcooling 15.00 F Motor Speed 3450.0 rpm

Maximum Error 2.8049 %
Average Error 0.6039 %
Standard Deviation 0.8327 %

$$F(T_c,T_e)=-5.3548*10^{-5}T_c^2+1.1118*10^{-2}T_c-6.8077*10^{-5}T_e^2 -2.0087*10^{-3}T_e+6.5030*10^{-5}T_cT_e-9.9646*10^{-2}$$

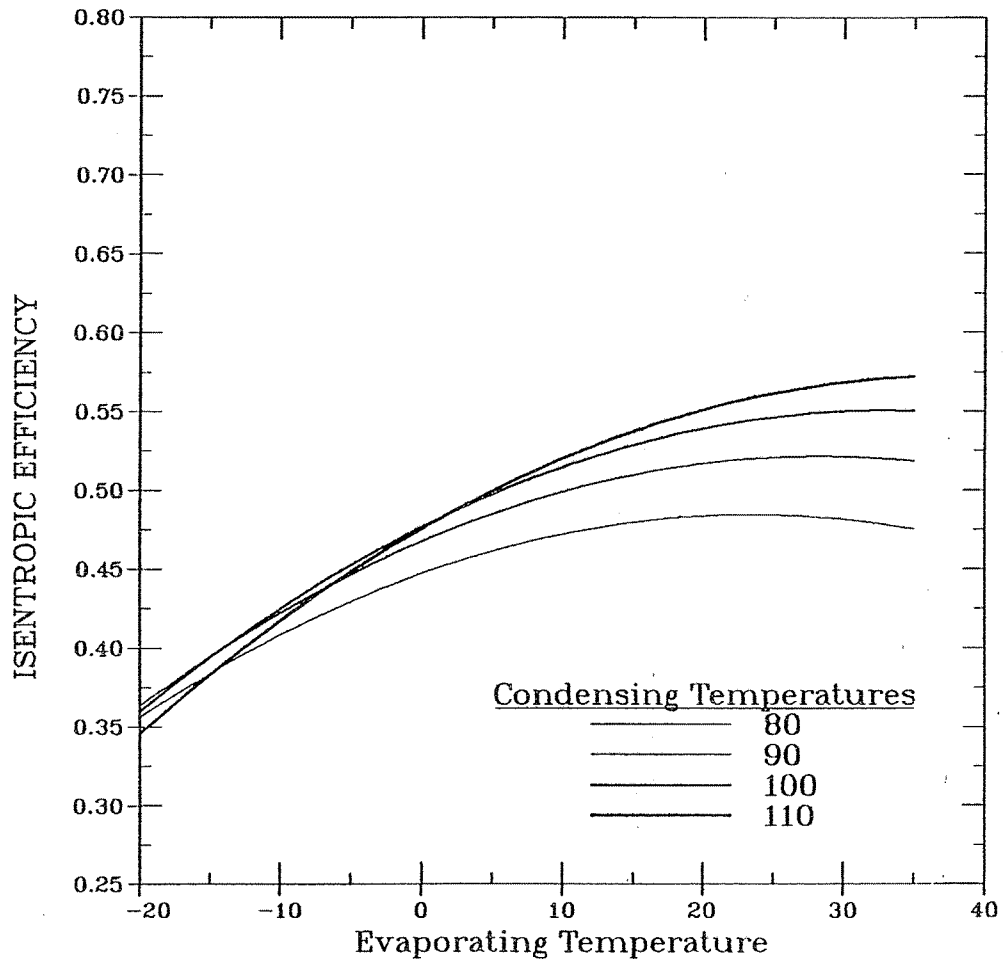

Fig. 5.3. Graphical output from compressor map-fitting routine showing derived isentropic efficiency data and curve fit.

ORNL–DWG 86–8037

SAMPLE COMPRESSOR DATA
VOLUMETRIC EFFICIENCY

Superheat 20.00 F Displacement 3.640 in^3
Subcooling 15.00 F Motor Speed 3450.0 rpm

Maximum Error 4.4967 %
Average Error 0.8256 %
Standard Deviation 1.1639 %

$$F(T_c,T_e) = 5.4328*10^{-6}T_c^2 - 4.5529*10^{-3}T_c - 5.0401*10^{-5}T_e^2 + 9.8042*10^{-3}T_e - 6.9020*10^{-6}T_cT_e + 9.6039*10^{-1}$$

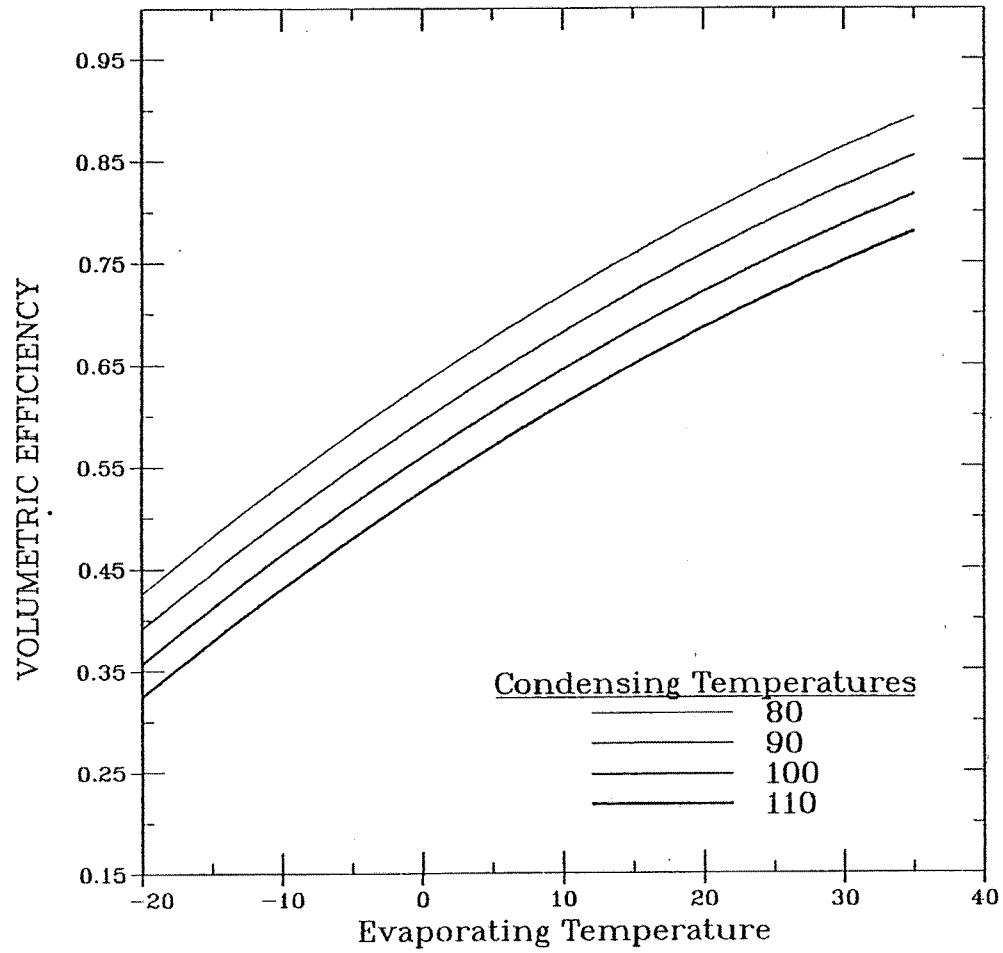

Fig. 5.4. Graphical output from compressor map-fitting routine showing derived volumetric efficiency data and curve fit.

where

$\dot{m}_r$ = refrigerant mass flow rate (lbm/h),

Δh_{isen} = enthalpy change from shell outlet to shell inlet assuming isentropic compression (Btu/lbm),

$\dot{w}_{input}$ = power input to the compressor (Btu/h).

The coefficients for the curve fits to the efficiencies are printed out although these are not used in the HPDM. They are used by the version of the fitting program that generates the plots (as in Figs. 5.1 through 5.4).

6. CONVERSION OF THE APF MODEL TO SUBROUTINE FUNCT1

6.1 INTRODUCTION

The HPDM and the APF model have been used extensively at ORNL in conjunction with other programs such as numerical optimization routines, contour plotting programs, and codes that simply estimate a gradient of the steady-state or annual performance with respect to different design parameters. It has been convenient to have "main programs" that could easily fit into any of these applications.

Before proceeding, a minor point merits a few words. The discussion that follows deals specifically with the APF model and changes that have been made to it because our most recent work has been with that particular program. Similar modifications could be, and in the past have been, made to the steady-state HPDM. It is convenient to talk about a specific program, and the APF model was chosen. Some other code could have been chosen just as easily.

6.2 THE SUBROUTINE FUNCT1

Much of what follows is motivated by the requirements of a particular numerical optimization package available at ORNL. Many of our applications began with studies for optimal heat pump design, and subroutines were developed that were consistent with the needs of the optimization package. The "optimizer" required that

1. the user's program be set up as a subroutine named FUNCT1,
2. the independent parameters (e.g., compressor displacement, air flow rates) be passed to FUNCT1 as the elements of a double precision array X,
3. the independent parameters be limited within specified lower and upper limits ($a_i < X_i < b_i$), and
4. ideally the lower and upper limits on the independent parameters be -1 and $+1$.

These were accepted as fixed criteria that defined certain aspects of our subroutines.

The main program for the APF model was converted to the subroutine FUNCT1. This was done by putting a SUBROUTINE statement at the beginning with the appropriate parameter list (see the listing in Appendix L) and by replacing the STOP statement at the end with a RETURN statement. An "objective function" for the optimization was added toward the end of the program (see Chap. 8 for more discussion of objective functions), even though it is irrelevent to some applications such as contour plotting. The calls to subroutines DATAIN and TABLES were removed so they would not be invoked each time FUNCT1 was called (they need to be put into whatever main program is used with FUNCT1). And finally, a call to a transformation routine, TRNSFM, was added.

6.3 THE TRANSFORMATION ROUTINE TRNSFM

Once the user accepts the requirement that the independent design variables be passed to FUNCT1 in an array X, a way is needed to get those design variables into and out of that array. Subroutine TRNSFM has been set up to do that. In the process, it also converts single precision numbers to double precision and scales the data so that

$$-1 \leqslant X_i \leqslant +1 \ . \tag{6.1}$$

Describing what good scaling is prior to getting into an optimization is difficult, yet it is essential that the objective function and constraints be "well scaled" so that the optimization will converge to a solution in a reasonable length of time. The manuals for the software library used at ORNL simply state that a unit step in each variable direction must have an approximately equal effect in magnitude of the resulting change in the objective function and in each of the constraints. That may not be entirely clear to the user.

In one of our own applications, we set out to constrain the steady-state cooling capacity at 35°C (95°F) to a fixed value. We discovered, none too surprisingly, that the constraint depended much more heavily on the compressor displacement than it did on the indoor air flow rate. The optimization algorithm got hung up trying to get the best displacement within 10^{-6} mL (0.0001 in.^{3}) because the constraint was poorly scaled with respect to the objective function. Also, it did nothing with the air flow (or any of the other variables) because that variable was poorly scaled with respect to the compressor displacement.

The optimization considers a "unit step" in each variable as a fixed percentage of the specified range for that variable. We were able to improve the scaling of one variable with respect to the others by selecting broader or narrower ranges for each. Unfortunately, a feel for what is good scaling and what is not came only through experience. There was more to do than select ranges, though, because for some esoteric mathematical reason the authors of the optimization routines recommended that each variable have an upper limit of +1 and a lower limit of −1. This amounts to working in a nondimensional space and is not hard to accommodate.

Although the scaling transformation used is general, the subroutine listed in Appendix L is specific to our own uses. An array ISWTCH is used to identify which design variables are to be used in the array X. Table 6.1 identifies the design parameters that we assigned through the ISWTCH array. If, for example, ISWTCH(5)=3, then X(5) will contain data for the outdoor volumetric air flow rate. The corresponding lower and upper limits for the air flow rate are passed in the array elements A(5) and B(5), respectively.

TRNSFM performs either of two linear transformations depending on whether design variables are being used to initialize the X array or if data from the X array are being transformed back into the original design variables. The first of these two functions is performed using a transformation similar to the one shown in Eq. 6.2 for the outdoor air flow rate. The inverse function of computing the design variable from the normalized X variable is shown in Eq. 6.3.

$$X(3) = \frac{2(QAO) - A(3) - B(3)}{B(3) - A(3)} \ , \tag{6.2}$$

Table 6.1. Correspondence of physical design variables and switch settings

1	Total compressor displacement, in.^{3}
2	Indoor air flow rate, ft^3/min
3	Outdoor air flow rate, ft^3/min
4	Number of equivalent parallel refrigerant circuits in indoor heat exchanger
5	Number of equivalent parallel refrigerant circuits in outdoor heat exchanger
6	Number of refrigerant tube rows in indoor heat exchanger
7	Number of refrigerant tube rows in outdoor heat exchanger
8	Fraction of total heat exchanger surface area in indoor coil (not used simultaneously with item 9)
9	Fraction of total heat exchanger surface area in outdoor coil (not used simultaneously with item 8)
10	Specified level of condenser subcooling for cooling mode (when a fixed condenser subcooling is used in lieu of a specific flow control device)
11	Specified condenser subcooling for heating mode (when a fixed condenser subcooling is used in lieu of a specific flow control device)
12	Fin pitch of the indoor coil, fins per inch
13	Fin pitch for the outdoor coil, fins per inch
14	Capillary flow factor for cooling mode (when a capillary tube is used for flow control device)
15	Capillary flow factor for heating mode, dimensionless
16	Slope of specified condenser subcooling curve when subcooling is specified as a function of ambient temperature for cooling mode operation
17	Slope of specified condenser subcooling curve for heating mode when subcooling is specified as a function of ambient temperature

$$QAO = \frac{X(3)\{B(3) - A(3)\} + A(3) + B(3)}{2} \quad . \tag{6.3}$$

An input variable, IDIR, is used to specify the "direction" of the transformation (i.e., whether Eq. 6.2 or 6.3 is used).

The standard design parameters can be read by DATAIN from the HPDM as usual and passed to TRNSFM through common blocks. As X is varied by an optimization or contour plotting routine, the design variables can be computed and passed back to the APF model and HPDM through the same common blocks. The arrays ISWTCH, A, and B need to be assigned in the main program and made available to TRNSFM. This is done in

our codes by reading them as input data and passing them to FUNCT1 in common blocks. They are then passed to TRNSFM via the argument list.

6.4 THE SUBROUTINE SETVAR

Some of the variables in Table 6.1 affect only the cooling mode performance while others affect only the heating mode calculations. Others, of course, affect both modes. Subroutine SETVAR was written to work in conjunction with TRNSFM and FUNCT1 to eliminate repetitious calculations. It sets switches that identify whether the latest changes in the X values will affect just the heating season performance, the cooling season performance, or both. For example, if the annual performance of several different heat pumps is to be computed and in configuring the systems only the capillary flow factor for the heating mode has been changed, there is no need to repeat the cooling season calculations for each of them. SETVAR is used to indicate this to the subroutines doing the steady-state calculations. (Little overhead is associated with repeating the APF calculations.) The switch settings from SETVAR are conveyed to subroutine STEADY so that only the necessary steady-state computations are performed. In this way, previous results are used whenever possible.

6.5 CONCLUSION

The conversion of the main program, either from the APF model or the HPDM, into a subroutine provides a code that can be called repetitively for many different combinations of design variables. The name FUNCT1 was selected to conform with requirements of a particular software library available at ORNL. TRNSFM was written to transform between the engineering design variables of the HPDM and the required parameters for FUNCT1. SETVAR was written to reduce redundant calculations. Together, they can be used under the control of optimization or contour plotting routines to perform hundreds, or even thousands, of APF or steady-state calculations.

7. CONTOUR PLOTS

7.1 INTRODUCTION

A common approach to analyzing the effects of two independent parameters on the operation of a mechanical system, such as a heat pump, is to hold one of them fixed while varying the other over a selected range of values. Doing this several times enables one to construct a family of curves such as those in Fig. 7.1. This particular example shows the dependence of annual performance factor (the dependent variable) on the indoor and outdoor volumetric air flow rates (the independent variables).

This means of displaying data becomes more complicated, however, when more and more data are added to it. Figure 7.1 shows three curves, each for a constant outdoor air flow rate. Figure 7.2 shows the same three curves as dashed lines with a fourth, solid curve added for an outdoor air flow rate of 1415 L/s (3000 ft^3/min). The curves are already beginning to overlap and cross each other, which makes them difficult to read and use. This overlapping display is carried to extremes when two or more families of curves are superimposed to examine simultaneous effects on more than one dependent variable. Figure 7.3 shows the dependence of two variables, APF and design cooling capacity at 35°C (95°F), on the indoor air flow rate for several fixed outdoor air flow rates. Not only is the figure hard to read, but the reader may find it often difficult and sometimes

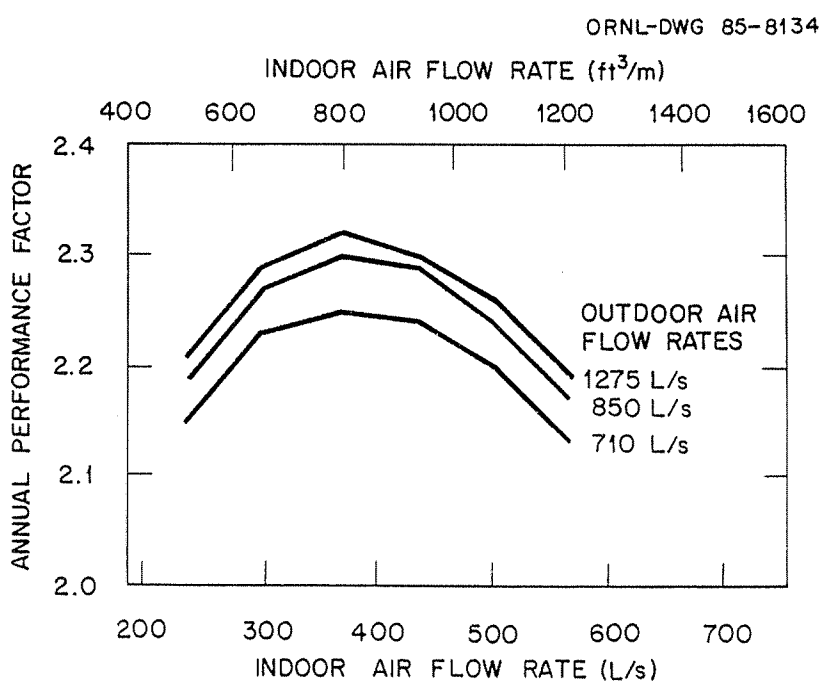

Fig. 7.1. Dependence of annual performance factor on indoor and outdoor air flow rates of 710, 850, and 1275 L/s (1500, 1800, and 2700 ft^3/min).

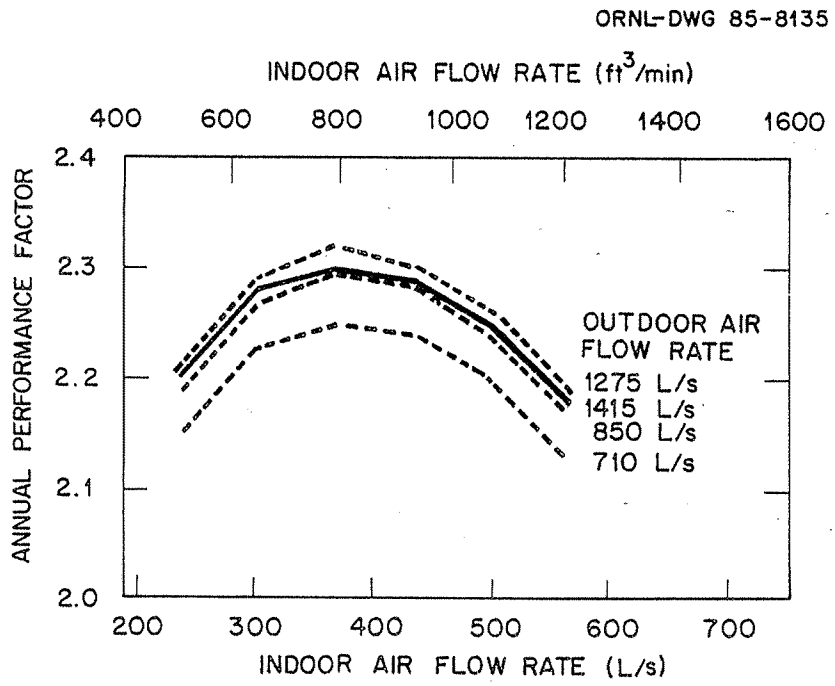

Fig. 7.2. Dependence of annual performance factor on indoor and outdoor flow rates of 710, 850, 1275, and 1415 L/s (1500, 1800, 2700, and 3000 ft^3/min).

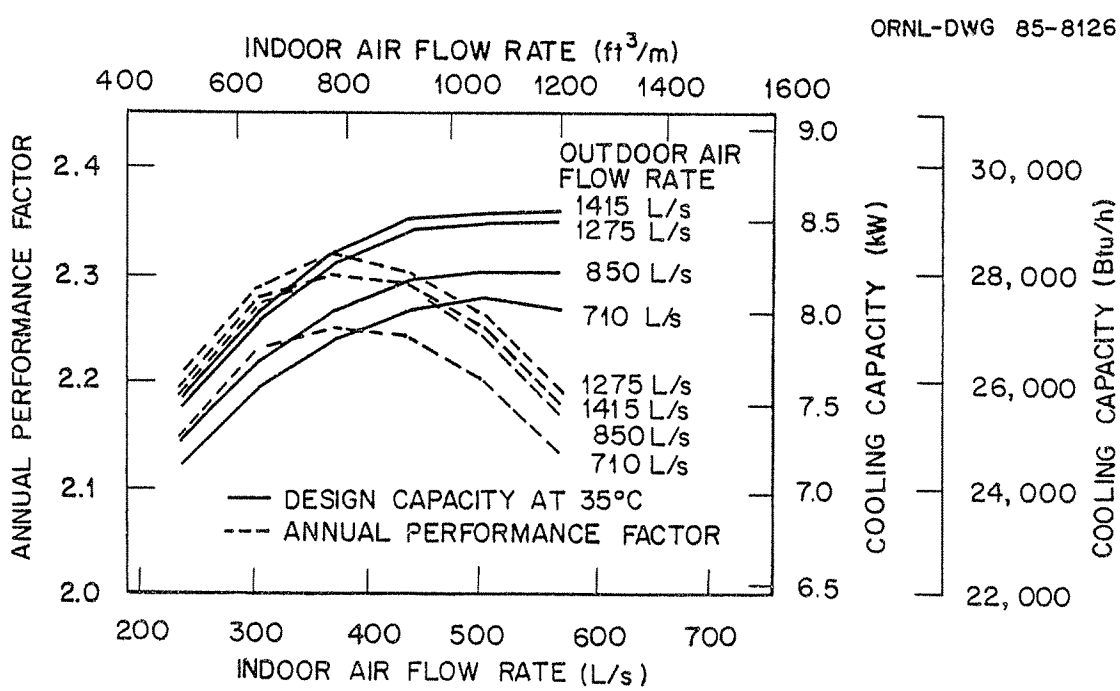

Fig. 7.3. Dependence of design cooling capacity and annual performance factor on indoor and outdoor air flow rates.

impossible to discern how the air flow rates could be varied simultaneously to find a better, or best, APF while maintaining a specified, fixed design cooling capacity. Interpolation between independent variable lines is also required, which is in some cases inaccurate and in other cases incorrect.

The data in Fig. 7.2 could be separated, or spread out, by displaying it as a three-dimensional perspective plot as in Fig. 7.4. In this case, the indoor and outdoor air-flow rates lie on the *x-y* plane, and the corresponding annual performance forms a surface in the third dimension. This makes the data easy to visualize but hard to read. It is very difficult to find the coordinates of a point lying on the surface.

A third way of looking at the data is to use a contour plot. This loses some of the visual aspects of a perspective drawing but is much more valuable in providing quantitative information. Figure 7.4 includes several curves of constant APF superimposed on the surface. These are broken lines where they reach the boundaries of the region but form "concentric rings" as they near the peak. These "contours" of constant APF can be projected down to the *x-y* plane to form a two-dimensional plot like that shown in Fig. 7.5. This contains many more contours than were shown in Fig. 7.4, which makes it easier to interpolate between them. The four curves that are shown in Fig. 7.2 now correspond to the four bold horizontal lines in Fig. 7.5.

ORNL-DWG 86-8105

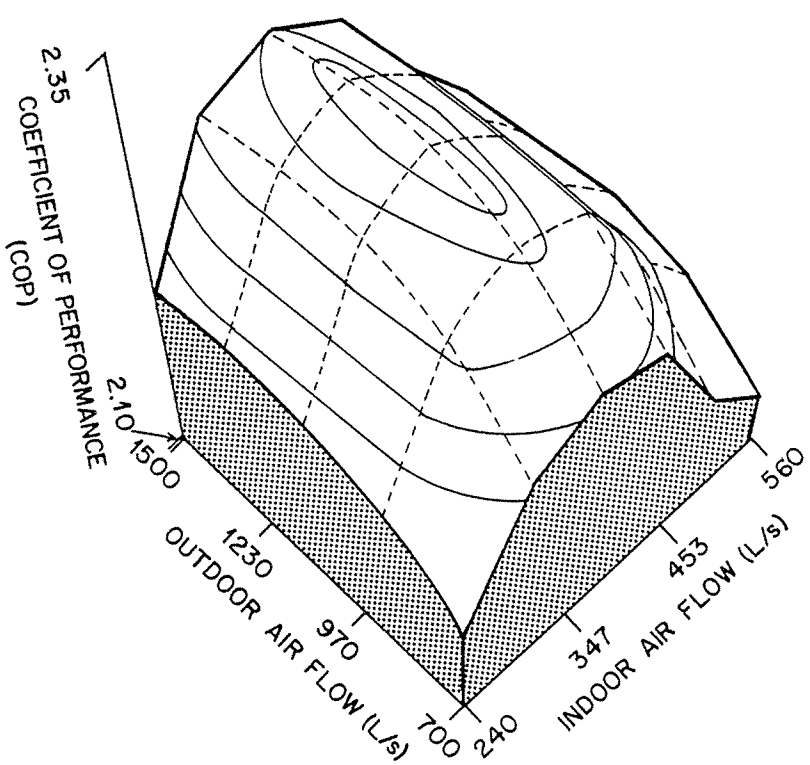

Fig. 7.4. Perspective drawing of the relationship between annual performance factor and indoor and outdoor air flow rates.

ORNL-DWG 85-8148

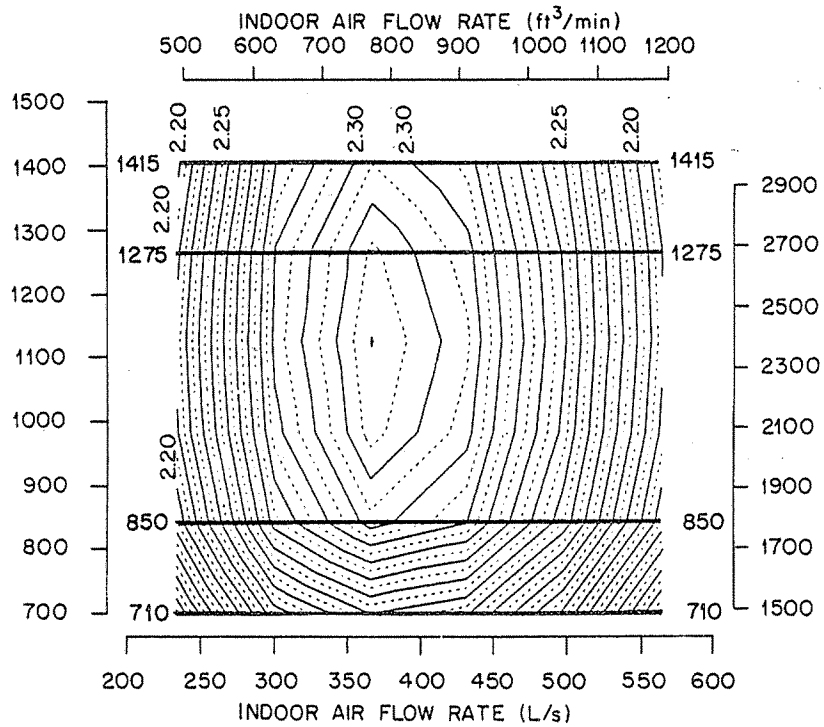

Fig. 7.5. Contour plot showing dependence of annual performance factor on indoor and outdoor air flow rates.

7.2 MULTIPLE FUNCTIONS OF COMMON VARIABLES

An additional advantage held by this display of data is that several dependent variables can be considered simultaneously. The data in Fig. 7.3 can be displayed as a contour plot in a similar way. In this case, the two families of curves (i.e., APF and cooling capacity at 35°C) define two surfaces, and consequently there are two sets of contours. Figure 7.6 shows the contours of APF that are in Fig. 7.5, and it also has lines of constant cooling capacity. It is now fairly easy to see that the highest APF lies on, or very close to, the curve for a design cooling capacity of 8.2 kW. In fact, this is a two-dimensional check of an optimization we set up to maximize the APF with the constraint requiring a cooling capacity of 8.2 kW at 35°C.

Contour plots are a means of displaying an additional dimension that can be hard to see in large families of parametric curves. They spread the data out and even allow for more information to be added without obscuring what is already there.

However useful contour plots may be, they can be very time consuming to construct with a handheld calculator and a piece of graph paper. Points on each of the contour levels are found by interpolating the dependent variable values in both independent variables. This is not too unpleasant for the first point or two, but it gets laborious by the fiftieth or sixtieth point. This process is well suited to computer-generated plots and, in spite of the length of the explanation that follows, it is not that difficult to do.

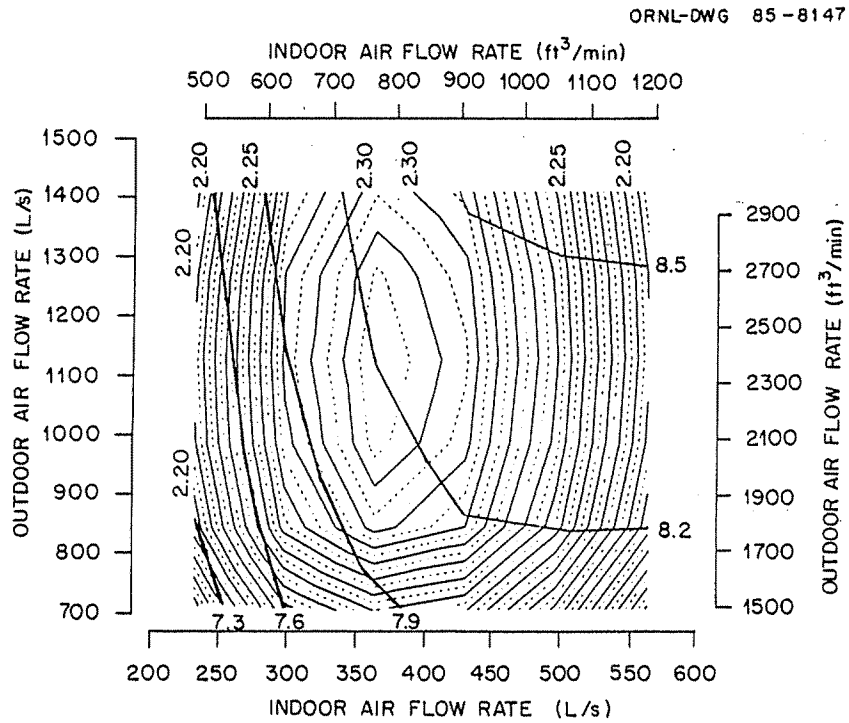

Fig. 7.6. Contour plot showing dependence of annual performance factor and design cooling capacity on indoor and outdoor flow rates.

7.3 DATA GENERATION

The process of creating a contour plot really consists of two distinct steps: generating the data for the plot and generating the plot itself. We have chosen for our own purposes to keep these tasks separate. Whether it be APFs, design cooling capacity, or any of the other possible dependent variables, data must be available to the plotting task on a "rectangular mesh" of points for whatever two independent variables are used. If these happen to be the two air flows, as in the preceding figures, then the APF model needs to be run at every point on a selected grid or mesh of indoor air flow rates and outdoor air flow rates. The points used to generate the plots in Figs. 7.5 and 7.6 are identified in Fig. 7.7. In this case six indoor and outdoor air flow rates were used for a total of 36 data points.

The modifications to the APF model described in Chap. 5 make it very easy to generate the data for a contour plot. All that is needed is a main program that does the following:

- Records information about the independent variables for use by the plotting program (i.e., number of values used for each independent variable, the desired axis labels, etc.)
- Invokes the APF model for each combination of the independent variables
- Records the computed data that will go into the contour plots (e.g., APFs, design cooling capacities, comparison of sensible heat transfer ratios to total heat transfer ratios at selected cooling temperatures, etc.)

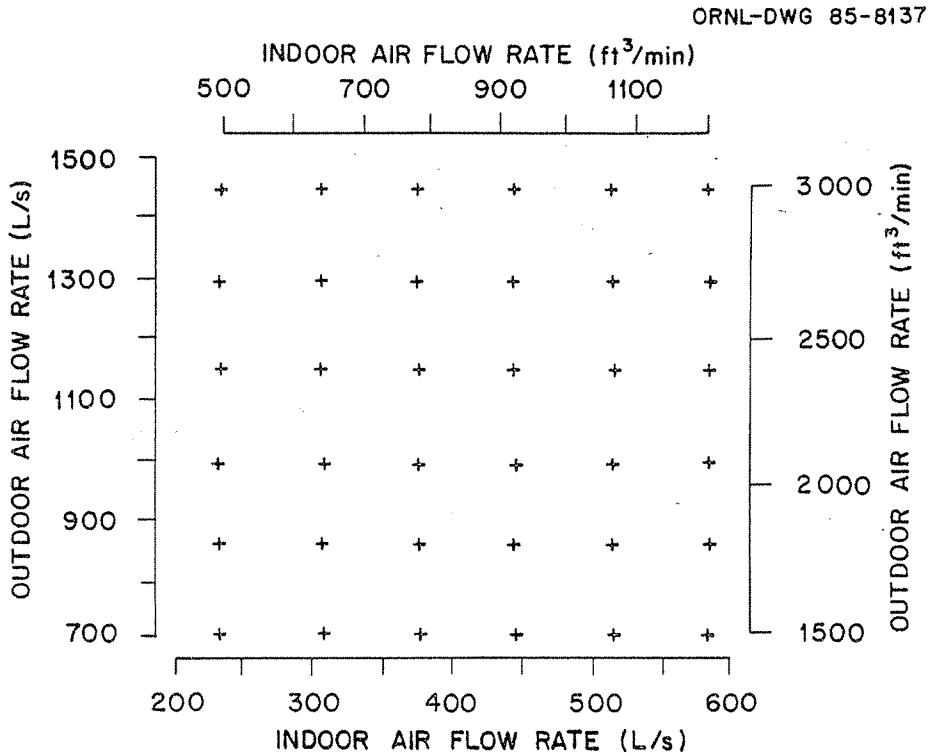

Fig. 7.7. Rectangular grid of data points for contour plots.

These data can then be read from a data file by a separate program that handles contour plotting.

Most of our own uses of contour plots have been in conjunction with heat pump design optimizations in which the best design is selected by using a numerical optimization package. The design parameters for this optimized heat pump can be recorded in the output data file so the contour plot can include detailed labels and also mark the best design point.

7.4 ID HEADER BLOCK

Appendixes M and N contain listings of the driving routine, DRIVER, which generates data for the contour plotting routines, and CONPLT, which draws the contour plots. Although the plotting program is discussed later, it is of interest here because of the transfer of data between the two codes. The main program in Appendix M writes data to logical unit number 18 that can be used as input data by the plotting code. An example of this data is shown in Exhibit 7.1. DRIVER makes use of information from three sources: an input data file read directly by DRIVER, the standard input data file for the steady-state heat pump model, and axis labels and identification information assigned in a BLOCK DATA routine. These data are all written into the first twelve lines of the output data set. This header block consists of the following:

```
OPTIMIZED SINGLE-SPEED HEAT PUMP WITH CAPILLARY TUBES
I?NDOOR @A?IR @F?LOW @R?ATE (FT"E.5H.7?3"EXHX?/MIN)@$
I?NDOOR @A?IR @F?LOW @R?ATE (@L/?S)@$
O?UTDOOR @A?IR @F?LOW @R?ATE (FT"E.5H.7?3"EXHX?/MIN)@$
O?UTDOOR @A?IR @F?LOW @R?ATE (@L/?S)@$
        2        6     500.0    1200.0     848.5
        3        6    1500.0    3000.0    2427.0
    848.5   2427.0    2.6780    5.0750    8.5130    0.0       0.0       3.0000
      3.0      2.5       2.0    2.1150    2.7443    2.3499  797.8425
    500.0 1500.0 1800.0 2100.0 2400.0 2700.0 3000.0
 APF        2.209  2.232  2.242  2.244  2.237  2.223
 COPH       1.956  1.955  1.953  1.947  1.937  1.920
 COPC       2.653  2.732  2.775  2.796  2.800  2.793
 I2R       1172.9 1128.4 1090.5 1058.5 1033.6 1011.1
 Q(95)     23599. 23994. 24275. 24488. 24665. 24819.
 CNSTRAINT   32.0   32.0   32.0   32.0   32.0   32.0
 S-T(82)   0.0    0.0    0.0    0.0    0.0    0.0
 S-T(95)   0.0    0.0    0.0    0.0    0.0    0.0
 SS-COP     2.438  2.428  2.419  2.399  2.370  2.331
 SS-CAP    14267. 14497. 14694. 14860. 14998. 15101.
 SS-COP     3.088  3.073  3.056  3.038  3.014  2.981
 SS-CAP    24833. 25208. 25530. 25797. 25963. 26223.
 SS-COP     3.088  3.187  3.241  3.270  3.277  3.272
 SS-CAP    25571. 25913. 26167. 26365. 26497. 26652.
 SS-COP     2.609  2.703  2.753  2.780  2.792  2.793
 SS-CAP    23599. 23994. 24275. 24488. 24665. 24819.
    640.0 1500.0 1800.0 2100.0 2400.0 2700.0 3000.0
 APF        2.281  2.308  2.320  2.323  2.319  2.305
 COPH       2.055  2.055  2.053  2.048  2.038  2.023
 COPC       2.661  2.744  2.789  2.813  2.821  2.814
 I2R       1052.5 1008.7  968.9  934.7  907.8  887.9
 Q(95)     24935. 25407. 25733. 25988. 26200. 26367.
 CNSTRAINT   32.0   32.0   32.0   32.0   32.0   32.0
 S-T(82)   0.0    0.0    0.0    0.0    0.0    0.0
 S-T(95)   0.0    0.0    0.0    0.0    0.0    0.0
 SS-COP     2.527  2.518  2.506  2.486  2.457  2.417
 SS-CAP    14880. 15098. 15304. 15476. 15614. 15723.
 SS-COP     3.128  3.234  3.293  3.325  3.338  3.332
 SS-CAP    27163. 27574. 27874. 28104. 28291. 28434.
 SS-COP     2.642  2.742  2.796  2.827  2.844  2.846
 SS-CAP    24935. 25407. 25733. 25988. 26200. 26367.
    780.0 1500.0 1800.0 2100.0 2400.0 2700.0 3000.0
 APF        2.304  2.337  2.349  2.352  2.348  2.334
 COPH       2.106  2.114  2.110  2.103  2.094  2.078
 COPC       2.622  2.707  2.752  2.777  2.785  2.779
 I2R        961.6  904.0  869.6  836.7  808.5  795.0
 Q(95)     25771. 26290. 26645. 26926. 27150. 27335.
 CNSTRAINT   32.0   32.0   32.0   32.0   32.0   32.0
 S-T(82)   0.0    0.0    0.0    0.0    0.0    0.0
 S-T(95)   0.0    0.0    0.0    0.0    0.0    0.0
 SS-COP     2.549  2.552  2.536  2.515  2.486  2.449
 SS-CAP    15343. 15646. 15809. 15972. 16115. 16236.
 SS-COP     3.396  3.385  3.365  3.342  3.319  3.290
 SS-CAP    26722. 27188. 27563. 27882. 28140. 28264.
```

Exhibit 7.1. Sample data file for contour plots.

SS-COP	3.101	3.209	3.269	3.303	3.316	3.311
SS-CAP	28145.	28601.	28927.	29181.	29379.	29533.
SS-COP	2.622	2.725	2.780	2.814	2.831	2.835
SS-CAP	25771.	26290.	26645.	26926.	27150.	27335.
920.0	1500.0	1800.0	2100.0	2400.0	2700.0	3000.0
APF	2.293	2.326	2.338	2.339	2.333	2.319
COPH	2.128	2.135	2.129	2.119	2.106	2.089
COPC	2.548	2.632	2.676	2.700	2.709	2.704
I2R	870.9	819.0	792.4	774.5	759.3	747.2
Q(95)	26112.	26867.	27201.	27499.	27740.	27939.
CNSTRAINT	32.0	32.0	32.0	32.0	32.0	32.0
S-T(82)	0.0	0.0	0.0	0.0	0.0	0.0
S-T(95)	0.0	0.0	0.0	0.0	0.0	0.0
SS-COP	2.535	2.533	2.520	2.504	2.478	2.443
SS-CAP	15827.	16086.	16263.	16445.	16600.	16725.
SS-COP	3.424	3.415	3.396	3.373	3.347	3.316
SS-CAP	27413.	27910.	28299.	28627.	28886.	29015.
SS-COP	3.024	3.131	3.191	3.224	3.237	3.234
SS-CAP	28755.	29250.	29603.	29868.	30074.	30238.
SS-COP	2.553	2.670	2.719	2.753	2.771	2.777
SS-CAP	26112.	26867.	27201.	27499.	27740.	27939.
1060.0	1500.0	1800.0	2100.0	2400.0	2700.0	3000.0
APF	2.247	2.276	2.283	2.291	2.285	2.275
COPH	2.120	2.120	2.113	2.104	2.092	2.078
COPC	2.436	2.514	2.548	2.588	2.597	2.593
I2R	788.8	761.9	744.6	726.1	710.5	697.4
Q(95)	26284.	26854.	27259.	27566.	27816.	28019.
CNSTRAINT	32.0	32.0	32.0	32.0	32.0	32.0
S-T(82)	0.0	0.0	0.0	0.0	0.0	0.0
S-T(95)	0.0	0.0	0.0	0.0	0.0	0.0
SS-COP	2.483	2.485	2.474	2.460	2.437	2.405
SS-CAP	16303.	16577.	16752.	16941.	17100.	17233.
SS-COP	3.388	3.381	3.364	3.341	3.316	3.296
SS-CAP	28041.	28541.	28947.	29278.	29540.	29798.
SS-COP	2.892	2.993	3.038	3.095	3.108	3.106
SS-CAP	28826.	29336.	29634.	30160.	30372.	30539.
SS-COP	2.457	2.553	2.609	2.642	2.661	2.667
SS-CAP	26284.	26854.	27259.	27566.	27816.	28019.
1200.0	1500.0	1800.0	2100.0	2400.0	2700.0	3000.0
APF	2.176	2.204	2.215	2.218	2.214	2.205
COPH	2.083	2.084	2.078	2.070	2.058	2.046
COPC	2.309	2.382	2.422	2.445	2.454	2.451
I2R	735.3	707.8	690.6	671.4	655.5	642.5
Q(95)	26239.	26826.	27236.	27565.	27820.	28027.
CNSTRAINT	32.0	32.0	32.0	32.0	32.0	32.0
S-T(82)	0.0	0.0	0.0	0.0	0.0	0.0
S-T(95)	0.0	0.0	0.0	0.0	0.0	0.0
SS-COP	2.411	2.414	2.405	2.394	2.374	2.346
SS-CAP	16852.	17132.	17307.	17502.	17664.	17797.
SS-COP	3.308	3.303	3.288	3.267	3.243	3.226
SS-CAP	28680.	29182.	29592.	29925.	30189.	30457.
SS-COP	2.741	2.835	2.889	2.922	2.935	2.934
SS-CAP	28847.	29373.	29748.	30038.	30256.	30422.
SS-COP	2.332	2.423	2.475	2.510	2.528	2.535
SS-CAP	26239.	26826.	27236.	27565.	27820.	28027.

Exhibit 7.1 (continued)

- **Line 1**—a title for the run, taken from the HPDM component data file (read by DATAIN)
- **Lines 2 and 3**—a label for the horizontal axis in English units followed by a label in Standard Internationale (SI) units (from BLOCK DATA)
- **Line 4**—the slope and intercept for converting from English to SI units for the variable on the horizontal axis (from BLOCK DATA)
- **Lines 5 and 6**—a label for the vertical axis in English units followed by a label in SI units (from BLOCK DATA)
- **Line 7**—the conversion factors to transform from English units to SI units for the variable on the vertical axis (from BLOCK DATA)
- **Line 8**—the number of data points in the horizontal direction, the lower and upper limits of that variable in English units (from the input data to DRIVER), and the initial value of that parameter (from the input data for the HPDM)
- **Line 9**—the number of data points in the vertical direction and the lower and upper limits of that variable in English units (from the input data to DRIVER) and the initial value of that parameter (from the input data for the HPDM)
- **Lines 10 and 11**—the initial component configuration (from the input data for the HPDM), i.e., the indoor and outdoor air flow rates, the compressor displacement, the frontal areas of the two heat exchangers, the specified condenser subcoolings for refrigerant flow control in cooling and heating modes, the number of parallel refrigerant circuits for each coil, the number of tube rows in each heat exchanger
- **Line 12**—the HSPF, CSPF, APF, and annual resistance heat requirements at the initial configuration

The header block is followed by several lines that describe what data are stored in the remainder of the file. One line gives the number of dependent variables that are stored for each point in the rectangular mesh. In the example in Exhibit 7.1, this number is 5. This line is followed with data giving the number of letters in the title for each derived variable and the title for each variable. This information is specified as part of the driving program, and DRIVER must be modified to change it. Several blocks of data follow that contain the information necessary to draw the contours.

7.5 DATA BLOCKS FOR CONTOURS

The "data descriptor" (ID header) block is followed by several blocks of data for the contours. Each of these is preceded by a line of data with the value of the horizontal coordinate and the values of the vertical coordinates (e.g., a single indoor air flow rate and each of the outdoor air flow rates in Fig. 7.7). In the case shown in Exhibit 7.1, the remainder of these blocks consists of

- APFs at each combination of the fixed horizontal coordinate and the set of vertical coordinates
- Corresponding heating season performance factors (HSPFs)
- Corresponding cooling season performance factors (CSPFs)
- Annual power consumption for supplemental resistance heat
- Cooling capacity at 35°C (95°F)

Selection of data for use in the contour plots is arbitrary, of course, and other users will undoubtedly change this list to better meet their own needs. Common blocks have been set up throughout the APF and steady-state models to bring these data back to the main program where they can be saved for later processing.

7.6 CONTOUR PLOTTING

The contour plotting programs included in the Design Tool Package were not developed at ORNL. In fact, we do not even know their complete history. Sometime in the unknown past they resided at the Naval Ocean System Center (NOSC) in San Diego, California. By one means or another they came to Oak Ridge and were incorporated in a plotting package named GENCON. The only known changes between GENCON and the NOSC versions pertained to replacing CALCOMP plotting calls with calls to the DISSPLA package. These changes were made by B. A. Clark of Union Carbide Corporation, Nuclear Division, prior to our use of GENCON.

GENCON was selected for our own purposes in 1980 because it could handle arbitrarily spaced data that were of interest to us at that time. There were, and are, other routines that do as well or better than GENCON, but this was the only one that could handle our data at that time. We modified GENCON as needs arose and renamed only to avoid confusion for users of the unmodified code at ORNL. This program is still essentially the result of development by other people.

Figure 7.8 shows the hierarchy of subroutine calls in CONPLT. All the names enclosed in solid rectangles are DISSPLA graphics routines that are described in Appendix G. Each of these "blocks" has a specific purpose, which appears in parentheses beneath it. The specific purpose may be just setting internal parameters or it may be drawing and labeling curves. The remaining twelve routines are described below.

7.6.1 The Routine CONPLT

CONPLT itself serves primarily as a driving routine for CONTUR. INDATA is called to read all the input data saved by DRIVER, and a number of graphics routines are called to assign parameter values for the plots (e.g., page dimensions, orientation of numbers labeling the vertical axis, character sets). CONTUR is then called for each of the dependent data sets (e.g., APF, HSPF, design cooling capacity) provided in the input data that are to be plotted.

7.6.2 The Routine BLOCK DATA

BLOCK DATA is used to assign initial values to a number of plotting parameters. These include such things as the dimensions of the page for each plot, the character height for labels, the lengths of the axes, and the position of the origin of the plot with respect to the lower left corner of the page. All of these values are specified in inches.

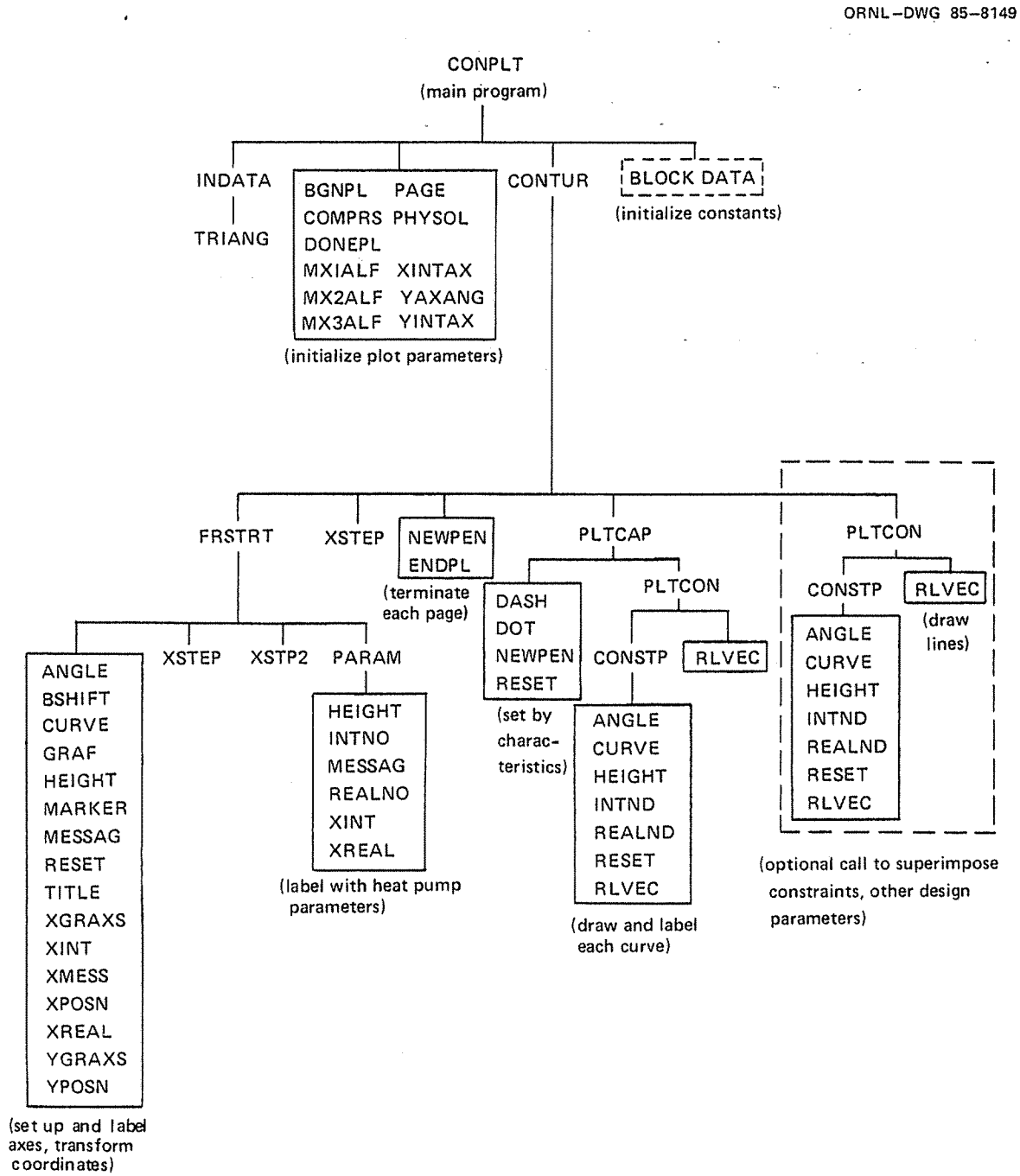

Fig. 7.8. Hierarchy of subroutine calls in contour plotting package CONPLT.

7.6.3 The Routine FRSTRT

FRSTRT sets up the axes for the plot, in both English and SI units, and separately labels the plot with the heat pump design configuration at the base point. These data, which are essentially the major input data to the steady-state heat pump model, include such things as the heat exchanger frontal areas, number of tube rows and refrigerant circuits, and the compressor displacement. Two of these independent variables will be used for the X and Y axes of the contour plots, with the remaining variables held fixed. XSTEP and XSTP2 are called to establish limits for the English and SI axes, respectively, that span all the data values and also provide a convenient step size along the axes.

7.6.4 The Routines XSTEP and XSTP2

These two routines are set up to find convenient limits and step lengths for the axes on the plot; they are essentially the same. (These are set up so the axis limits will be powers of 10 times 1.0, 2.0, 2.5, or 5.0.) The argument list for XSTEP includes the array of independent parameters for that particular axis. XSTEP scans this array to find the highest and lowest values and then works with those. The parameter list for XSTP2 includes the known upper and lower limits for the SI axis (these are known from the transformed limits of the English unit axes).

Both of these subroutines are designed to find a lower bound that is less than the minimum data point to be plotted along that axis and an upper bound that exceeds the highest one. They do this in such a way that there are not too many (more than 7) or too few (less than 3) labeled tick marks on the axis. The step size for the axis is computed to be powers of 10 times 1.0, 2.0, 2.5, or 5.0.

XSTEP is also called from CONTUR to get round numbers for the contour levels.

7.6.5 The Routine PARAM

PARAM is described fairly well in the preceding description of FRSTRT. It labels each plot with most of the data for the heat pump design model (an identifying design configuration). Although not an essential function, it is a convenient feature when plots are saved for future reference or when a number of different heat pumps are being analyzed.

7.6.6 The Routine PLTCAP

PLTCAP is little more than a driving routine for the two subroutines PLTCON and CONSTP that were written at the NOSC. We wrote it to enhance the appearance of the contour plots available from the original GENCON package. Major contour lines are drawn with thick solid lines. Intermediate contours, halfway between the major levels, are drawn with lighter, dashed lines. Minor divisions are drawn with light dotted lines if there are not more than 30 contour levels on the plot. These are left out if there are more than 30 contour levels.

7.6.7 The Routine TRIANG

Although TRIANG is pictured as one of the first routines on Fig. 7.8, it is described here because it works so closely with PLTCON and CONSTP. TRIANG is used to generate a mesh of triangular elements from the rectangular grid of points represented by the two independent variables in the input data set. This "triangulation" is essential to the processes described in PLTCON and CONSTP because interpolations in the dependent variables are performed to compute where each contour line crosses each mesh element. Because this triangulation is completely transparent to the user, it is not necessary to understand it to use or even to modify CONPLT.

TRIANG is one of the few routines from the original GENCON package that has been extensively modified (in fact it was replaced altogether). We experienced some difficulty with the original version of TRIANG; when we no longer needed the capability of plotting arbitrarily spaced data, we wrote our own triangulation routine.

CONPLT requires data on a uniform, rectangular grid. The number of points in the grid, NXY, is the product of the number of points in the horizontal direction, NX, and the number in the vertical direction, NY. Figure 7.9 shows a sample grid and the corresponding triangulation for five points in the horizontal direction and four points in the vertical direction. Each grid point is identified by a small number just to the left of it and each triangular mesh element by a larger number in the center of the triangle. Nodes of the grid are numbered from the bottom to the top of the mesh and from left to right, the same order in which the data are read by INDATA. The triangular mesh elements are numbered from left to right and from bottom to top.

TRIANG communicates information to CONSTP and PLTCON through the array ITRI. The elements of ITRI identify the vertices of each mesh element and the indices of each adjacent mesh element. For each mesh element JTRI, ITRI(1,JTRI), ITRI(2,JTRI), and ITRI(3,JTRI) contain the indices of the vertices of mesh element JTRI. In Fig. 7.9, ITRI(1,12), ITRI(2,12), and ITRI(3,12) represent the vertices of triangular element 12

ORNL-DWG 85-8138

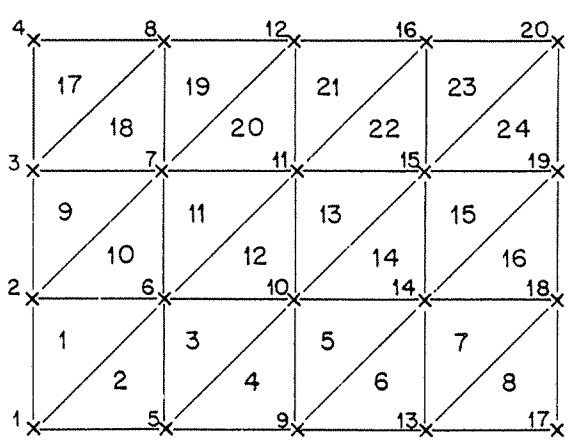

Fig. 7.9. Identification of nodes and mesh elements in triangulation of input data for contour plots.

with the grid nodes 6, 10, and 11, respectively. The next three elements of ITRI are used to identify the mesh elements that share vertices, or edges, with element JTRI. ITRI(4,JTRI) is set to the index of the only other triangular mesh element that has ITRI(1,JTRI) and ITRI(2,JTRI) as two of its vertices. In the preceding example, the two vertices are grid nodes 6 and 10 and the mesh element is 3; therefore, ITRI(4,12)=3. ITRI(5,JTRI) and ITRI(6,JTRI) are assigned in a similar fashion. ITRI(5,JTRI) points to the mesh element that shares the vertices identified by ITRI(2,JTRI) and ITRI(3,JTRI). ITRI(6,JTRI) points to the mesh element that shares vertices ITRI(3,JTRI) and ITRI(1,JTRI). Any of these three values is set to 0 if the corresponding vertices are on the boundary of the plotting area (i.e., if there is not another mesh element with those vertices).

A final element of this array, ITRI(7,JTRI), is used as a flag when tracing each contour level. It is initally set to 0 for every element in the mesh when each contour level is drawn. It is reset to 1 as that mesh element is examined to see whether the current contour level, or line, passes through that mesh element.

The first dimension of ITRI is always set to 7. The second dimension corresponds to the maximum number of triangular mesh elements that can be handled by CONPLT. This has been set at 500 and should be large enough for almost all cases. The number must be at least $2 \times (NX - 1)(NY - 1)$, which is the actual number of mesh elements in the triangularization.

7.6.8 The Routines PLTCON and CONSTP

These two subroutines are the heart of the contour plotting package. PLTCON examines each contour level in turn and finds a mesh element that is crossed by the corresponding contour line. CONSTP starts with the mesh element identified by PLTCON and traces the contour until it either reaches a boundary element or closes on itself. CONSTP interpolates between the coordinates of the vertices of the mesh elements that the contour line crosses. It stores these interpolated coordinates in work space arrays, XW and YW, until it reaches the end of the contour or the workspaces are filled. At that point it draws and labels the curve defined by the interpolated coordinates. PLTCON and CONSTP communicate with each other using the seventh element of ITRI to identify which mesh elements have been examined to see whether the contour line passes through them.

7.7 OPTIONAL CALL TO PLTCON

A dashed box on the right side of Fig. 7.9 surrounding an additional call to PLTCON shows that PLTCON can be used to overlay contours of a different dependent variable on top of the plot drawn by PLTCAP. The plot of APF and design cooling capacity shown in Fig. 7.6 is an example of this. In that case, PLTCON was called with an array of design cooling capacities and a set of contour values that included 7.3, 7.6, 7.9, 8.2, and 8.5 kW (25,000, 26,000, 27,000, 28,000, and 29,000 Btu/h).

The listing of CONPLT in Appendix N does not include this optional call to PLTCON. The user needs to exercise some care and discretion in superimposing one set of

contours on another. It is very easy to put so much on the same graph that none of it can be read. We prefer to either plot separate graphs for each variable specified in the input data or to superimpose just a single curve representing some desired fixed design condition [e.g., design cooling capacity at 35°C (95°F)] on the other calculated quantities.

7.8 CONCLUSION

Contour plots can be generated by the computer with relatively little effort. These are very useful in investigating the dependence of one, two, and possibly more dependent quantities on simultaneous changes in two independent variables.

8. NUMERICAL OPTIMIZATION OF HEAT PUMP DESIGN

8.1 INTRODUCTION

The term "optimization" can mean many things; in our applications, and all that is dealt with here, we refer to a particular category, nonlinear optimization with nonlinear constraints. In general terms that means:

> minimize $f(\mathbf{X})$ where $\mathbf{X}$ is a vector with N elements subject to the M constraints, $C(\mathbf{X})$, which can be either equalities, inequalities, or lower and upper bounds,
>
> $$C_j(\mathbf{X}) = 0 \qquad 1 \leqslant j \leqslant NEQ\,,$$
>
> $$C_{j+NEQ}(\mathbf{X}) \geqslant 0 \qquad 1 \leqslant j \leqslant NINEQ\,, \tag{8.1}$$
>
> $$1_j \leqslant C_{j+NEQ+NINEQ}(\mathbf{X}) \leqslant U_j \qquad 1 \leqslant j \leqslant NRANGE\,,$$
>
> where $M = NEQ + NINEQ + NRANGE$ and $a_i \leqslant x_i \leqslant b_i$ for $1 \leqslant i \leqslant N$.

The objective function f can be a nonlinear function of N independent variables x_i, $1 \leqslant i \leqslant N$. The goal is to find the values of the x_i that give the lowest possible value of $f(\mathbf{X})$ while still satisfying the M nonlinear constraining functions, $C_j(\mathbf{X})$, $1 \leqslant j \leqslant M$.

A few observations should be drawn to avoid confusion later on.

- A function $f(\mathbf{X})$ can be maximized by finding the minimum of $F(\mathbf{X}) = -f(\mathbf{X})$.
- Nonzero equality constraints $c_j(\mathbf{X}) = z_j$ [and inequalities $c_j(\mathbf{X}) \geqslant z_j$] can be handled by imposing $k_j(\mathbf{X}) = c_j(\mathbf{X}) - z_j = 0$ [$k_j(\mathbf{X}) = c_j(\mathbf{X}) - z_j \geqslant 0$]
- Upper limits can be imposed on inequalities $c_j(\mathbf{X}) \leqslant z_j$, by setting the constraint to $k_j(\mathbf{X}) = z_j - c_j(\mathbf{X}) \geqslant 0$.

The original problem, then, is perhaps more general than it might appear at first glance. Strict inequalities, such as $c_j(\mathbf{X}) > 0$, cannot be handled by the software we have used. The mathematical reasons for this are beyond the realm of this discussion.

It might be helpful to pose a specific example of an optimization problem instead of leaving it with a mathematical definition. The following example is from our own line of work:

> Find the compressor displacement and the indoor and outdoor air flow rates that (1) give the highest heat pump steady-state COP at 8.3°C (47°F), (2) also provide 7.0 kW (24,000 Btu/h) of cooling at 35°C (95°F) ambient temperature, and (3) have a supply air temperature at −3.3°C (26°F) ambient temperature that is at least 32°C (90°F) in the heating mode.

In this case the objective function could be:

f(displacement, indoor air flow, outdoor air flow) $= -$COP .

Other functions are possible, and in fact may be preferable, as discussed in Sect. 8.6. In this case, however, finding the minimum of f will correspond to the largest COP at 8.3°C (47°F). If the displacement and air flows are identified with the elements of a vector **X**, the two constraints could be written as:

$$c_1(\mathbf{X}) = \dot{Q}_{ss,35}(\mathbf{X}) - 7.0 = 0 \tag{8.2}$$

and

$$c_2(\mathbf{X}) = T_{supply,-3}(\mathbf{X}) - 32 \geqslant 0 ,$$

where $\dot{Q}_{ss,35}$ and $T_{supply,-3}$ are the cooling capacity at 35°C (95°F) and the heating mode supply air temperature at -3.3°C (26°F), respectively. Although it has not been stated explicitly in this example, it might be worthwhile to set upper and lower limits on the air flow rates. The two constraints may or may not be sufficient to keep all the variables within desirable limits. All of our work has included user-supplied limits on the permissible ranges for the independent variables.

8.2 UNCONSTRAINED VS CONSTRAINED OPTIMIZATION

Historically, unconstrained optimization has been around since the inception of calculus, and a broad body of mathematical literature and theory has been developed on the subject. Imposing constraints, however, has always generated problems. These constraints were pretty much avoided until the advent of digital computers. The high computational speed of computers made it practical to solve a sequence of unconstrained problems $\{g^k(\mathbf{X})\}_{k=1}^{\infty}$, whose solutions $\mathbf{X}^k$ converge to the solution of the constrained problem:

For each k, $\mathbf{X}^k$ is a vector of N elements that minimizes $g^k(x)$, and if

$$\lim_{k\to\infty} \mathbf{X}_i^k = \mathbf{X}_i^* , \qquad \text{for } 1 \leqslant i \leqslant N ,$$

then $\mathbf{X}^* = (x_1^*, x_2^*, \ldots, x_n^*)$ is the minimum of $f(\mathbf{X})$, and $c_j(\mathbf{X}^*)$ is satisfied for each constraining function, $1 \leqslant j \leqslant M$.

Constrained problems could thus be solved by solving a series of unconstrained problems.

8.3 SEQUENTIAL AUGMENTED LAGRANGIANS

There are a number of ways to combine the objective function and the constraints to get a sequence of unconstrained problems that can be used. Some of these have better

computational properties than others. One approach is to use a sequence of quadratic penalty functions as shown in Eq. 8.3.

$$g^k(\mathbf{X}) = f(\mathbf{X}) + \rho^k \sum_{j=1}^{m} c_j(\mathbf{X})\ c_j(\mathbf{X}) \ . \tag{8.3}$$

It can be shown that for a sufficiently large ρ^k, the minimum of $g^k(\mathbf{X})$ coincides with the constrained minimum of $f(\mathbf{X})$. Unfortunately, as ρ^k increases, the stability of the algorithms used to solve for $\mathbf{X}$ decreases. This sequence of unconstrained problems leads to solving systems of equations that are nearly linearly dependent. These are unstable numerically and cannot be solved economically.

An alternative to the penalty function approach is to use a sequence of augmented Lagrangians as shown in Eq. 8.4.

$$g^k(\mathbf{X}) = f(\mathbf{X}) - \sum_{j=1}^{m} \lambda_j c_j(\mathbf{X}) + \rho^k \sum_{j=1}^{m} c_j(\mathbf{X})\ c_j(\mathbf{X}) \ . \tag{8.4}$$

The λ_j, called Lagrange multipliers, are selected in a manner that improves the stability of the solution algorithms. The software packages that we have used are based on solving the sequence $\{g^k(\mathbf{K})\}$ of augmented Lagrangians.

One difficulty with using an algorithm that relies on solving a sequence of unconstrained problems is in determining when to call a halt to the computations. Some programs use a liberal bias and stop earlier than others. In so doing they may save on computer time but miss the solution. Other algorithms are very conservative and seem determined to search for the precise solution regardless of cost.

Our own experiences are with some of the latter routines. We constrain the computer run by the maximum length of CPU time it can use and the maximum number of times it is allowed to evaluate the objective function. We print out the values of the objective function, the constraints, and the augmented Lagrangian each time they are computed. If the optimization is stopped in the middle because of the limit on CPU time or function evaluations, we may choose to restart it. If the optimization seems to be making good progress, we will use the best point from one computer run as the starting point for the next one. If there is no discernable progress, we may decide to halt the whole process. In this event, we generally use contour plots of our original objective function with the constraints superimposed on them to ascertain if we are sufficiently close to the optimum values for the design variables. Contour plots can be used to check the progress of the optimization process, and in fact sometimes they indicate that a likely solution is actually far removed from the minimum. In those instances the problem needs to be adjusted in order to converge to a true solution.

8.4 GRADIENTS

At each combination of the independent variables $\mathbf{X}$, the gradient of the augmented objective function $\nabla g^k(\mathbf{X})$ is a vector that points in the direction of greatest increase in g^k.

Changing the values of x_i so that **X** lies on the vector $\nabla g^k(\mathbf{X})$ will result in increasing values of $g^k(\mathbf{X})$, at least when **X** is fairly close to the initial point **X**. Changing the components x_i so they lie on $-\nabla g^k(\mathbf{X})$ will result in decreasing values of $g^k(\mathbf{X})$.

Many optimization routines rely on the use of gradients to select these "search directions" that determine how to alter the independent variables simultaneously and reduce the objective function, $g(\mathbf{X})$. Some of these routines require the user to supply a subroutine that computes the gradient of the objective function analytically. We considered these overly demanding for our heat pump analysis and did not use them. Although this approach would have required less computer time than some of the alternatives, we would have had to write the partial derivatives of the annual performance of a heat pump, for example, as an explicit function of the compressor displacement, refrigerant tube rows, etc.

The route we chose uses a numerical approximation to the gradient using difference formulas. Either a forward difference is used, as in Eq. 8.5, or a central difference as in Eq. 8.6.

$$\frac{\partial g^k}{\partial x_i}\Big|_{\mathbf{X}=\mathbf{X}^*} = \frac{g^k(\mathbf{X}^* + \delta\epsilon_i) - g^k(\mathbf{X}^*)}{\delta} , \tag{8.5}$$

$$\frac{\partial g^k}{\partial x_i}\Big|_{\mathbf{X}=\mathbf{X}^*} = \frac{g^k(\mathbf{X}^* + \delta\epsilon_i) - 2g^k(\mathbf{X}^*) + g^k(\mathbf{X}^* - \delta\epsilon_i)}{2\delta} . \tag{8.6}$$

Both of these approximations are derived from Taylor's theorem, and either one is useful, particularly when the partial derivatives cannot be expressed directly as a function of the x_i.

The software package designed to do this is set up to use the square root of the computer's machine precision for the gradient step or perturbation δ in Eqs. 8.5 and 8.6. This may be fine in many problems, but in our heat pump analysis and many types of engineering problems this caused the terms in the numerators to differ by less than the accuracy of the objective function. (This is the consequence of the iterative processes in the steady-state calculations and does not even involve the true accuracies of the programs.) Consequently, we obtained numerical noise in the numerator and a completely inaccurate approximation (zero significant digits).

This problem was circumvented by replacing the library subroutine X02AAF, which computes the step size δ, X02AAF. The replacement routine sets the step size for each component of the gradient based on the permissible range for the corresponding independent variable. As described later, we specify ranges for each design variable, an upper and a lower limit:

$$a_i \leqslant x_i \leqslant b_i .$$

Then δ is set to be 10% of the distance from x_i to the furthest end point of the range as shown in Eq. 8.7.

$$\delta = \max\left\{\frac{x_i - a_i}{10}, \frac{b_i - x_i}{10}\right\} . \tag{8.7}$$

This seems to give us sufficient accuracy in the gradient calculations if the problem is well scaled (as explained later).

8.5 MINIMIZATION ALONG A SEARCH DIRECTION

As mentioned earlier, the optimization routine computes the gradient of the augmented Lagrangian in order to establish a search direction (the negative of the gradient). It then varies all the design variables simultaneously to move along this vector. The optimization in N independent variables has thus become a subproblem of minimizing a function of just one variable, the distance in the search direction from the initial point (see Fig. 8.1).

This minimization in a single variable can be solved using bisection methods or with the more sophisticated root-solving algorithms. The routine in the package we use employs a quasi-Newton algorithm to find this minimum in one dimension. It is based on a numerical approximation to the derivative df/dt, where t is the parameterizing variable (the distance in the search direction).

This one-dimensional subproblem raises questions that need to be addressed. The gradient at best reflects the behavior of the objective function (or the augmented function)

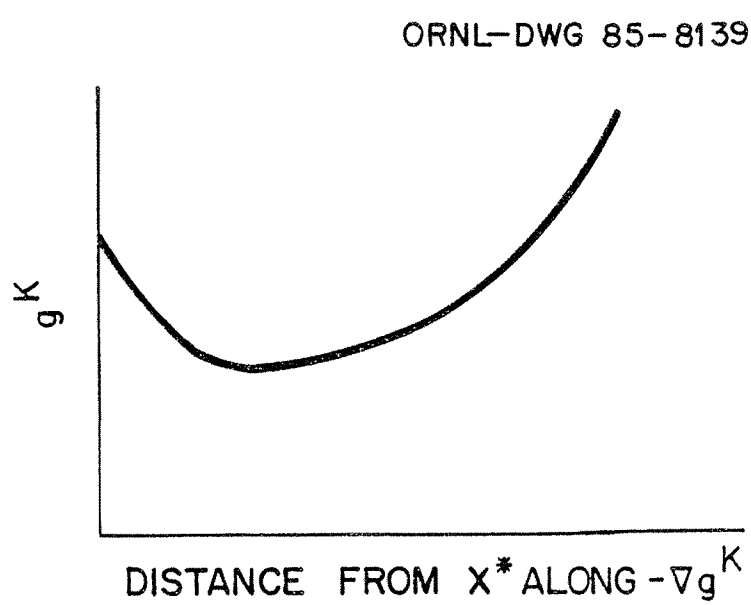

Fig. 8.1. Graph showing a minimum of a function of a single variable.

close to the initial point X. How far do you allow the optimization routine to move in the search direction before recomputing the gradient? Also, how carefully do you solve for the minimum along this line since it may be only one of many iterations in solving one of the augmented functions? Do you try to save time by taking big steps in the search direction and risk overshooting the solution?

Most gradient-based searches either expect the user to supply answers to these questions or they answer them for you. An iteration that is going on intolerably long may be trying to solve each subproblem to too great an accuracy. A solution that gets into trouble with unacceptably large (or small) parameters may be allowing too large a step in the search direction.

8.6 SCALING

The objective function can be poorly scaled in a number of ways. Problems can occur that relate to the sensitivity of the objective function with respect to each of the independent variables, as well as problems that relate to the relative magnitudes of the objective function and the constraints.

8.6.1 Objective Functions and Independent Variables

Figure 8.2 is a contour plot of a well-scaled objective function with just two independent variables. The contour levels are nearly elliptical without a great difference between the lengths of the major and minor axes. The search direction from any pair of x_1 and x_2 will point more or less toward the center of the ellipses.

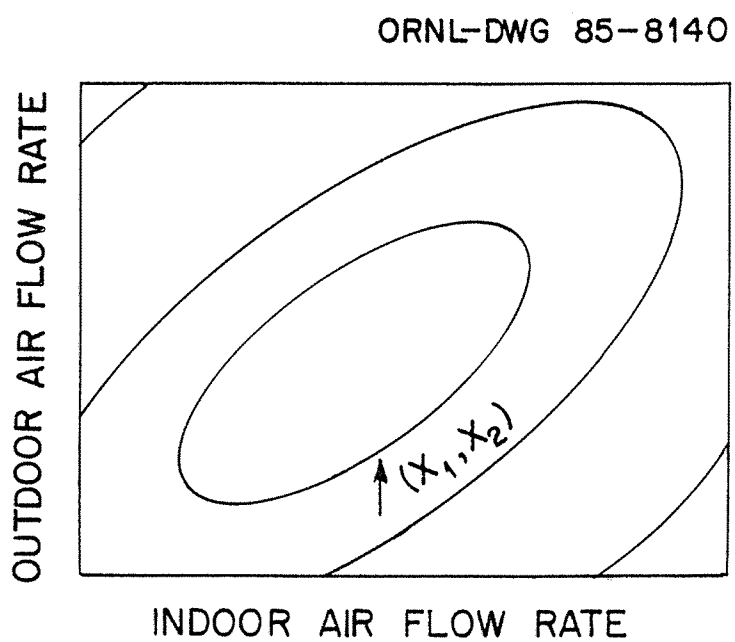

Fig. 8.2. Sample contour plot of a well-scaled function.

Figure 8.3 is a contour plot of a poorly scaled objective function. Although the function has nearly elliptical contour levels, as in the well-scaled example, the major and minor axes of the ellipses differ substantially. There is essentially a deep, narrow valley in the objective function. The search direction will be practically perpendicular to the major axes, and the optimization program will spend a lot of time trying to find the lowest point in that direction (it will need to use very small steps to avoid overshooting the minimum and ending up on the other side). There may never be any movement along the major axis, and the actual optimum point may not be found.

Ideally, a "unit" step in each coordinate direction should produce approximately the same magnitude of change in the objective function. We tried to achieve this end through scaling of the independent variables. Mathematically it is convenient for the optimization package to restrict the independent variables to the range $-1 \leqslant x_i < 1$. We used a simple linear transformation to accomplish this. If the original design variable is limited so that $a_i \leqslant x_i \leqslant b_i$, then the transformed variable is computed by Eq. 8.8.

$$Z_i = \frac{2X_i - a_i - b_i}{b_i - a_i} \quad . \tag{8.8}$$

The optimization was thus performed using the transformed variables. The intervals $[a_i,b_i]$ are then adjusted to give well-behaved contours.

In one sense the intervals are set to restrict the design variables to reasonable values. They are also set so that a unit change in each independent, transformed variable has approximately an equal effect on the objective function. Adding or subtracting 0.1 to or from any z_i (where $-1 \leqslant z_i \leqslant 1$) is equivalent to adding or subtracting $(b_i - a_i)/10$ to or

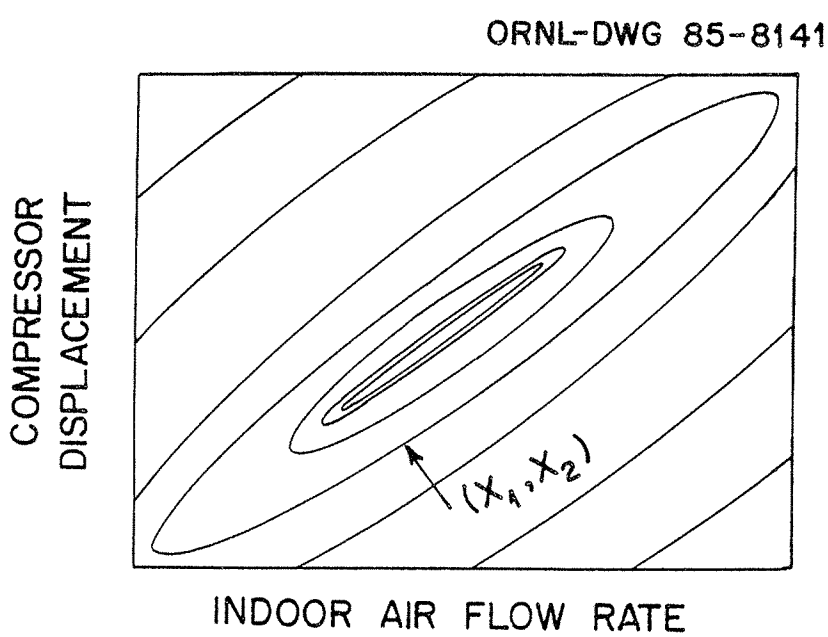

Fig. 8.3. Sample contour plot of a poorly scaled function.

from x_i. If an optimization seems overly sensitive to changes in the compressor displacement, for instance, and does not alter the air flow appreciably, we might cut down the range of the displacement or broaden the ranges for the air flows. This amounts to compressing or stretching one of the axes in Fig. 8.3 and getting a better behaved function. That transformation does not guarantee that everything gets better, but it usually improves the optimization process and we see some progress in the objective function, with changes in most of the parameters.

8.6.2 Objective Functions and Constraints

Not only do the design variables need to be scaled with respect to each other, but the objective function and the constraints need to be balanced. If a constraint is much smaller than the objective function, the solutions for the first several augmented Lagrangians may wander far from the desired (constrained) design. The problem will eventually be forced back to the constraint (as ρ^k is made progressively larger), but a lot of computer time is wasted in the process. Conversely, if the values of the constraint are too large with respect to the objective function, the solution may converge very slowly. Figure 8.4 shows a contour plot of an arbitrary objective function with a single constraining curve superimposed on it. The true constrained minimum in this case occurs at (x_1^*, x_2^*), the point at which the constraining curve is tangent to the contours of the objective function. If the constraint is not too small with respect to the objective function, the optimization will move quickly from an arbitrary initial point P_1 to a feasible point P_2 (one that lies on the constraint). However, if the constraint is too demanding, the optimization may have to use extremely small steps to move along the curving constraint, from P_2 to P_3 to P_4, etc., toward the true minimum. This iteration would move more quickly with a less demanding, smaller constraint because the iterations could lie near the curved line and not necessarily right on it.

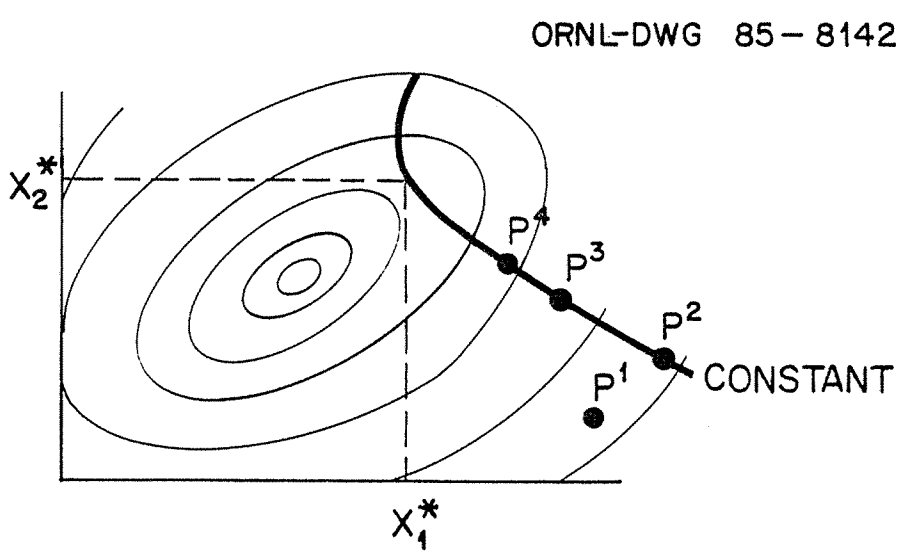

Fig. 8.4. Example of a contour plot with a superimposed constraint line.

There are two things to watch for relative to the scaling of the constraint. A lot of computer time may be used trying to track right along the constraint. Progress of the iterations can be so slow that the user thinks the process is close to the solution and that any further refinements are unnecessary. The solution could in fact be quite removed from what the user decides is close enough. If progress is agonizingly slow, the user may wish to check what is going on with contour plots.

Our scaling of objective functions and constraints has been fairly arbitrary. The optimization of APFs, for example, used an objective function of the form in Eq. 8.9 and a single constraint like Eq. 8.10,

$$f(\mathrm{X}) = a(APF(\mathrm{X}) - APF_0) \ , \tag{8.9}$$

$$C(\mathrm{X}) = b[\dot{Q}_{35}(\mathrm{X}) - \dot{Q}_{\mathrm{design},35}]/\dot{Q}_{\mathrm{design},35} \ , \tag{8.10}$$

where APF_0 is some representative performance factor, $\dot{Q}_{\mathrm{design},35}$ is the desired design capacity, and a and b are multiplicative constants.

The values of a, b, and APF_0 were all adjusted in either of two ways. The first was to manually adjust the value as part of the "manual" iteration of computer runs. If a job was working fairly well, no adjustments were made. If it seemed to be wandering too far from the constraint, a would be decreased or b would be increased. An alternative to these ad hoc adjustments was to examine the gradients of the objective function and the augmented Lagrangian. This led to the development of a program (independent of the optimization process itself) to evaluate the gradients of the proposed objective functions.

8.7 THE MAIN PROGRAM GRADIE

It can be very helpful to know what the most important variables are in an optimization problem before starting out to solve it. More often than not, engineering judgment and experience will indicate what the major variables should be, but this may not be the case after the scaling transformations and constraints are applied. Scaling may cause variables that should be important to be completely swamped by one or two others because of the way the initial variable ranges were chosen. Our own experience, for example, has been that the compressor displacement will dominate all of the other heat pump variables if the capacity is constrained unless we are careful about the scaling.

A main program named GRADIE was developed to approximate the gradient of the objective function and the augmented Lagrangian. This requires that the user provide some initial values and ranges for the independent variables and some multipliers as in Eqs. 8.9 and 8.10. This program uses FUNCT1 (as described in Chap. 6) to compute the objective function and a subroutine named CON1 to compute the values of the constraints. Examples of these routines are given in Appendix O.

GRADIE uses the central difference formula of Eq. 8.6 to compute each component of the gradient of the objective function and of the augmented Lagrangian. This process involves evaluating the objective function and the constraints at the initial point and after a positive and a negative perturbation in each coordinate direction. The Lagrange multipliers, λ_j^k, in Eq. 8.6 should be set to 0 unless the user has some knowledge of what they should be. Some optimization routines print out estimates of these during the course of their analysis, so these numbers may be available for some "mid-stream" adjustments to the scaling. The value of ρ^k should be small, and positive, unless good estimates of the Lagrange multipliers are used (in which case corresponding values of ρ^k are also available from the optimization program).

GRADIE prints out a short table showing the components of each gradient and also the numbers that went into computing them (the numerators and denominators). Users should watch that the numerators in Eq. 8.6 do not drop to meaningless levels. If they do, the corresponding range for that variable should be broadened to get a greater change between the function value at the initial point and at the perturbed point.

The user can check the table printed by GRADIE and see that the most important variables (in an engineering sense) do in fact have the larger values in the gradient (either positive or negative). It may be necessary to adjust the scaling if there is too great a difference in the magnitudes of these components. Variables with very small or insignificant components in the gradient may be dropped, at least from the early analysis, to reduce computational time or even selected separately from contour plots.

Although GRADIE is independent of any particular optimization package and is not used by them, it can be a useful tool in setting up a problem. It helps in judging the scaling of the independent parameters as well as in assessing the balance between the constraints and the objective function. Source code is provided in Appendix O so users can modify it and substitute different algorithms for incorporating the constraints or approximating the gradients.

8.8 UNFINISHED BUSINESS

A few questions come to mind that have not yet been addressed. First, how does one work with variables that can take on only a few fixed, discrete values? This could be something like the number of rows of refrigerant tubes in a heat exchanger or the displacement of a compressor that is available in predetermined sizes. Special optimization programs are available that are designed to handle only discrete variables; however, we do not have experience with any of these. An alternative approach is to assume a continuum of values for the discrete variables and then select the best, closest available value after optimizing the design. We have used the latter approach with no problems and are satisfied with the results we have achieved.

Second, how does one know if the optimization routine found the absolute minimum of the function? The answer to this is not very reassuring. Mathematically there is no way to guarantee that the program found the absolute minimum of a general, nonlinear function. Contour plots can be used to see if there are any "hills" that keep the search algorithms from finding a better point, or optimizations can be run from widely varying initial points to see if there are any other "local" minima. Generally, these two checks are enough to instill confidence in the results, but there is no guarantee that the point found is the best.

9. CHANGES TO THE STEADY-STATE DESIGN MODEL SINCE ORNL/CON-80

A number of changes have been made to the steady-state heat pump design model since it was documented in ORNL/CON-80 in 1981. A few minor modifications were made to correct small errors that had been discovered in the code. The major computational changes related to unnecessary iterations in the compressor submodels, repetitious calculations of refrigerant properties, and calculation of the contact conductance between the fins and the tubes in the heat exchangers.

In the original version of the heat pump model, initial estimates were made for saturation temperatures and exit low-side superheat at the heat exchangers. The compressor subroutine then evaluated the conditions at the compressor inlet and exit iteratively using guesses for the refrigerant mass flow rate to calculate pressure and temperature changes in the connecting refrigerant lines. These iterations were found to be costly in computational time. In the revised version, the computations start at the compressor shell inlet and exit and proceed outward to the heat exchangers. Next, starting guesses are made for shell inlet and exit saturation temperatures, and the compressor inlet superheat value is specified. An estimate of the refrigerant mass flow rate is no longer needed. The required evaporator exit superheat is computed in the compressor model and passed to the evaporator and TXV routines for use as in the previous documentation. These changes are reflected in new input data description sheets found in Appendix P.

A change was made in the refrigerant properties routines to speed up the model. Subroutines TSAT and SPVOL were modified to avoid iterative recalculation of values if the subroutine arguments were unchanged from the previous call. These changes reduce overall computational time by 30 to 40%. The changes involve the addition of a separate BLOCK DATA for each subroutine to initialize some parameters and ensure that internal parameters are saved from one call of the subroutine to the next. The use of multiple BLOCK DATA subroutines could cause problems on some computer systems; these may need to be consolidated with the main BLOCK DATA for the program.

For validation purposes, a change was made that allows measured fan power values to be specified directly rather than being calculated. This is particularly useful if one is mainly concentrating on validating the heat exchanger and compressor models and wants to look at the fan power predictions separately or not at all.

One significant engineering calculation change was made in revisions to the contact conductance calculations. First, heat transfer resistance equations in the heat exchanger models were changed to apply the contact conductance resistance along the entire length of the tube (collared fins) rather than just at the point of contact of a fin (uncollared fins). Next, rather than have the user specify contact conductance values (which are somewhat nebulous quantities at best), an algorithm to calculate them was built into the program. The user can now either use the computed value directly or a specified multiple of it. The correlation is a function of fin thickness, fin spacing, and the tube outside diameter.[9] For a wet coil, the contact conductance is increased by a factor of 1.33, as suggested in ref. 9.

The other significant engineering change was in the capillary tube model. The capillary tube correlations were extended to handle two-phase refrigerant at the tube inlet. The

equations for this were obtained from an empirical fit to capillary tube flow factor curves in the *ASHRAE Equipment Handbook.*[10]

Remaining changes are in the areas of evaporator superheat iterations and revised output formats. The iteration logic in subroutine EVAPR concerning the convergence to a specified superheat was redone to minimize convergence difficulties that have plagued this routine. Next, WRITE statements and formats were changed throughout the program to make the output more useful and understandable.

The organization of the input data was also changed to group information in a more logical order. The input data under the new format are described in Appendix P.

REFERENCES

1. R. D. Ellison and F. A. Creswick, *A Computer Simulation of Steady-State Performance of Air-to-Air Heat Pumps*, ORNL/CON-16, Oak Ridge National Laboratory, March 1978.

2. R. D. Ellison et al., "Heat Pump Modeling: A Progress Report," *Proceedings of the Fourth Annual Heat Pump Technology Conference, Oklahoma State University, Stillwater, Oklahoma, April 9–10, 1979*, Oklahoma State University, 1979.

3. S. K. Fischer and C. K. Rice, *A Steady-State Computer Design Model for Air-to-Air Heat Pumps*, ORNL/CON-80, Oak Ridge National Laboratory, December 1981.

4. S. K. Fischer and C. K. Rice, *The Oak Ridge Heat Pump Models: I. A Steady-State Computer Design Model for Air-to-Air Heat Pumps*, ORNL/CON-80/R1, Oak Ridge National Laboratory, August 1983.

5. C. K. Rice et al., *Design Optimization and the Limits of Steady-State Heating Efficiency for Conventional Single-Speed Air-Source Heat Pumps*, ORNL/CON-63, Oak Ridge National Laboratory, October 1981.

6. S. K. Fischer and C. K. Rice, "System Design Optimization and Design Validation for Single-Speed Heat Pumps," *ASHRAE Trans.* **91**(2a and b), 509–522 (1985).

7. S. K. Fischer and C. K. Rice, "Computer-Aided Heat Pump Design and Optimization," *Proceedings of the DOE Heat Pump Contractors' Program Integration Meeting*, CONF-810672, March 1982.

8. C. K. Rice and S. K. Fischer, "A Comparative Analysis of Single- and Continuously Variable-Capacity Heat Pump Concepts," pp. 57–65, *Proceedings of the DOE/ORNL Heat Pump Conference: Research and Development on Heat Pumps for Space Conditioning Applications, Washington, D.C., Dec. 11–13, 1984*, CONF-841231, Oak Ridge National Laboratory, August 1985.

9. P. W. Eckels, *Contact Conductance of Mechanically Expanded Plate Finned Tube Heat Exchangers*, presented at the AIChE-ASME Heat Transfer Conference, Salt Lake City, Utah, 1977.

10. *ASHRAE Equipment Handbook*, Chapter 20, American Society of Heating, Refrigerating, and Air-Conditioning Engineers, 1983.

Appendix A

INPUT DATA DEFINING AMBIENT CONDITIONS FOR STEADY-STATE CALCULATIONS

2					
16.70	0.700	70.90	0.560	95.00	5.75
46.90	0.660	71.00	0.540	110.00	30.25
2					
74.90	0.450	79.20	0.550	112.75	40.25
95.00	0.380	78.80	0.570	120.70	47.00

Appendix B

INPUT DATA FOR COMPRESSOR MAP MODEL TO DO HEATING AND COOLING CALCULATIONS

```
         2
         1
         0          7.0
         0        30.40
      38.2        121.1
         2        3.051     3450.00       0.0     0.095
-1.429E-04    3.635E-02  -1.915E-04  -5.141E-03  3.552E-04  -3.453E-01   3.64E+00   20.0E+00
 4.458E-03   -2.039E+00   8.709E-02   9.108E+00  -3.483E-02   3.034E+02
-1.429E-04    3.635E-02  -1.915E-04  -5.141E-03  3.552E-04  -3.453E-01   3.64E+00   20.0E+00
 4.458E-03   -2.039E+00   8.709E-02   9.108E+00  -3.483E-02   3.034E+02
      78.8        0.57
    1054.5        0.22        6.0         0.0
     3.889         4.0       2.51       0.866       1.00       113.0
       2.0        14.0     0.0050      0.3950     0.3710       128.3      225.0        1.0
      95.0        0.38
    1911.0        0.16          1
     4.484         3.0       2.51        1.08       1.25        48.0
       2.0        13.0     0.0060      0.3950     0.3710       128.3      225.0        1.0
         0           2          2
     150.0      1000.0      100.0
    0.2555       50.00     0.6860       31.00     0.6860        2.00
    0.7930        5.00     0.5610        2.00
```

Appendix C

LISTINGS OF NEW SUBROUTINES FOR THE COMBINED APF/STEADY-STATE MODEL

On microfiche

Appendix D

SAMPLES OF SYSTEM COMPARISONS

Sample Output from Program TABULA

SYSTEM PERFORMANCE COMPARISONS

SYSTEM #1, FILE NAME: EXAMPLE.DAT
TEST CASE #1: HIGH EFFICIENCY HEAT PUMP

SYSTEM #2, FILE NAME: SAMPLE.DAT
TEST CASE #2: DESIGN OPTIMIZED FOR BEST SEASONAL PERFORMANCE

	#1	#2	
COMPRESSOR			
DISPLACEMENT	2.907	2.678	CU IN
SHELL HEAT LOSS	0.095	0.095	TIMES COMPRESSOR POWER
DIAMETER OF DUCTS	6.000	6.000	INCHES

	INDOOR HEAT EXCHANGER #1	INDOOR HEAT EXCHANGER #2	OUTDOOR HEAT EXCHANGER #1	OUTDOOR HEAT EXCHANGER #2	
AIR FLOW RATE	997.0	848.5	1820.0	2427.0	CFM
FACE VELOCITY	273.9	167.4	363.3	285.2	FT/MIN
FRONTAL AREA	3.640	5.070	5.010	8.510	SQ FT
TUBE ROWS	4.0	2.5	3.0	2.0	
REFRIGERANT CIRCUITS	2.4	3.0	2.4	3.0	
FRACTION OF HX AREA	0.492	0.427	0.508	0.573	
CAPILLARY FLOW FACTOR	3.673	3.530	3.035	2.248	
FIN THICKNESS	0.005	0.005	0.006	0.006	INCHES
VERTICAL TUBE SPACING	1.000	1.000	1.250	1.250	INCHES
HORIZONTAL TUBE SPACING	0.072	0.072	1.080	1.080	INCHES
OUTSIDE DIAMETER OF TUBES	0.395	0.395	0.395	0.395	INCHES

	HEATING SEASON #1	HEATING SEASON #2	HEATING SEASON -	COOLING SEASON #1	COOLING SEASON #2	COOLING SEASON -	ANNUAL #1	ANNUAL #2	ANNUAL -	
PERFORMANCE FACTORS	2.002	2.118	-5.79	2.483	2.750	-10.75	2.186	2.354	-7.69	%
POWER CONSUMPTION										
STEADY-STATE										
COMPRESSOR	3091.	3221.	-130.	2637.	2515.	122.	5727.	5736.	-9.	KWH
INDOOR FAN	484.	265.	219.	368.	187.	181.	852.	452.	400.	KWH
OUTDOOR FAN	322.	224.	98.	120.	132.	-12.	442.	356.	86.	KWH
SUBTOTAL	3897.	3710.	187.	3125.	2834.	291.	7021.	6544.	477.	KWH
RESISTANCE HEAT	830.	744.	86.				830.	744.	86.	KWH
FROSTING/DEFROSTING	608.	577.	31.				608.	577.	31.	KWH
CYCLING LOSSES	619.	598.	21.	591.	520.	71.	1210.	1117.	93.	KWH
TOTAL	5954.	5629.	325.	3716.	3354.	362.	9670.	8983.	687.	KWH

SYSTEM PERFORMANCE COMPARISONS

SYSTEM #1, FILE NAME: EXAMPLE.DAT
TEST CASE #1: HIGH EFFICIENCY HEAT PUMP

SYSTEM #2, FILE NAME: SAMPLE.DAT
TEST CASE #2: DESIGN OPTIMIZED FOR BEST SEASONAL PERFORMANCE

COMPRESSOR & HEAT EXCHANGER CAPACITIES:

OUTDOOR TEMPERATURE (F)	COMPRESSOR CAPACITY (BTU/HR) #1	#2	-	CONDENSER CAPACITY (BTU/HR) #1	#2	-	EVAPORATOR CAPACITY (BTU/HR) #1	#2	-
-10.0	3011.	3717.	-706.	4729.	6653.	-1924.	2885.	4134.	-1249.
0.0	3628.	4163.	-535.	7943.	9852.	-1909.	5497.	6815.	-1318.
10.0	4208.	4630.	-422.	11615.	13291.	-1676.	8544.	9663.	-1119.
20.0	4776.	5118.	-342.	15534.	16703.	-1169.	11795.	12542.	-747.
30.0	5393.	5635.	-242.	19702.	20442.	-740.	15269.	15769.	-500.
40.0	5979.	6222.	-243.	23956.	24617.	-661.	18935.	19352.	-417.
50.0	6606.	6902.	-296.	28716.	29131.	-415.	23075.	23187.	-112.
60.0	7300.	7757.	-457.	34038.	34095.	-57.	27710.	27285.	425.
70.0	7355.	6662.	693.	40381.	37780.	2601.	33981.	32073.	1908.
75.0	7511.	6910.	601.	39569.	37277.	2292.	33027.	31313.	1714.
80.0	7726.	7162.	564.	38844.	36749.	2095.	32040.	30506.	1534.
85.0	7921.	7412.	509.	37857.	36123.	1734.	30870.	29664.	1206.
90.0	8167.	7666.	501.	37047.	35491.	1556.	29842.	28779.	1063.
95.0	8337.	7921.	416.	36186.	34823.	1363.	28801.	27860.	941.
100.0	8503.	8170.	333.	35294.	34130.	1164.	27773.	26924.	849.

POWER CONSUMPTIONS & COP'S:

OUTDOOR TEMPERATURE (F)	INDOOR FAN (W) #1	#2	-	OUTDOOR FAN (W) #1	#2	-	COMPRESSOR (W) #1	#2	-	COP #1	#2	-
-10.0	283.8	156.7	127.1	138.3	127.0	11.3	975.0	1203.3	-228.3	1.195	1.164	0.031
0.0	283.7	156.7	127.0	135.8	126.3	9.5	1174.7	1347.7	-173.0	1.638	1.474	0.164
10.0	283.4	156.6	126.8	133.4	125.7	7.7	1362.3	1499.1	-136.8	2.072	2.068	0.004
20.0	283.2	156.5	126.7	131.2	125.2	6.0	1546.2	1656.9	-110.7	2.466	2.605	-0.139
30.0	282.9	156.4	126.5	189.4	128.0	61.4	1745.9	1824.4	-78.5	2.730	2.914	-0.184
40.0	282.6	156.3	126.3	206.1	132.7	73.4	1935.7	2014.3	-78.6	3.012	3.199	-0.187
50.0	282.2	156.1	126.1	232.6	148.0	84.6	2138.6	2234.6	-96.0	3.277	3.424	-0.147
60.0	281.7	155.9	125.8	249.0	158.1	90.9	2363.3	2511.3	-148.0	3.544	3.591	-0.047
70.0	354.4	175.2	179.2	117.0	123.6	-6.6	2381.1	2156.9	224.2	3.366	3.755	-0.389
75.0	354.1	175.2	178.9	116.3	123.6	-7.3	2431.8	2237.0	194.8	3.212	3.549	-0.337
80.0	354.5	175.2	179.3	115.6	123.7	-8.1	2501.4	2318.8	182.6	3.040	3.348	-0.308
85.0	353.9	175.1	178.8	114.9	123.7	-8.8	2564.3	2399.7	164.6	2.865	3.156	-0.291
90.0	352.3	175.1	177.2	114.3	123.8	-9.5	2644.2	2482.0	162.2	2.698	2.969	-0.271
95.0	350.7	175.0	175.7	113.6	123.8	-10.2	2699.1	2564.4	134.7	2.557	2.790	-0.233
100.0	348.9	175.0	173.9	112.9	123.9	-11.0	2752.7	2645.0	107.7	2.423	2.620	-0.197

SYSTEM PERFORMANCE COMPARISONS

SYSTEM #1, FILE NAME: EXAMPLE.DAT
TEST CASE #1: HIGH EFFICIENCY HEAT PUMP

SYSTEM #2, FILE NAME: SAMPLE.DAT
TEST CASE #2: DESIGN OPTIMIZED FOR BEST SEASONAL PERFORMANCE

COMPRESSOR AND FAN EFFICIENCIES:

OUTDOOR TEMPERATURE (F)	COMPRESSOR VOLUMETRIC EFFICIENCY			TOTAL COMPRESSOR EFFICIENCY			OUTDOOR FAN EFFICIENCY			INDOOR FAN EFFICIENCY			COMPRESSOR ONLY COP		
	#1	#2	-	#1	#2	-	#1	#2	-	#1	#2	-	#1	#2	-
-10.0	0.441	0.479	-0.038	0.446	0.376	0.070	0.245	0.177	0.068	0.220	0.220	-0.000	1.421	1.620	-0.199
0.0	0.496	0.544	-0.048	0.454	0.425	0.029	0.245	0.175	0.070	0.220	0.220	-0.000	1.981	2.142	-0.161
10.0	0.549	0.601	-0.052	0.474	0.467	0.007	0.244	0.172	0.072	0.220	0.220	0.000	2.498	2.598	-0.100
20.0	0.598	0.651	-0.053	0.495	0.502	-0.007	0.244	0.169	0.075	0.220	0.220	0.000	2.944	2.954	-0.010
30.0	0.645	0.691	-0.046	0.515	0.532	-0.017	0.247	0.181	0.066	0.220	0.220	-0.000	3.306	3.283	0.023
40.0	0.686	0.720	-0.034	0.534	0.555	-0.021	0.245	0.193	0.052	0.220	0.220	0.000	3.626	3.581	0.045
50.0	0.719	0.737	-0.018	0.554	0.575	-0.021	0.242	0.215	0.027	0.220	0.220	-0.000	3.934	3.820	0.115
60.0	0.744	0.744	0.000	0.573	0.589	-0.016	0.239	0.224	0.015	0.220	0.220	-0.000	4.220	3.978	0.242
70.0	0.799	0.798	0.001	0.569	0.535	0.034	0.238	0.151	0.087	0.220	0.220	-0.000	4.969	5.132	-0.163
75.0	0.789	0.790	-0.001	0.579	0.541	0.038	0.238	0.150	0.088	0.220	0.220	-0.000	4.768	4.882	-0.115
80.0	0.778	0.781	-0.003	0.583	0.546	0.037	0.238	0.148	0.090	0.220	0.220	-0.000	4.550	4.644	-0.094
85.0	0.767	0.772	-0.005	0.588	0.550	0.038	0.237	0.147	0.090	0.220	0.220	0.000	4.326	4.411	-0.085
90.0	0.756	0.763	-0.007	0.590	0.554	0.036	0.237	0.146	0.091	0.220	0.220	0.000	4.105	4.190	-0.085
95.0	0.745	0.753	-0.008	0.597	0.557	0.040	0.237	0.145	0.092	0.220	0.220	0.000	3.928	3.979	-0.051
100.0	0.735	0.743	-0.008	0.604	0.559	0.045	0.236	0.144	0.092	0.220	0.220	0.000	3.757	3.781	-0.024

PRESSURE DROPS:

OUTDOOR TEMPERATURE (F)	INDOOR HEAT EXCHANGER AIR-SIDE (INCHES WATER)			INDOOR HEAT EXCHANGER REFRIGERANT-SIDE (PSIA)			OUTDOOR HEAT EXCHANGER AIR-SIDE (INCHES WATER)			OUTDOOR HEAT EXCHANGER REFRIGERANT-SIDE (PSIA)			EXPANSION DEVICE HIGH-SIDE/LOW-SIDE (PSIA)		
	#1	#2	-	#1	#2	-	#1	#2	-	#1	#2	-	#1	#2	-
-10.0	0.533	0.346	0.187	0.52	0.19	0.33	0.159	0.079	0.080	2.39	1.33	1.06	115.7	126.1	-10.4
0.0	0.533	0.346	0.187	0.73	0.26	0.47	0.155	0.077	0.078	3.04	1.79	1.25	118.3	132.6	-14.3
10.0	0.532	0.345	0.187	0.99	0.36	0.63	0.152	0.076	0.076	3.88	2.36	1.52	121.9	139.7	-17.8
20.0	0.532	0.345	0.187	1.32	0.50	0.82	0.150	0.074	0.076	4.87	3.06	1.81	126.3	146.0	-19.7
30.0	0.531	0.345	0.186	1.79	0.64	1.15	0.218	0.081	0.137	6.19	3.82	2.37	130.4	153.8	-23.4
40.0	0.531	0.345	0.186	2.35	0.78	1.57	0.236	0.090	0.146	7.68	4.59	3.09	134.9	165.1	-30.2
50.0	0.530	0.345	0.185	2.92	0.88	2.04	0.263	0.112	0.151	9.28	5.36	3.92	142.0	181.6	-39.6
60.0	0.529	0.344	0.185	3.46	0.92	2.54	0.279	0.124	0.155	10.95	6.05	4.90	152.5	207.3	-54.8
70.0	0.665	0.387	0.278	18.91	6.88	12.03	0.130	0.065	0.065	3.24	1.79	1.45	119.8	117.5	2.3
75.0	0.665	0.387	0.278	18.92	6.92	12.00	0.129	0.065	0.064	3.15	1.76	1.39	130.5	127.9	2.6
80.0	0.666	0.387	0.279	18.97	6.96	12.01	0.129	0.064	0.065	3.05	1.72	1.33	142.2	139.1	3.1
85.0	0.665	0.386	0.279	18.91	6.99	11.92	0.128	0.064	0.064	2.93	1.67	1.26	154.3	150.9	3.4
90.0	0.662	0.386	0.276	18.90	7.01	11.89	0.127	0.063	0.064	2.82	1.62	1.20	167.4	163.6	3.8
95.0	0.659	0.386	0.273	18.93	7.03	11.90	0.126	0.063	0.063	2.70	1.57	1.13	180.8	176.9	3.9
100.0	0.655	0.386	0.269	18.92	7.04	11.88	0.125	0.062	0.063	2.59	1.51	1.08	194.8	190.8	4.0

SYSTEM PERFORMANCE COMPARISONS

SYSTEM #1, FILE NAME: EXAMPLE.DAT
TEST CASE #1: HIGH EFFICIENCY HEAT PUMP

SYSTEM #2, FILE NAME: SAMPLE.DAT
TEST CASE #2: DESIGN OPTIMIZED FOR BEST SEASONAL PERFORMANCE

MISCELLANEOUS DATA:

OUTDOOR TEMPERATURE (F)	REFRIGERANT FLOW RATE (LBM/HR) #1	#2	-	POWER / UNIT FLOW (KW/LBM) #1	#2	-	OUTDOOR PRESSURE DROP (INCHES WATER) #1	#2	-	SPECIFIC SPEED #1	#2	-
-10.0	81.8	82.1	-0.3	0.0	0.0	0.0	0.159	0.079	0.080	140.0	272.8	-132.8
0.0	108.3	110.2	-1.9	0.0	0.0	0.0	0.155	0.077	0.078	142.2	277.0	-134.8
10.0	139.6	142.9	-3.3	0.0	0.0	0.0	0.152	0.076	0.076	144.3	281.3	-137.0
20.0	175.1	180.4	-5.3	0.0	0.0	0.0	0.150	0.074	0.076	146.4	285.5	-139.1
30.0	218.1	221.6	-3.4	0.0	0.0	0.0	0.218	0.081	0.137	110.2	266.9	-156.7
40.0	265.3	266.6	-1.3	0.0	0.0	0.0	0.236	0.090	0.146	103.9	247.7	-143.8
50.0	317.8	314.1	3.7	0.0	0.0	0.0	0.263	0.112	0.151	95.8	210.5	-114.7
60.0	375.8	364.2	11.6	0.0	0.0	0.0	0.279	0.124	0.155	91.8	194.5	-102.7
70.0	444.4	412.6	31.8	0.0	0.0	0.0	0.130	0.065	0.065	162.2	314.7	-152.5
75.0	442.9	412.7	30.3	0.0	0.0	0.0	0.129	0.065	0.064	163.0	316.4	-153.4
80.0	441.9	412.6	29.3	0.0	0.0	0.0	0.129	0.064	0.065	164.0	318.1	-154.1
85.0	438.2	411.8	26.4	0.0	0.0	0.0	0.128	0.064	0.064	164.9	319.9	-155.0
90.0	436.2	411.1	25.1	0.0	0.0	0.0	0.127	0.063	0.064	165.8	321.7	-155.9
95.0	434.6	410.2	24.4	0.0	0.0	0.0	0.126	0.063	0.063	166.7	323.6	-156.9
100.0	432.7	409.2	23.5	0.0	0.0	0.0	0.125	0.062	0.063	167.7	325.5	-157.8

OUTDOOR TEMPERATURE (F)	CONDENSER SUBCOOLING (F) #1	#2	-	CAPILLARY FLOW FACTOR #1	#2	-	SUPPLY AIR TEMPERATURE #1	#2	-	SENSIBLE TO TOTAL RATIO #1	#2	-
-10.0	0.0	0.0	0.0	3.035	2.248	0.787	121.9	132.6	-10.7	1.000	1.000	0.000
0.0	0.0	0.0	0.0	3.035	2.248	0.787	124.9	136.1	-11.2	1.000	1.000	0.000
10.0	0.0	0.0	0.0	3.035	2.248	0.787	128.2	139.8	-11.5	1.000	1.000	0.000
20.0	0.0	2.9	-2.9	3.035	2.248	0.787	131.8	143.4	-11.6	1.000	1.000	0.000
30.0	0.0	11.3	-11.3	3.035	2.248	0.787	135.6	147.4	-11.8	0.959	0.999	-0.040
40.0	7.2	20.4	-13.2	3.035	2.248	0.787	139.5	151.9	-12.4	0.932	0.974	-0.042
50.0	14.9	30.4	-15.5	3.035	2.248	0.787	143.8	156.7	-12.9	0.877	0.939	-0.062
60.0	23.5	42.3	-18.8	3.035	2.248	0.787	148.7	162.0	-13.4	0.806	0.884	-0.078
70.0	26.1	25.7	0.4	3.673	3.530	0.143	57.4	55.6	1.8	0.694	0.663	0.031
75.0	23.3	23.3	0.0	3.673	3.530	0.143	57.7	56.0	1.8	0.702	0.669	0.033
80.0	20.7	20.8	-0.1	3.673	3.530	0.143	58.1	56.3	1.8	0.712	0.675	0.037
85.0	17.7	18.1	-0.4	3.673	3.530	0.143	58.6	56.7	1.9	0.720	0.682	0.038
90.0	14.9	15.6	-0.7	3.673	3.530	0.143	59.0	57.1	1.9	0.731	0.690	0.041
95.0	12.1	12.9	-0.8	3.673	3.530	0.143	59.4	57.5	1.8	0.743	0.699	0.044
100.0	9.3	10.2	-0.9	3.673	3.530	0.143	59.7	57.9	1.8	0.756	0.709	0.047

SYSTEM PERFORMANCE COMPARISONS

SYSTEM #1, FILE NAME: EXAMPLE.DAT
TEST CASE #1: HIGH EFFICIENCY HEAT PUMP

SYSTEM #2, FILE NAME: SAMPLE.DAT
TEST CASE #2: DESIGN OPTIMIZED FOR BEST SEASONAL PERFORMANCE

SATURATION TEMPERATURES:

OUTDOOR TEMPERATURE (F)	ENTERING COMPRESSOR (F) #1	#2	-	LEAVING COMPRESSOR (F) #1	#2	-	ENTERING CONDENSER (F) #1	#2	-	LEAVING CONDENSER (F) #1	#2	-
-10.0	-14.3	-14.2	-0.1	75.0	79.0	-4.0	75.0	79.0	-4.0	74.8	78.9	-4.1
0.0	-6.5	-6.1	-0.4	78.9	84.3	-5.4	78.9	84.3	-5.4	78.6	84.2	-5.6
10.0	1.1	1.8	-0.7	83.4	89.9	-6.5	83.4	89.8	-6.4	83.0	89.7	-6.7
20.0	8.3	9.7	-1.4	88.3	95.2	-6.9	88.2	95.1	-6.9	87.7	94.9	-7.2
30.0	15.9	17.5	-1.6	93.4	101.0	-7.6	93.3	100.9	-7.6	92.6	100.7	-8.1
40.0	23.2	25.4	-2.2	98.7	108.0	-9.3	98.5	107.9	-9.4	97.7	107.7	-10.0
50.0	30.7	33.3	-2.6	104.9	116.4	-11.5	104.8	116.3	-11.5	103.8	116.1	-12.3
60.0	38.4	41.5	-3.1	112.3	127.0	-14.7	112.2	126.9	-14.7	111.1	126.7	-15.6
70.0	44.1	44.7	-0.6	107.4	102.4	5.0	107.4	102.4	5.0	106.3	101.8	4.5
75.0	44.7	45.3	-0.6	111.1	106.2	4.9	111.0	106.1	4.9	110.0	105.6	4.4
80.0	45.4	45.9	-0.5	114.9	110.1	4.8	114.9	110.0	4.9	113.9	109.5	4.4
85.0	45.8	46.5	-0.7	118.6	114.0	4.6	118.5	113.9	4.6	117.7	113.4	4.3
90.0	46.4	47.2	-0.8	122.5	118.0	4.5	122.4	118.0	4.4	121.7	117.5	4.2
95.0	47.0	47.8	-0.8	126.4	122.1	4.3	126.4	122.1	4.3	125.6	121.6	4.0
100.0	47.6	48.5	-0.9	130.3	126.1	4.2	130.2	126.1	4.1	129.6	125.7	3.9

OUTDOOR TEMPERATURE (F)	ENTERING EVAPORATOR (F) #1	#2	-	LEAVING EVAPORATOR (F) #1	#2	-
-10.0	-10.7	-12.1	1.4	-14.3	-14.1	-0.2
0.0	-2.4	-3.7	1.3	-6.4	-6.1	-0.3
10.0	5.6	4.6	1.0	1.1	1.9	-0.8
20.0	13.4	12.9	0.5	8.4	9.8	-1.4
30.0	21.7	21.1	0.6	16.0	17.6	-1.6
40.0	29.7	29.3	0.4	23.3	25.5	-2.2
50.0	37.7	37.3	0.4	30.8	33.4	-2.6
60.0	45.9	45.5	0.4	38.5	41.5	-3.0
70.0	56.4	49.7	6.7	45.0	45.4	-0.4
75.0	56.9	50.3	6.6	45.6	46.1	-0.5
80.0	57.5	51.0	6.5	46.3	46.7	-0.4
85.0	57.7	51.5	6.2	46.6	47.3	-0.7
90.0	58.2	52.1	6.1	47.2	47.9	-0.7
95.0	58.8	52.8	6.0	47.8	48.5	-0.7
100.0	59.3	53.4	5.9	48.4	49.2	-0.8

SYSTEM PERFORMANCE COMPARISONS

SYSTEM #1, FILE NAME: EXAMPLE.DAT
TEST CASE #1: HIGH EFFICIENCY HEAT PUMP

SYSTEM #2, FILE NAME: SAMPLE.DAT
TEST CASE #2: DESIGN OPTIMIZED FOR BEST SEASONAL PERFORMANCE

REFRIGERANT TEMPERATURES:

OUTDOOR TEMPERATURE (F)	ENTERING COMPRESSOR (F)			LEAVING COMPRESSOR (F)			ENTERING CONDENSER (F)			LEAVING CONDENSER (F)		
	#1	#2	-	#1	#2	-	#1	#2	-	#1	#2	-
-10.0	-7.3	-7.2	-0.1	233.2	278.7	-45.5	168.5	215.0	-46.5	74.8	78.9	-4.1
0.0	0.5	0.9	-0.4	221.4	245.5	-24.1	172.7	198.2	-25.5	78.6	84.2	-5.6
10.0	8.1	8.8	-0.7	209.4	223.8	-14.4	171.9	187.6	-15.7	83.0	89.7	-6.7
20.0	15.3	16.7	-1.4	200.0	209.1	-9.1	170.4	180.9	-10.5	87.7	92.0	-4.3
30.0	22.9	24.5	-1.6	192.8	200.6	-7.8	169.3	177.9	-8.6	92.6	89.4	3.2
40.0	30.2	32.4	-2.2	187.7	197.2	-9.5	168.7	178.7	-10.0	90.5	87.3	3.2
50.0	37.7	40.3	-2.6	185.5	198.5	-13.0	169.9	183.2	-13.3	88.9	85.7	3.2
60.0	45.4	48.5	-3.1	186.2	204.8	-18.6	173.3	191.9	-18.6	87.6	84.4	3.2
70.0	51.1	51.7	-0.6	171.8	167.3	4.5	160.9	155.3	5.6	80.2	76.1	4.1
75.0	51.7	52.3	-0.6	176.1	172.6	3.5	165.3	160.7	4.6	86.7	82.3	4.4
80.0	52.4	52.9	-0.5	181.2	178.0	3.2	170.4	166.3	4.1	93.2	88.7	4.5
85.0	52.8	53.5	-0.7	186.3	183.6	2.7	175.6	172.0	3.6	100.0	95.3	4.7
90.0	53.4	54.2	-0.8	192.0	189.3	2.7	181.2	177.7	3.5	106.8	101.9	4.9
95.0	54.0	54.8	-0.8	196.7	195.1	1.6	186.1	183.6	2.5	113.5	108.7	4.8
100.0	54.6	55.5	-0.9	201.5	200.8	0.7	190.9	189.4	1.5	120.3	115.5	4.8

OUTDOOR TEMPERATURE (F)	ENTERING EVAPORATOR (F)			LEAVING EVAPORATOR (F)		
	#1	#2	-	#1	#2	-
-10.0	-10.7	-12.1	1.4	-14.3	-14.1	-0.2
0.0	-2.4	-3.7	1.3	-6.4	-6.1	-0.3
10.0	5.6	4.6	1.0	1.6	2.2	-0.6
20.0	13.4	12.9	0.5	10.1	11.8	-1.7
30.0	21.7	21.1	0.6	19.0	20.8	-1.8
40.0	29.7	29.3	0.4	27.1	29.3	-2.2
50.0	37.7	37.3	0.4	35.3	37.8	-2.5
60.0	45.9	45.5	0.4	43.5	46.1	-2.6
70.0	56.4	49.7	6.7	49.8	50.1	-0.3
75.0	56.9	50.3	6.6	50.5	50.6	-0.1
80.0	57.5	51.0	6.5	50.6	50.9	-0.3
85.0	57.7	51.5	6.2	51.1	51.9	-0.8
90.0	58.2	52.1	6.1	52.0	52.6	-0.6
95.0	58.8	52.8	6.0	52.5	53.3	-0.8
100.0	59.3	53.4	5.9	53.5	54.0	-0.5

SYSTEM PERFORMANCE COMPARISONS

SYSTEM #1, FILE NAME: EXAMPLE.DAT
TEST CASE #1: HIGH EFFICIENCY HEAT PUMP

SYSTEM #2, FILE NAME: SAMPLE.DAT
TEST CASE #2: DESIGN OPTIMIZED FOR BEST SEASONAL PERFORMANCE

ENTHALPIES:

OUTDOOR TEMPERATURE (F)	ENTERING COMPRESSOR (BTU/LBM) #1	#2	·	LEAVING COMPRESSOR (BTU/LBM) #1	#2	·	ENTERING CONDENSER (BTU/LBM) #1	#2	·	LEAVING CONDENSER (BTU/LBM) #1	#2	·	CONDENSER ENTHALPY CHANGE #1	#2	·
-10.0	104.1	104.1	0.0	140.9	149.4	-8.5	128.7	137.2	-8.5	68.2	53.1	15.1	60.5	84.1	-23.6
0.0	104.9	104.9	0.0	138.4	142.7	-4.3	129.2	133.6	-4.4	53.7	42.7	11.0	75.5	90.9	-15.4
10.0	105.7	105.8	-0.1	135.8	138.2	-2.4	128.7	131.2	-2.5	44.2	37.8	6.4	84.5	93.4	-8.9
20.0	106.4	106.5	-0.1	133.7	134.9	-1.2	128.0	129.4	-1.4	38.8	36.8	2.0	89.2	92.6	-3.4
30.0	107.2	107.3	-0.1	131.9	132.7	-0.8	127.3	128.2	-0.9	37.0	36.0	1.0	90.3	92.2	-1.9
40.0	107.9	108.1	-0.2	130.4	131.4	-1.0	126.6	127.6	-1.0	36.3	35.3	1.0	90.3	92.3	-2.0
50.0	108.6	108.8	-0.2	129.3	130.8	-1.5	126.2	127.6	-1.4	35.8	34.8	1.0	90.4	92.8	-2.4
60.0	109.2	109.5	-0.3	128.7	130.8	-2.1	126.0	128.1	-2.1	35.4	34.4	1.0	90.6	93.7	-3.1
70.0	109.7	109.8	-0.1	126.3	125.9	0.4	124.0	123.5	0.5	33.2	31.9	1.3	90.8	91.6	-0.8
75.0	109.8	109.8	0.0	126.7	126.6	0.1	124.5	124.2	0.3	35.1	33.8	1.3	89.4	90.4	-1.0
80.0	109.8	109.9	-0.1	127.3	127.2	0.1	125.1	124.8	0.3	37.2	35.8	1.4	87.9	89.0	-1.1
85.0	109.9	109.9	0.0	128.0	127.9	0.1	125.7	125.5	0.2	39.3	37.8	1.5	86.4	87.7	-1.3
90.0	109.9	110.0	-0.1	128.7	128.6	0.1	126.4	126.2	0.2	41.4	39.9	1.5	85.0	86.3	-1.3
95.0	110.0	110.0	0.0	129.2	129.4	-0.2	126.9	126.9	0.0	43.6	42.0	1.6	83.3	84.9	-1.6
100.0	110.0	110.1	-0.1	129.7	130.1	-0.4	127.4	127.6	-0.2	45.8	44.2	1.6	81.6	83.4	-1.8

OUTDOOR TEMPERATURE (F)	ENTERING EVAPORATOR (BTU/LBM) #1	#2	·	LEAVING EVAPORATOR (BTU/LBM) #1	#2	·	EVAPORATOR ENTHALPY CHANGE #1	#2	·
-10.0	67.0	51.9	29.1	102.2	102.3	-0.1	35.2	50.4	-30.2
0.0	52.7	41.8	26.1	103.5	103.6	-0.1	50.8	61.8	-17.8
10.0	43.4	37.1	17.0	104.6	104.7	-0.1	61.2	67.6	-9.5
20.0	38.2	36.2	5.5	105.6	105.7	-0.1	67.4	69.5	-3.0
30.0	36.5	35.5	2.8	106.5	106.6	-0.1	70.0	71.1	-1.5
40.0	35.9	34.9	2.9	107.3	107.5	-0.2	71.4	72.6	-1.7
50.0	35.5	34.5	2.9	108.1	108.3	-0.2	72.6	73.8	-1.6
60.0	35.2	34.2	2.9	108.8	109.1	-0.3	73.6	74.9	-1.7
70.0	32.9	31.7	3.8	109.4	109.4	0.0	76.5	77.7	-1.5
75.0	34.9	33.6	3.9	109.4	109.5	-0.1	74.5	75.9	-1.8
80.0	36.9	35.5	3.9	109.5	109.5	0.0	72.6	74.0	-1.9
85.0	39.0	37.5	4.0	109.5	109.6	-0.1	70.5	72.1	-2.2
90.0	41.2	39.6	4.0	109.6	109.6	0.0	68.4	70.0	-2.3
95.0	43.4	41.8	3.8	109.6	109.7	-0.1	66.2	67.9	-2.5
100.0	45.6	44.0	3.6	109.7	109.7	0.0	64.1	65.7	-2.4

SYSTEM PERFORMANCE COMPARISONS

SYSTEM #1, FILE NAME: EXAMPLE.DAT
TEST CASE #1: HIGH EFFICIENCY HEAT PUMP

SYSTEM #2, FILE NAME: SAMPLE.DAT
TEST CASE #2: DESIGN OPTIMIZED FOR BEST SEASONAL PERFORMANCE

PRESSURES:

OUTDOOR TEMPERATURE (F)	ENTERING COMPRESSOR (PSIA) #1	#2	-	LEAVING COMPRESSOR (PSIA) #1	#2	-	ENTERING CONDENSER (PSIA) #1	#2	-	LEAVING CONDENSER (PSIA) #1	#2	-
-10.0	28.3	28.4	-0.1	147.0	156.1	-9.1	146.9	156.0	-9.1	146.4	155.8	-9.4
0.0	33.7	33.9	-0.2	155.8	168.7	-12.9	155.7	168.6	-12.9	155.0	168.3	-13.3
10.0	39.5	40.2	-0.7	166.5	182.8	-16.3	166.4	182.7	-16.3	165.4	182.3	-16.9
20.0	45.9	47.2	-1.3	178.6	197.0	-18.4	178.4	196.8	-18.4	177.1	196.3	-19.2
30.0	53.3	55.0	-1.7	192.1	213.6	-21.5	191.8	213.3	-21.5	190.0	212.7	-22.7
40.0	61.4	64.0	-2.6	206.8	234.8	-28.0	206.4	234.5	-28.1	204.1	233.7	-29.6
50.0	70.5	73.9	-3.4	225.3	262.2	-36.9	224.9	261.8	-36.9	221.9	261.0	-39.1
60.0	81.0	85.3	-4.3	248.6	300.1	-51.5	248.1	299.7	-51.6	244.6	298.8	-54.2
70.0	89.4	90.2	-0.8	232.9	217.7	15.2	232.7	217.5	15.2	229.5	215.8	13.7
75.0	90.3	91.2	-0.9	244.4	229.0	15.4	244.3	228.9	15.4	241.1	227.2	13.9
80.0	91.3	92.2	-0.9	257.1	241.2	15.9	256.9	241.1	15.8	253.9	239.4	14.5
85.0	91.9	93.1	-1.2	269.6	254.0	15.6	269.4	253.9	15.5	266.5	252.2	14.3
90.0	92.9	94.2	-1.3	283.4	267.7	15.7	283.3	267.5	15.8	280.5	265.9	14.6
95.0	93.9	95.2	-1.3	297.8	282.0	15.8	297.6	281.9	15.7	294.9	280.3	14.6
100.0	94.8	96.3	-1.5	312.5	296.8	15.7	312.4	296.7	15.7	309.8	295.2	14.6

OUTDOOR TEMPERATURE (F)	ENTERING EVAPORATOR (PSIA) #1	#2	-	LEAVING EVAPORATOR (PSIA) #1	#2	-
-10.0	30.7	29.7	1.0	28.3	28.4	-0.1
0.0	36.7	35.7	1.0	33.7	33.9	-0.2
10.0	43.5	42.6	0.9	39.6	40.2	-0.6
20.0	50.8	50.3	0.5	46.0	47.3	-1.3
30.0	59.6	58.9	0.7	53.4	55.1	-1.7
40.0	69.2	68.6	0.6	61.5	64.1	-2.6
50.0	79.9	79.4	0.5	70.7	74.0	-3.3
60.0	92.1	91.5	0.6	81.1	85.5	-4.4
70.0	109.7	98.3	11.4	90.8	91.4	-0.6
75.0	110.6	99.3	11.3	91.7	92.4	-0.7
80.0	111.7	100.3	11.4	92.7	93.4	-0.7
85.0	112.2	101.3	10.9	93.2	94.3	-1.1
90.0	113.1	102.3	10.8	94.2	95.3	-1.1
95.0	114.1	103.4	10.7	95.1	96.3	-1.2
100.0	115.0	104.4	10.6	96.0	97.4	-1.4

Sample Output from Program COMPAR

COMPARISON OF STEADY-STATE
COMPONENT POWER CONSUMPTION
(HEATING SEASON CALCULATIONS)

SYSTEM #1, FILE NAME: EXAMPLE.DAT
TEST CASE #1: HIGH EFFICIENCY HEAT PUMP

SYSTEM #2, FILE NAME: SAMPLE.DAT
TEST CASE #2: DESIGN OPTIMIZED FOR BEST SEASONAL PERFORMANCE

	HOURS OF OPERATION				COMPRESSOR				INDOOR FAN				
TEMP (F)	#1 (HR)	#2 (HR)	- (HR)	CUMUL (HR)	#1 (W)	#2 (W)	- (W)	CUMUL (KWH)	#1 (W)	#2 (W)	- (W)	CUMUL (KWH)	#1 (W)
-13.	1.0	1.0	0.0	0.0	914.7	1159.5	-244.8	-0.2	283.9	156.7	127.2	0.1	139.
-8.	1.0	1.0	0.0	0.0	1014.8	1231.9	-217.1	-0.5	283.8	156.7	127.1	0.3	137.
-3.	4.0	4.0	0.0	0.0	1114.9	1304.3	-189.3	-1.2	283.7	156.7	127.1	0.8	136.
2.	9.0	9.0	0.0	0.0	1212.3	1377.9	-165.6	-2.7	283.6	156.6	127.0	1.9	135.
7.	21.0	21.0	0.0	0.0	1305.6	1453.6	-148.0	-5.8	283.5	156.6	126.9	4.6	134.
12.	41.0	41.0	0.0	0.0	1398.6	1530.7	-132.2	-11.2	283.4	156.6	126.8	9.8	133.
17.	98.0	98.0	0.0	0.0	1490.8	1609.9	-119.1	-22.9	283.2	156.5	126.7	22.2	131.
22.	167.0	167.0	0.0	0.0	1586.1	1690.8	-104.7	-40.4	283.1	156.5	126.6	43.3	142.
27.	277.7	271.6	6.2	6.2	1686.0	1774.3	-88.3	-54.0	283.0	156.4	126.6	79.5	172.
32.	331.9	327.5	4.4	10.6	1783.9	1862.4	-78.5	-71.8	282.8	156.4	126.5	122.1	192.
37.	292.7	289.6	3.1	13.7	1878.7	1957.3	-78.6	-88.7	282.7	156.3	126.4	159.6	201.
42.	212.8	211.3	1.5	15.2	1976.3	2058.3	-82.1	-103.2	282.5	156.3	126.3	186.7	211.
47.	135.6	135.3	0.3	15.4	2077.7	2168.5	-90.7	-114.9	282.3	156.2	126.1	203.8	224.
52.	79.1	79.4	-0.2	15.2	2183.6	2289.9	-106.3	-123.8	282.1	156.1	126.0	213.8	235.
57.	33.8	34.0	-0.3	14.9	2295.9	2428.3	-132.4	-128.9	281.8	156.0	125.8	218.0	244.
62.	6.1	6.1	-0.1	14.9	2408.3	2566.6	-158.4	-130.1	281.6	155.9	125.7	218.7	252.

STEADY-STATE COMPONENT	SYSTEM #1	SYSTEM #2	DIFFERENCE
COMPRESSOR POWER	3091.	3221.	-130. KWH
INDOOR FAN POWER	484.	265.	219. KWH
OUTDOOR FAN POWER	322.	224.	98. KWH
TOTAL STEADY STATE	3896.	3710.	186. KWH
RESISTANCE HEAT	830.	744.	86. KWH
FROSTING/DEFROSTING LOSSES	608.	577.	32. KWH
CYCLING LOSSES	619.	598.	22. KWH
TOTAL POWER CONSUMPTION	5954.	5628.	326. KWH

COMPARISON OF STEADY-STATE
COMPONENT POWER CONSUMPTION
(COOLING SEASON CALCULATIONS)

SYSTEM #1, FILE NAME: EXAMPLE.DAT
TEST CASE #1: HIGH EFFICIENCY HEAT PUMP

SYSTEM #2, FILE NAME: SAMPLE.DAT
TEST CASE #2: DESIGN OPTIMIZED FOR BEST SEASONAL PERFORMANCE

	HOURS OF OPERATION				COMPRESSOR				INDOOR FAN				OUTDOOR FAN			
TEMP (F)	#1 (HR)	#2 (HR)	- (HR)	CUMUL (HR)	#1 (W)	#2 (W)	- (W)	CUMUL (KWH)	#1 (W)	#2 (W)	- (W)	CUMUL (KWH)	#1 (W)	#2 (W)	- (W)	CUMUL (KWH)
67.	32.1	33.5	-1.4	-1.4	2350.7	2108.8	241.8	4.8	354.5	175.3	179.3	5.5	117.4	123.6	-6.2	-0.4
72.	116.6	121.1	-4.6	-6.0	2401.4	2189.0	212.4	19.5	354.2	175.2	179.0	25.6	116.7	123.6	-6.9	-1.7
77.	202.3	209.2	-6.9	-12.8	2459.7	2269.7	189.9	42.4	354.3	175.2	179.0	60.6	116.0	123.7	-7.6	-4.1
82.	262.5	269.5	-7.0	-19.9	2526.6	2351.2	175.4	71.9	354.3	175.2	179.1	106.4	115.3	123.7	-8.4	-7.2
87.	266.0	271.0	-5.0	-24.9	2596.3	2432.6	163.6	103.3	353.3	175.1	178.2	152.9	114.7	123.7	-9.1	-10.2
92.	141.0	143.1	-2.1	-27.0	2666.1	2515.0	151.1	119.3	351.7	175.1	176.6	177.4	114.0	123.8	-9.8	-11.9
97.	19.8	20.0	-0.2	-27.2	2720.5	2596.6	123.9	121.2	350.0	175.0	175.0	180.9	113.3	123.9	-10.6	-12.1

STEADY-STATE COMPONENT	SYSTEM #1	SYSTEM #2	DIFFERENCE
COMPRESSOR POWER	2637.	2515.	121. KWH
INDOOR FAN POWER	368.	187.	181. KWH
OUTDOOR FAN POWER	120.	132.	-12. KWH
TOTAL STEADY STATE	3124.	2834.	290. KWH
RESISTANCE HEAT	0.	0.	0. KWH
FROSTING/DEFROSTING LOSSES	0.	0.	0. KWH
CYCLING LOSSES	591.	520.	71. KWH
TOTAL POWER CONSUMPTION	3715.	3354.	361. KWH

COMPARISON OF DYNAMIC
POWER CONSUMPTION
(HEATING SEASON CALCULATIONS)

SYSTEM #1, FILE NAME: EXAMPLE.DAT
TEST CASE #1: HIGH EFFICIENCY HEAT PUMP

SYSTEM #2, FILE NAME: SAMPLE.DAT
TEST CASE #2: DESIGN OPTIMIZED FOR BEST SEASONAL PERFORMANCE

	HOURS OF OPERATION				CYCLING LOSSES				FROSTING & DEFROSTING LOSSES				
TEMP (F)	#1 (HR)	#2 (HR)	- (HR)	CUMUL (HR)	#1 (W)	#2 (W)	- (W)	CUMUL (KWH)	#1 (W)	#2 (W)	- (W)	CUMUL (KWH)	#1 (KW
-13.	1.0	1.0	0.0	0.0	0.0	0.0	0.0	0.0	0.0	0.0	0.0	0.0	10.
-8.	1.0	1.0	0.0	0.0	0.0	0.0	0.0	0.0	0.0	0.0	0.0	0.0	9.
-3.	4.0	4.0	0.0	0.0	0.0	0.0	0.0	0.0	0.0	0.0	0.0	0.0	8.
2.	9.0	9.0	0.0	0.0	0.0	0.0	0.0	0.0	0.0	0.0	0.0	0.0	6.
7.	21.0	21.0	0.0	0.0	0.0	0.0	0.0	0.0	0.0	0.0	0.0	0.0	5.
12.	41.0	41.0	0.0	0.0	0.0	0.0	0.0	0.0	74.5	68.9	5.6	0.2	3.
17.	98.0	98.0	0.0	0.0	0.0	0.0	0.0	0.0	221.8	226.8	-5.0	-0.3	2.
22.	167.0	167.0	0.0	0.0	0.0	0.0	0.0	0.0	408.6	419.6	-11.0	-2.1	1.
27.	277.7	271.6	6.2	6.2	34.0	46.1	-12.1	-3.1	443.0	359.5	83.5	23.3	0.
32.	331.9	327.5	4.4	10.6	203.0	200.4	2.6	-1.3	432.0	427.7	4.3	26.6	0.
37.	292.7	289.6	3.1	13.7	391.7	377.3	14.4	4.1	618.2	609.4	8.8	31.1	0.
42.	212.8	211.3	1.5	15.2	624.8	599.0	25.8	10.4	319.3	318.5	0.8	31.8	0.
47.	135.6	135.3	0.3	15.4	950.4	908.4	42.0	16.4	0.0	0.0	0.0	31.8	0.
52.	79.1	79.4	-0.2	15.2	1268.4	1217.2	51.2	20.2	0.0	0.0	0.0	31.8	0.
57.	33.8	34.0	-0.3	14.9	1600.3	1551.0	49.4	21.4	0.0	0.0	0.0	31.8	0.
62.	6.1	6.1	-0.1	14.9	1863.5	1825.3	38.2	21.5	0.0	0.0	0.0	31.8	0.

STEADY-STATE COMPONENT	SYSTEM #1	SYSTEM #2	DIFFERENCE
COMPRESSOR POWER	3091.	3221.	-130. KWH
INDOOR FAN POWER	484.	265.	219. KWH
OUTDOOR FAN POWER	322.	224.	98. KWH
TOTAL STEADY STATE	3896.	3710.	186. KWH
RESISTANCE HEAT	830.	744.	86. KWH
FROSTING/DEFROSTING LOSSES	608.	577.	32. KWH
CYCLING LOSSES	619.	598.	22. KWH
TOTAL POWER CONSUMPTION	5954.	5628.	326. KWH

COMPARISON OF DYNAMIC
POWER CONSUMPTION
(COOLING SEASON CALCULATIONS)

SYSTEM #1, FILE NAME: EXAMPLE.DAT
TEST CASE #1: HIGH EFFICIENCY HEAT PUMP

SYSTEM #2, FILE NAME: SAMPLE.DAT
TEST CASE #2: DESIGN OPTIMIZED FOR BEST SEASONAL PERFORMANCE

	HOURS OF OPERATION				CYCLING LOSSES				FROSTING & DEFROSTING LOSSES				RESISTANCE HEAT			
TEMP (F)	#1 (HR)	#2 (HR)	- (HR)	CUMUL (HR)	#1 (W)	#2 (W)	- (W)	CUMUL (KWH)	#1 (W)	#2 (W)	- (W)	CUMUL (KWH)	#1 (KW)	#2 (KW)	- (KW)	CUMUL (KWH)
67.	32.1	33.5	-1.4	-1.4	1932.2	1636.6	295.7	7.2	0.0	0.0	0.0	0.0	0.0	0.0	0.0	0.0
72.	116.6	121.1	-4.6	-6.0	1343.5	1136.0	207.4	26.2	0.0	0.0	0.0	0.0	0.0	0.0	0.0	0.0
77.	202.3	209.2	-6.9	-12.8	836.3	709.9	126.5	46.9	0.0	0.0	0.0	0.0	0.0	0.0	0.0	0.0
82.	262.5	269.5	-7.0	-19.9	402.5	348.0	54.5	58.7	0.0	0.0	0.0	0.0	0.0	0.0	0.0	0.0
87.	266.0	271.0	-5.0	-24.9	273.4	236.2	37.2	67.5	0.0	0.0	0.0	0.0	0.0	0.0	0.0	0.0
92.	141.0	143.1	-2.1	-27.0	168.4	141.8	26.6	70.9	0.0	0.0	0.0	0.0	0.0	0.0	0.0	0.0
97.	19.8	20.0	-0.2	-27.2	48.0	35.5	12.6	71.1	0.0	0.0	0.0	0.0	0.0	0.0	0.0	0.0

STEADY-STATE COMPONENT	SYSTEM #1	SYSTEM #2	DIFFERENCE
COMPRESSOR POWER	2637.	2515.	121. KWH
INDOOR FAN POWER	368.	187.	181. KWH
OUTDOOR FAN POWER	120.	132.	-12. KWH
TOTAL STEADY STATE	3124.	2834.	290. KWH
RESISTANCE HEAT	0.	0.	0. KWH
FROSTING/DEFROSTING LOSSES	0.	0.	0. KWH
CYCLING LOSSES	591.	520.	71. KWH
TOTAL POWER CONSUMPTION	3715.	3354.	361. KWH

Appendix E

LISTINGS OF PROGRAMS TO GENERATE SYSTEM COMPARISONS

On microfiche

Appendix F

LISTING OF PROGRAM TO PLOT STEADY-STATE AND DYNAMIC HEAT PUMP PERFORMANCE

On microfiche

Appendix G

DESCRIPTION OF GRAPHICS SUBROUTINES

All of the programs in the Design Tool Package that make use of computer graphics rely on the DISSPLA software package, which is commercially available from ISSCO, Inc., of San Diego, California. Because of the strong similarities among most graphics packages, however, it is not difficult to convert a program from one set of subroutine calls to another *if it is clear what each subroutine is intended to do.* Most of the subroutines will have a direct counterpart in the new graphics package. A few very specialized subroutines may not be replaceable with a single call in the converted program if they can be handled by it at all. In most of these cases, these subroutines perform functions that only enhance the appearance of the graph and can be left out altogether without losing very much.

The following DISSPLA subroutines are used by programs in the Design Tool Package and are described here to facilitate translating programs from this software library to any other one.

ANGLE(ANG)—Causes subsequent lines of text drawn with MESSAG, REALNO, and INTNO to be written at an angle of ANG degrees counterclockwise from horizontal.

BGNPL(I)—Used to begin or initialize a plot; sets defaults for all "internal" parameters. Argument I is used to determine level and disposition of diagnostic messages.

BLNK1(XMIN,XMAX,YMIN,YMAX,IFRAME)—Used to "blank out" a portion of the plot so lines cannot be drawn in that area; reset with RESET('BLNK1') so that part of the graph can be used later. XMIN and XMAX define the horizontal coordinates of the blanked region in inches from the origin. YMIN and YMAX define the vertical coordinates of the blanked region in inches from the origin. IFRAME is the number of times to draw the outline, or frame, of the blanked region.

BSHIFT(XSHIFT,YSHIFT)—Shifts the physical origin of the plotting region XSHIFT inches horizontally and YSHIFT inches vertically with respect to the current location of the physical origin.

COMPRS—Invokes a "device-independent" driver, which routes plotting commands to a disk file for subsequent postprocessing to a particular graphics device.

CURVE(X,Y,N,I)—Draws the curve defined by the points stored in the arrays X and Y. N is the number of points in the curve (no larger than the dimensions of X and Y), and I is a flag used to specify how frequently to draw a symbol, or marker, on the curve (0 = draw the line only; >0 = a straight line with a marker at every I*th* point; <0 = markers only, no line connecting the points, at every −I*th* point).

DASH—Changes default line drawing parameters so that subsequent lines are composed of short dashes instead of solid lines, reset to solid lines with RESET('DASH').

DONEPL—Terminates plot generation, dumps buffers, closes output disk files, etc.

DOT—Changes default line drawing parameters so that subsequent lines are drawn with dots, reset to solid lines with RESET('DOT').

ENDGR(I)—Terminates a particular graph, or subplot, and restores some default parameters so a new set of axes and a new plot can be drawn on the same page as the one just completed. Parameter I pertains to a printed summary of vectors drawn, etc., and has no particular significance.

ENDPL(I)—Closes out the drawing of a page by dumping all the buffers, etc., and advances the paper (for hardcopy plotters). Argument I controls printing of summary information on the plot and also on the computer listing (given a nonzero value).

GRAF(XMIN,XSTP,XMAX,YMIN,YSTP,YMAX)—Sets up and draws the user's axes. XMIN, XMAX, and XSTP are the minimum, maximum, and step length between tick marks for the horizontal axis in the units of the graph; YMIN, YMAX, and YSTP are the corresponding parameters for the vertical axis.

GRID(IHOR,IVERT)—Draws a grid on the plot area with IHOR grid lines for each axis step on the horizontal axis and IVERT grid lines for each step on the vertical axis.

HEIGHT(HITE)—Defines the height of alphanumeric characters used for drawing character strings. HITE is the height of the letters in inches.

INTAXS—Causes tick marks on the axes to be labeled with integers whenever possible.

INTNO(INTEGER,XPT,YPT)—Draws the character string for the integer stored in INTEGER at a position XPT inches to the right of the origin and YPT inches up from the origin.

MARKER(ISYM)—Overrides the default counter and causes the next call to subroutine CURVE to use marker number ISYM for locating points on the plot (0 = small circle, 1 = small circle, 2 = triangle, etc.)

MESSAG(LSTRING,NLSTRN,XPT,YPT)—Draws the character string, or message, stored in LSTRING on the plot. NLSTRN is the number of characters in the message (NSTRN=100 can be used for "self-counting" strings in lieu of the actual number of characters). XPT and YPT are the horizontal and vertical distances from the lower left hand corner of the plot (the origin) to the point to start drawing the message (in inches).

MX1ALF(ALFBT,ICHAR)—Defines an alphabet, or character set, to use in drawing text or messages. ICHAR is an alphanumeric character [e.g., '(' or 1H<] that initiates the alphabet specified by ALFBT (e.g., 'STAND' for standard upper

case or 6HL/CSTD for lower case standard letters). MX2ALF and MX3ALF are comparable to MX1ALF and therefore multiple character sets are available within a plot.

NEWPEN(I)—Is used to change the color of the pen (or ink) used in the plot. This subroutine is device dependent; for some plotters it will change the color of the lines being drawn, and for others it will change the width of the lines. Parameter I specifies the color or width.

NUMODE(LNUMODE)—Changes mode setting parameters that control the appearance of the plot. It is used in the compressor map fitting plots with LNUMODE equal to 'LEAD SPACE' and 4HPLUS to precede *plotted* numbers with a leading space or with a plus sign.

OREL(XREL,YREL)—Causes a relative shift of the origin of a plot so that subsequent lines are drawn with respect to the new origin instead of the original one. This is useful to separate several plots drawn on the same page. XREL is the distance (in inches) to shift horizontally to the right of the current origin, and YREL is the vertical distance (in inches) to shift.

PAGE(XPAGE,YPAGE)—Defines the dimensions of the page for the plot, XPAGE inches horizontally and YPAGE inches vertically.

PHYSOR(XORG,YORG)—Defines the position of the origin for the plot with respect to the lower left corner of the page, XORG inches to the right of the left edge and YORG inches up from the bottom.

REALNO(X,IX,XPT,YPT)—Draws the numerical string for the value of the number X using IX places to the right of the decimal point. XPT and YPT are the distances to the right and up from the origin of the plot to place the left-most character of the number.

RESET('option name')—Resets internal plotting parameters to their default values. It is used with the options 'NUMODE', 'BLNKS', 'DOT', 'DASH', and 'ANGLE' to return to the standard form of plotting (e.g., no areas blanked out, text drawn on horizontal lines).

RLVEC(XFROM,YFROM,XTO,YTO,IVEC)—Draws a vector, or line, from the point specified by XFROM and YFROM (in coordinate units) to the point given by XTO and YTO. IVEC specifies whether to put an arrowhead on the vector.

SCLPIC(FACTOR)—Changes the size of the markers used to locate data points in calls to CURVE by the multiplicative constant FACTOR.

SIMPLX—Sets a character font that has fairly smooth, rounded letters and characters but uses a simple, single stroke for each letter.

TITLE(LTITLE,NLTITL,XTITLE,NXTITL,YTITLE,NYTITL,XAXIS,YAXIS)—Sets the title for a plot, the axis labels, and the lengths of each axis. LTITLE is a character string specifying the title for the plot; NTITL is the number of

letters in LTITLE; XTITLE and YTITLE are character strings containing the labels for the horizontal and vertical axes. Their respective lengths are NXTITL and NYTITL. XAXIS and YAXIS are the lengths of the horizontal and vertical axes in inches.

VECTOR(XFROM,YFROM,XTO,YTO,IVEC)—Draws a vector from the point (XFROM,YFROM) to (XTO,YTO), where the coordinates are with respect to inches from the physical origin (XORG,YORG). IVEC controls the shape and size of an arrowhead to draw on the vector (0 for none).

XGRAXS(XMIN,XSTP,XMAX,XAXIS,LXNAME,IXNAME,XPOS,YPOS)—Draws and labels a secondary horizontal axis. XMIN, XSTP, and XMAX are the same as in the primary axis routine GRAF; XAXIS is the length of the secondary axis in inches; LXNAME is the alphanumeric character string for the axis label; IXNAME is the number of characters in LXNAME; XPOS and YPOS are the horizontal and vertical displacements from the current physical origin for the origin of the new axis in inches.

XINT(INUM)—Is a function subroutine that returns the horizontal space required to draw the integer INUM in inches.

XINTAX—Sets parameters so the horizontal axis will be labeled with integers.

XMESS(LSTRNG,NLSTR)—Calculates the physical length required to draw the character string stored in LSTRNG based on the current character height. NLSTR is the number of characters in LSTRNG.

XPOSN(XVAL,YVAL)—Is a function subroutine that returns the horizontal distance from the physical origin to the point XVAL,YVAL in the units of the current axes.

XREAL(X,IX)—Returns the physical length (in inches) required to draw the character string corresponding to the number X using IX places to the right of the decimal point.

YAXANG(ANG)—Causes tick marks on the vertical axis to be labeled with numbers at an angle of ANG degrees from the horizontal.

YGRAXS(YMIN,YSTP,YMAX,YAXIS,LYNAME,IYNAME,XPOS,YPOS)—Draws and labels a secondary vertical axis. All of the parameters are comparable to those for GRAF and XGRAXS.

YINTAX—Causes the tick marks on the vertical axis to be labeled with integers.

Appendix H

LISTING OF COMPRESSOR MAP-FITTING ROUTINES

On microfiche

Appendix I

TRANSFORMATION OF COORDINATES FROM DIGITIZING TABLET

The Tektronix 4953 Digitizing Tablet has 1024 identifiable points in both the horizontal and vertical directions. The coordinates of a point that is digitized is thus sent back to the computer as an ordered pair of integers, each between 1 and 1024. It is then necessary for the user's software to convert these integers into coordinates relative to the axes of the graph that is being digitized.

This is done in the compressor map fitting program by requesting that the user type the values at the upper and lower ends of each axis and to digitize the end points. Figure I.1 is an exaggeration of the data for the horizontal axis showing:

- Rotation from the true horizontal (as far as the tablet is concerned)
- Tablet coordinates of the two end points of the axis, (IX_1,IY_1) and (IX_2,IY_2)
- Values at each end of the axis in graph units, A_1 and A_2

Ordinarily the difference between IY_1 and IY_2 will be small or 0 if the graph to be digitized is placed on the tablet carefully. There is likely to be a small angle of rotation θ, and this has to be taken into account when computing the coordinates of a point on the graph. It can be seen from Fig. I.1 that

$$\sin\theta = \frac{IY_2 - IY_1}{[(IX_2 - IX_1)^2 + (IY_2 - IY_1)^2]^{1/2}}, \tag{I.1}$$

$$\cos\theta = \frac{IX_2 - IX_1}{[(IX_2 - IX_1)^2 + (IY_2 - IY_1)^2]^{1/2}}. \tag{I.2}$$

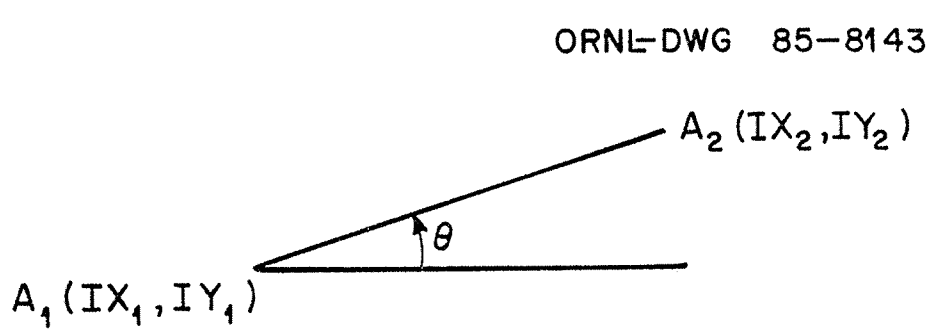

Fig. I.1. Layout on digitizing tablet showing coordinates of two points with exagerated variation from true horizontal.

Figure I.2 shows the same horizontal axis as that in Fig. I.1, but it includes an arbitrary point, (X,Y), within the domain of the graph. This point has tablet coordinates (IX_5,IY_5), which need to be transformed to graph coordinates. In this figure, the distance between A_1 and the projection of the point (X,Y) onto the line segment A_1A_2 has been labeled r. It is most convenient to consider r in tablet units, in which case

$$X = A_1 + \frac{r}{[(IX_2 - IX_1)^2 + (IY_2 - IY_1)^2]^{1/2}} (A_2 - A_1) \ . \tag{I.3}$$

The key to the transformation of variables is in expressing r in terms of the digitizer coordinates (IX_1,IY_1), (IX_2,IY_2), and (IX_5,IY_5). Of the many probable ways to do this, the one used in the map-fitting program is based on similar triangles, as shown in Fig. I.3. First, (IX_5,IY_5) is projected onto the horizontal line through (IX_1,IY_1), which identifies the point (IX_5,IY_1) in tablet units. For the sake of abbreviated reference later, call this point C_1, in whatever units you want.

Project this point onto the line segment A_1A_2 and let r_2 denote the distance from this point to A_1 in tablet units. Finally, extend the projection of (X,Y) onto A_1A_2 to project C_1 onto this extension at point C_2. It can be shown that the angle at (X,Y) is the same as the angle at A_1. If the distance between C_1 and C_2 is called r_3, then it is easy to see that

$$r = r_2 + r_3 \ , \tag{I.4}$$

and

$$r_2 = (IX_5 - IX_1) \cos\theta \ , \tag{I.5}$$

$$r_3 = (IY_5 - IY_1) \sin\theta \ . \tag{I.6}$$

Substituting Eqs. I.1 and I.2 into Eqs. I.6, I.5, and I.4 yields

$$r = \frac{(IX_5 - IX_1)(IX_2 - IX_1) + (IY_5 - IY_1)(IY_2 - IY_1)}{[(IX_2 - IX_1)^2 + (IY_2 - IY_1)^2]^{1/2}} \ , \tag{I.7}$$

and finally, substituting Eq. I.7 into Eq. I.3 gives

$$r = A_1 + \frac{(IX_5 - IX_1)(IX_2 - IX_1) + (IY_5 - IY_1)(IY_2 - IY_1)}{(IX_2 - IX_1)^2 + (IY_2 - IY_1)^2} (A_2 - A_1) \ . \tag{I.8}$$

ORNL-DWG 85-8145

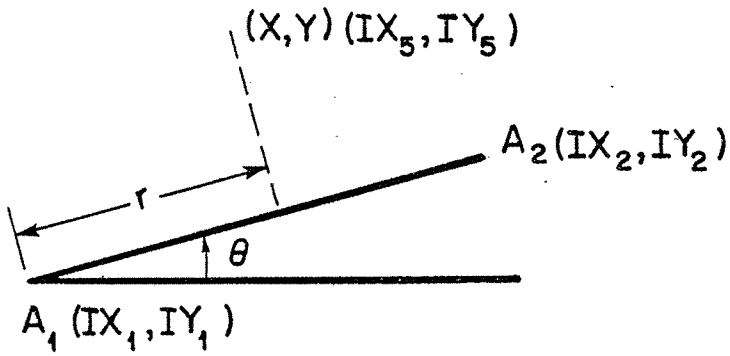

Fig. I.2. Layout on digitizing tablet identifying points and distances in "tablet" and "graph" units.

ORNL-DWG 85-8144

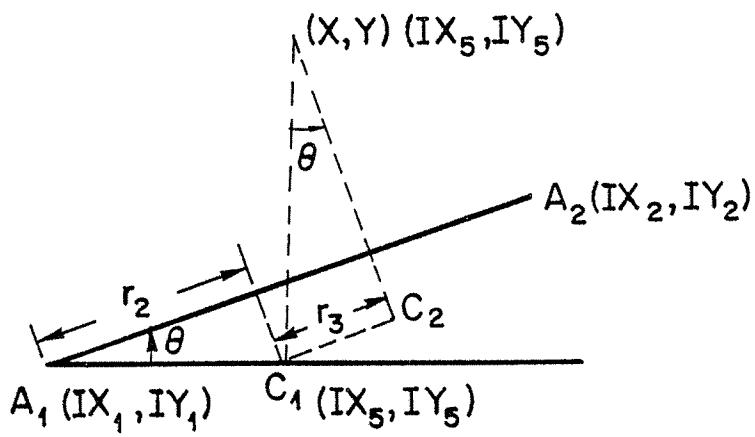

Fig. I.3. Layout on digitizing tablet showing points and distances used in the transformation of coordinates.

A similar set of manipulations can be performed for transforming the vertical coordinate Y from the tablet units into map units. Figure I.4 corresponds to Fig. I.3, and Eqs. I.9–I.12 correspond to Eqs. I.3–I.6.

$$Y = B_1 + \frac{r_2}{[(IX_4 - IX_3)^2 + (IY_4 - IY_3)^2]^{1/2}} (B_2 - B_1) \ . \tag{I.9}$$

ORNL-DWG 85-8146

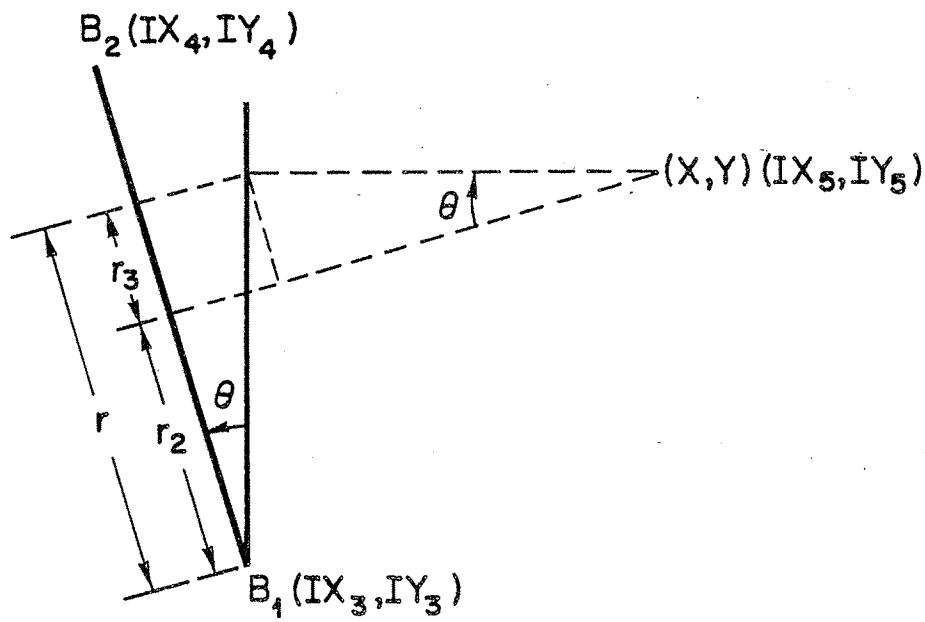

Fig. I.4. Layout on digitizing tablet showing points and distances used in the transformation of the vertical coordinates.

$$r_2 = r - r_3 \ . \tag{I.10}$$

$$r_3 = (IX_5 - IX_3)\sin\theta \ . \tag{I.11}$$

$$r = (IY_5 - IY_3)\cos\theta \ . \tag{I.12}$$

In this case, however, sin θ and cos θ can be given by Eqs. I.13 and I.14.

$$\sin\theta = \frac{IX_3 - IX_4}{[(IX_4 - IX_3)^2 + (IY_4 - IY_3)^2]^{1/2}} \ . \tag{I.13}$$

$$\cos\theta = \frac{IY_4 - IY_3}{[(IX_4 - IX_3)^2 + (IY_4 - IY_3)^2]^{1/2}} \ . \tag{I.14}$$

After all the appropriate substitutions and changes of signs, Y is given by Eq. I.15.

$$Y = B_1 + \frac{(IX_5 - IX_3)(IX_4 - IX_3) + (IY_5 - IY_3)(IY_4 - IY_3)}{(IX_4 - IX_3)^2 + (IY_4 - IY_3)^2} (B_2 - B_1) \ . \quad \text{(I.15)}$$

Appendix J

SOLUTION OF LEAST SQUARES PROBLEM IN COMPRESSOR CURVE FITTING

The compressor map-fitting program uses very general subroutines to solve a very specific least squares problem. The ORNL Heat Pump Design Model (HPDM) uses a "biquadratic" fit with six coefficients to specify the compressor performance as a function of the saturation variables at the compressor shell inlet and outlet. The form of this function is given by Eq. J.1.

$$f(x,y) = a_1x^2 + a_2x + a_3y^2 + a_4y + a_5xy + a_6 \ . \tag{J.1}$$

A linear least squares approach is used to solve for the coefficients a_i. Users of the HPDM may want to use more, or less, terms than the six shown, and the subroutines in the curve-fitting program are general enough so that the necessary changes are easy to make.

It is easiest to describe the least squares algorithms used by starting with the specific application in the map-fitting program and then looking at the generalized nature of the subroutines. The data that have been digitized or typed into the computer define the known values b_{ij}, where

$$f(x_i,y_j) = b_{ij} \ . \tag{J.2}$$

The object of the least squares approach is to minimize the function $F(\mathbf{a})$ given in Eq. J.3.

$$F(\mathbf{a}) = \sum_{ij} w_{ij}(a_1x_i^2 + a_2x_i + a_3y_j^2 + a_4y_j + a_5x_iy_j + a_6 - b_{ij})^2 \ . \tag{J.3}$$

The process of taking partial derivatives and setting them equal to zero results in the matrix equations given in J.4 and J.5.

$$\begin{pmatrix} \sum w_{ij}x_i^4 & \sum w_{ij}x_i^3 & \sum w_{ij}x_i^2y_j^2 & \sum w_{ij}x_i^2y_j & \sum w_{ij}x_i^3y_j & \sum w_{ij}x_i^2 \\ \sum w_{ij}x_i^3 & \sum w_{ij}x_i^2 & \sum w_{ij}x_iy_j^2 & \sum w_{ij}x_iy_j & \sum w_{ij}x_i^2y_j & \sum w_{ij}x_i \\ \sum w_{ij}x_i^2y_j^2 & \sum w_{ij}x_iy_j^2 & \sum w_{ij}y_j^4 & \sum w_{ij}y_j^3 & \sum w_{ij}x_iy_j^3 & \sum w_{ij}y_j^2 \\ \sum w_{ij}x_i^2y_j & \sum w_{ij}x_iy_j & \sum w_{ij}y_j^3 & \sum w_{ij}y_j^2 & \sum w_{ij}x_iy_j^2 & \sum w_{ij}y_j \\ \sum w_{ij}x_i^3y_j & \sum w_{ij}x_i^2y_j & \sum w_{ij}x_iy_j^3 & \sum w_{ij}x_iy_j^2 & \sum w_{ij}x_i^2y_j^2 & \sum w_{ij}x_iy_j \\ \sum w_{ij}x_i^2 & \sum w_{ij}x_i & \sum w_{ij}y_j^2 & \sum w_{ij}y_j & \sum w_{ij}x_iy_j & \sum w_{ij} \end{pmatrix} \begin{pmatrix} a_1 \\ a_2 \\ a_3 \\ a_4 \\ a_5 \\ a_6 \end{pmatrix} = \begin{pmatrix} \sum w_{ij}x_i^2b_{ij} \\ \sum w_{ij}x_ib_{ij} \\ \sum w_{ij}y_j^2b_{ij} \\ \sum w_{ij}y_jb_{ij} \\ \sum w_{ij}x_iy_jb_{ij} \\ \sum w_{ij}b_{ij} \end{pmatrix} \quad \text{(J.4)}$$

$$A\mathbf{a} = \mathbf{b} \ . \quad \text{(J.5)}$$

Two subroutines from the open literature,[1] DECOMP and SOLVE, are used to solve this system of equations for the coefficients a_i which make up the vector **a**. DECOMP performs a Gaussian decomposition with partial pivoting which transforms the matrix Eq. J.5 to an upper-triangular matrix system, Eq. J.6.

$$U\mathbf{a} = \mathbf{b}^* \ . \quad \text{(J.6)}$$

This is solved using "back-substitution" by the subroutine SOLVE.

The matrices in Eqs. J.4 and J.5 are only specific applications of a more general problem. In this case, the object is to minimize the function $F(\mathbf{a})$ given in Eq. J.7.

$$F(\mathbf{a}) = \sum_{ij} w_{ij} \left[\sum_{k=1}^{k} a_k p_k(x_i) q_k(y_j) - b_{ij} \right]^2 \ . \quad \text{(J.7)}$$

In the earlier example, $p_1(x) = x^2$ and $q_1(y) = 1$, etc. The normal equations for this system can be derived, setting partial derivatives with respect to a_i to 0 just as before, to get a linear system of K equations in K unknowns. This can be written in matrix form as in Eq. J.8.

$$A\mathbf{a} = \mathbf{b} \ , \quad \text{(J.8)}$$

where

$$A_{IJ} = \sum_{ij} w_{ij} p_I(x_i) q_I(y_j) p_J(x_i) q_j(y_j) \quad \text{(J.9)}$$

and

$$b_I = \sum_{ij} w_{ij} p_I(x_i) q_I(y_j) b_{ij} \ . \quad \text{(J.10)}$$

Subroutine FIT of the compressor map-fitting program incorporates the specific functions $p_k(x)$ and $q_k(y)$ of Eq. J.1 in setting up the general matrix A and vector $\mathbf{b}$ of Eqs. J.9 and J.10. Although there is no direct correspondence between variable names in the subroutine and functions in the equations, the translation from one to the other is not very difficult. Modifications to the form of the fit in Eq. J.1 lead to straightforward changes to FIT.

REFERENCE

1. G. E. Forsythe, M. A Malcolm, and C. B. Moler, *Computer Methods for Mathematical Computations*, Prentice-Hall, Inc., Englewood Cliffs, N.J., 1977, pp. 30–36.

Appendix K

PLOTTING VERSION OF SUBROUTINE FIT

On microfiche

Appendix L

LISTING OF SUBROUTINE FUNCT1

On microfiche

Appendix M

LISTING OF DATA GENERATION PROGRAM DRIVER

On microfiche

Appendix N

LISTING OF CONTOUR PLOTTING PROGRAM CONPLT

On microfiche

Appendix O

LISTING OF SUBROUTINES FOR OPTIMIZATION AND PROGRAM GRADIE

On microfiche

Appendix P

DESCRIPTION OF REVISED INPUT DATA FORMAT FOR HEAT PUMP DESIGN MODEL

TITLE, OUTPUT, and MODE DATA

CARD #1 FORMAT(20A4)

ITITLE Descriptive title for system described by this set of data

CARD #2 FORMAT(8I10)

LPRINT Output switch to control the detail of printed results 1

=0, for minimum output with only an energy input and output summary printed
=1, for a summary of the system operating conditions and component performance calculations as well as the energy summary
=2, for output after each intermediate iteration converges
=3, for continous output during intermediate iterations

CARD #3 FORMAT(8I10)

NCORH Switch to specify cooling or heating mode 2

=1, for cooling mode
=2, for heating mode

SUPERHEAT / CHARGE INVENTORY DATA:

CARD #4 FORMAT(I10,7F10.4)

ICHRGE Switch for specifying compressor inlet superheat or system refrigerant charge 0

=0, specify refrigerant superheat (or quality) and compute the required system refrigerant charge

=1, estimate compressor inlet superheat and specify the system refrigerant charge, not yet available

SUPER if ICHRGE=0, the specified refrigerant superheat (or quality) at the compressor shell inlet (F^o or negative of the desired quality fraction), 18.7
if ICHRGE=1, an estimate of the refrigerant superheat (or quality) at the compressor shell inlet (F^o or negative of the desired quality fraction)

Variable Used Only If ICHRGE=1

REFCHG Specified system refrigerant charge (lbm)

FLOW CONTROL DEVICE DATA: the variables on the next card depend on the type of flow control device selected.

CARD #5 FORMAT(I10,7F10.4)

Fixed Condenser Subcooling:

IREFC	=0, for specified refrigerant subcooling at the condenser exit	0
DTROC	the specified refrigerant subcooling (or quality) at the condenser exit (F^o or negative of the desired quality fraction)	44.2

Thermostatic Expansion Valve:

IREFC	=1, for the thermostatic expansion valve	1
TXVRAT	The rated capacity of the TXV (tons)	2.0
STATIC	The static superheat setting for the TXV (F^o)	6.0
SUPRAT	The TXV superheat at rating conditions (F^o)	11.0
SUPMAX	The maximum effective operating superheat (F^o)	13.0
BLEEDF	The TXV bypass or bleed factor	1.15
NZTBOP	A switch to omit TXV nozzle and tube pressure drop calculations =0.0, to omit tube and nozzle pressure drops =1.0, to include tube and nozzle pressure drop calculations	0.0

Capillary Tube:

IREFC	=2, for a capillary tube expansion device	2
CAPFLO	The capillary tube flow factor, see ASHRAE Guide and Data Book, Equipment Vol. (1975), Fig. 41, p. 20.25	2.2
NCAP	The number of capillary tubes in parallel	1.0

Short Tube Orifice:

IREFC	=3, for a short tube orifice	3
ORIFD	The diameter of the short-tube orifice (inches)	0.0544

ESTIMATES OF THE LOW AND HIGH SIDE REFRIGERANT SATURATION TEMPERATURES:

CARD #6 FORMAT(8F10.4)

TSICMP	Estimate of the refrigerant saturation temperature at the compressor inlet (^{o}F)	30.0
TSOCMP	Estimate of the refrigerant saturation temperature at the compressor outlet (^{o}F)	115.0

COMPRESSOR DATA:

CARD #7 FORMAT(I10,7F10.4)

ICOMP	Switch to specify which compressor submodel is to be used, =1, for the efficiency and loss model, =2, for the map-based model	2
DISPL	Total compressor piston displacement (in^3)	4.520
SYNC	The synchronous compressor motor speed (rpm) when ICOMP=1 and FLMOT is specified on CARD #9;	(3600.)
	the rated compressor motor speed (rpm) when ICOMP=1 and FLMOT is to be calculated or when ICOMP=2	3450.
QCAN	The compressor shell heat loss rate (Btu/hr), used if CANFAC=0.0	0.0
CANFAC	Switch to control the method of specifying the compressor shell heat loss rate, QCAN =0.0, to specify QCAN explicitly <1.0, to calculate QCAN as a fraction of the compressor input power, POW, (i.e., QCAN = CANFAC * POW) 1.0, to calculate QCAN from the equation: QCAN = 0.90 * (1-motor*mechanical efficiency) * POW	0.35

EFFICIENCY AND LOSS MODEL COMPRESSOR DATA:

CARD #8 FORMAT(8F10.4)

VR	Compressor actual clearance volume ratio	0.06
EFFMMX	Maximum efficiency of the compressor motor	0.82
ETAISN	Isentropic efficiency of the compressor	0.70
ETAMEC	Mechanical efficiency of the compressor	0.80

CARD #9 FORMAT(I10,7F10.4)

MTRCLC	Switch to determine whether to calculate the full load motor power (FLMOT) or to use the input value =0, to calculate FLMOT =1, to use the input value of FLMOT	0
FLMOT	Compressor motor output at full load (kW) (not used if MTRCLC=1)	(2.15)
QHILO	Heat transfer rate from the compressor inlet line to the inlet gas (Btu/hr), used if HILOFC=0.0	300.0
HILOFC	Switch to determine internal heat transfer from the high side to the low side, QHILO =0.0, to specify QHILO explicitly <1.0, to calculate QHILO = HILOFC * POW 1.0, to calculate QHILO = 0.03 * POW	0.0

MAP-BASED COMPRESSOR MODEL INPUT DATA:

CARD #8 FORMAT(8E10.3)

CPOW(1)	Coefficient for the second order term in condensing temperature for the compressor power consumption	-1.509E-04
CPOW(2)	Coefficient for the linear term in condensing temperature for the compressor power consumption	4.089E-02

207. James Schulze, General Electric Company, Appliance Park, Building 1, Room 210, Louisville, KY 40225
208. Takao Senshu, Mechanical Engineering Research Laboratory, Hitachi, Ltd, 390 Muramatsu, Shimizu-shi, Shizuoka-ken, Japan
209. Samuel Shelton, Thermax, Inc., 296 14th Street NW, Atlanta, GA 30318
210. J. A. Smith, Test and Evaluation Branch, CE-113.2, Department of Energy, 1000 Independence Avenue SW, Washington, DC 20585
211. T. Statt, Energy Conversion Equipment Branch, CE-132, GF-217, Department of Energy, 1000 Independence Avenue SW, Washington, DC 20585
212. W. F. Stoecker, University of Illinois, 1206 West Green Street, Urbana, IL 61801
213. John Tenhunfeld, Heating and Cooling Products, Amana Refrigeration, Inc., Amana, IA 52204
214. W. H. Thielbahr, Energy Conservation Branch, Department of Energy, Idaho Operations Office, 550 Second Street, Idaho Falls, ID 83401
215. W. C. Thomas, Virginia Polytechnic Institute and State University, Mechanical Engineering Department, Blacksburg, VA 24061
216. Tommy Thompson, BDP Company, Division of Carrier Corporation, P.O. Box 70, Indianapolis, IN 46206
217. E. L. Tramel, Conservation and Energy Management Branch, Tennessee Valley Authority, 350-401 Building, Chattanooga, TN 37401
218. David Tree, Ray Herrick Laboratory, Purdue University, West Lafayette, IN 47907
219. Ralph Webb, Department of Mechanical Engineering, Pennsylvania State University, 208 Mechanical Engineering Building, University Park, PA 16802
220. Office of the Assistant Manager for Energy R&D, U.S. Department of Energy, Oak Ridge Operations, P.O. Box E, Oak Ridge, TN 37831

221–250. Technical Information Center, P.O. Box 62, Oak Ridge, TN 37831

154. Robert Fischer, Battelle-Columbus Laboratory, 505 King Avenue, Columbus, OH 43201
155. R. J. Fiskum, Energy Conversion Equipment Branch, CE-132, GF-217, Department of Energy, 1000 Independence Avenue SW, Washington, DC 20585
156. P. V. Gilli, Graz University of Technology, Kopernikusgasse 24, A-8010, Graz, Austria
157. S. M. Gillis, Dean, Graduate School, Duke University, 4875 Duke Station, Durham, NC 27706
158. Paul Glamm, The Trane Company, 3600 Pammell Creek Road, LaCrosse, WI 54601
159. L. R. Glicksman, Massachusetts Institute of Technology, 77 Massachusetts Avenue, Building 3-137, Cambridge, MA 02139
160. D. E. Grether, International Environmental Corporation, P.O. Box 25608, 5000 SW 7th Street, Oklahoma City, OK 73125
161. Russell Griffith, Copeland Corporation, Sydney, OH 45365
162. Marvin Gunn, Energy Conversion and Utilization Technology Division, CS-142, Forrestal Building, Department of Energy, Washington, DC 20585
163. H. Halozan, University of Technology, Inffeldgasse 25, A-8010 Graz, Austria
164. John Hackstedde, Tecumseh Products Company, Tecumseh, MI 49286
165. James Harnish, Unitary Products Engineering, York Division, Borg-Warner Corporation, P.O. Box 1592, York, PA 17405
166. D. T. Harrje, CEES, Engineering Quad, Princeton University, Princeton, NJ 08544
167. Floyd Hayes, The Trane Company, 3600 Pammell Creek Road, LaCrosse, WI 54601
168. Wayne Helmer, Southern Illinois University at Carbondale, School of Engineering and Technology, Department of Thermal and Environmental Engineering, Carbondale, IL 62901
169. Arlo Hendrickson, Trane CAC, Inc., Tyler, TX 75711
170. C. C. Hiller, Electric Power Research Institute, 3412 Hillview Avenue, P.O. Box 10412, Palo Alto, CA 94303
171. Michimasa Hori, System Development Department, Air-Conditioner Division, Matsushita Electric, 2275-3 Noji-Cho, Kusatsu, Shiga-Ken 525 Japan
172. T. Jacoby, Tecumseh Products Company, Tecumseh, MI 49286
173. Larry James, ER-33, R-330/GTN, U.S. Department of Energy, Washington, DC 20596
174. Heinz Jaster, Corporate Research and Development, General Electric Company, P.O. Box 43, Schenectady, NY 12345
175. Larry L. Jenkins, Professional Engineering Company, 2211 North 91st Court, Omaha, NE 68134
176. F. R. Kalhammer, Vice President, Electric Power Research Institute, 3412 Hillview Avenue, P.O. Box 10412, Palo Alto, CA 94303
177. R. E. Kasperson, Professor of Government and Geography, Graduate School of Geography, Clark University, Worcester, MA 01610
178. Herbert Kaufman, ARCO Comfort Products Company, 1271 Avenue of the Americas, New York, NY 10020
179. Rube Kelto, Tecumseh Products Company, Tecumseh, MI 49286
180. Kenneth Kountz, Institute of Gas Technology, Chicago, IL 60616
181. M. Lessen, Consulting Engineer, 12 Country Club Drive, Rochester, NY 141618

182. D. C. Lim, Energy Conversion Equipment Branch, CE-113.2, Department of Energy, 1000 Independence Avenue SW, Washington, DC 20585
183. Nance Lovvorn, Alabama Power Company, P.O. Box 2641, Birmingham, AL 35291
184. Ward MacArthur, Honeywell Inc., 1700 West Highway 36, St. Paul, MN 55113
185. F. C. McQuiston, Oklahoma State University, 301 Engineering North, Stillwater, OK 74078
186. Dick Merriam, Arthur D. Little, Inc., 32 Acorn Park, Cambridge, MA 02140
187. Jerry Miller, Copeland Corporation, Sydney, OH 45365
188. R. Scott Miller, General Electric Company, CRD-River Road, Building 37-615, Schenectady, NY 12345
189. J. P. Millhone, Office of Buildings Energy Research and Development, CE-11, Department of Energy, 1000 Independence Avenue SW, Washington, DC 20585
190. F. H. Morse, Office of Solar Heat Technologies, CE-31, Department of Energy, 1000 Independence Avenue SW, Washington, DC 20585
191. W. E. Murphy, Agricultural Engineering, University of Kentucky, Lexington, KY 40546
192. Dennis O'Neal, Department of Mechanical Engineering, Texas A&M University, College Station, TX 77843
193. Dan Myers, Refrigeration Systems, 4241 Hogue Road, Evansville, IN 47712
194. R. W. Newell, Rheem Manufacturing Company, 5600 Old Greenwood Road, P.O. Box 6444, Fort Smith, AR 72906
195. Jerald Parker, School of Mechanical and Aerospace Engineering, Oklahoma State University, 218 Engineer North, Stillwater, OK 74078
196. Michael Pate, Mechanical Engineering Department, 2043 ME/ESM Building, Iowa State University, Ames, IA 50011
197. Michael Perlsweig, FE-23, C-148/GTN, Department of Energy, Washington, DC 20596
198. Hung Pham, Copeland Corporation, Sydney, OH 45365
199. R. L. Puterbaugh, Vice President Consumer Products Engineering, White Consolidated Industries, Inc., 11770 Berea Road, Cleveland, OH 44111
200. Bob Rasmussen, Honeywell Inc., 10701 Lyndale Avenue South, Bloomington, MN 55420
201. V. Recchi, National Research Council, % O. T. B. Zona Industriale, Contrada del Parco, Bari, Italy
202. Gordon Reistad, Department of Mechanical Engineering, Oregon State University, Corvallis, OR 97331
203. Hal Rhea, Lennox Industries, Inc., P.O. Box 877, 1600 Metro Drive, Carrollton, TX 75006
204. Richard Rush, Mechanical Engineering Department, 2043 ME/ESM Building, Iowa State University, Ames, IA 50011
205. J. D. Ryan, Energy Conversion Equipment Branch, CE-113.2, Department of Energy, 1000 Independence Avenue SW, Washington, DC 20585
206. D. E. Scherpereel, Director, Mechanical Systems Research, Elisha Gray II—Research and Engineering Center, Monte Road, Benton Harbor, MI 49022

INTERNAL DISTRIBUTION

1. M. R. Ally
2. V. D. Baxter
3. J. L. Bledsoe
4. R. S. Carlsmith
5. F. C. Chen
6. J. Christian
7. F. A. Creswick
8. N. Domingo
9–13. C. J. Emerson
14. P. D. Fairchild
15. F. G. Farrell
16–20. S. K. Fischer
21. W. Fulkerson
22. W. L. Jackson
23. L. Jung
24. S. I. Kaplan
25. M. A. Kuliasha
26. F. C. Maienschein
27. J. F. Martin
28. S. H. McConathy
29. H. A. McLain
30. V. C. Mei
31. W. A. Miller
32. J. C. Moyers
33. C. L. Nichols
34. H. Perez-Blanco
35. C. K. Rice
36. T. J. Simmons
37. C. D. West
38. K. H. Zimmerman
39–113. Energy Conservation Distribution, Bldg. 9102-2, Room 218
114–115. Laboratory Records Department
116. Laboratory Records Department–RC
117. ORNL Patent Office
118–119. Central Research Library
120. Document Reference Section

EXTERNAL DISTRIBUTION

121. C. A. Allen, Energy Information Administration, EI-60, Forrestal Building, 1000 Independence Avenue SW, Washington, DC 20585
122. Lawrence Ambs, Department of Mechanical Engineering, University of Massachusetts, Amherst, MA 01003
123. John Andrews, Solar Technology Group, Building 701, Brookhaven National Laboratory, Upton, NY 11973
124. Ralph Badtram, McQuay Group, P.O. Box 1551, 13600 Industrial Park Boulevard, Minneapolis, MN 55440
125. James Bard, Executive Vice-President, Bard Manufacturing Company, Inc., P.O. Box 607, Bryan, OH 43506
126. E. K. Bastress, Energy Conversion and Utilization Technology Division, CS-142, Forrestal Building, Department of Energy, Washington, DC 20585
127. Charles H. Bemisderfer, Sundstrand Heat Transfer, Inc., 415 East Prairie Ronde Street, Dowagiac, MI 49047
128. J. Berghmans, Universitiet Leuven, Institut Mechanica, Celestynen Laan 300A, B-3030 Heverlee-Belgium

129. Carl Bergt, Trane CAC, Inc., 6200 Troup Highway, Tyler, TX 75711
130. Peter Bodett, Goodyear Tire and Rubber Company, 509 South Poplar Street, LaGrange, IN 46761
131. Ulrich Bonne, Honeywell Incorporated, 10701 Lyndale Avenue South, Corporate Technology Center, Materials and Processes Department, Bloomington, MN 55420
132. James E. Bose, School of Technology, Oklahoma State University, Stillwater, OK 74078
133. Ralph Bryant, Heil Quaker Corporation, 1136 Heil-Quaker Boulevard, P.O. Box 3005, Lavergne, TN 37086-1985
134. Charles Bullock, Research Division, Carrier Corporation, Carrier Parkway, Syracuse, NY 13201
135. J. G. Carbonell, Associate Professor of Computer Science Carnegie-Mellon University Pittsburgh, PA 15213
136. Raymond Cohen, Ray Herrick Laboratories, Purdue University, West Lafayette, IN 47907
137. W. R. Coleman, Residential and Commercial Services, American Electric Power Services, 180 East Broad, Columbus, OH 43201
138. Manuel Conde, Swiss Federal Institute of Technology, Energy Systems Laboratory, Zurich, Switzerland
139. James Crawford, Trane CAC, Inc., 6200 Troup Highway, Tyler, TX 75711
140. Jerry Dapper, BDP Company, Division of Carrier Corporation, P.O. Box 70, Indianapolis, IN 46206
141. Glen Deming, Foster Miller, Inc., 350 Second Avenue, Waltham, MA 02254
142. R. J. Denny, Air-Conditioning and Refrigeration Institute, 1815 North Fort Meyer Drive, Arlington, VA 22209
143. Irvin Derks, Manager Engineering Development, Bard Manufacturing Company, P.O. Box 607, Bryan, OH 43506
144. Richard Devos, ICG Keeprite Corporation, Research and Development Center, Route 14, Box 12, Boones Creek Road, Johnson City, TN 37615
145. David A. Didion, Mechanical Systems Section, Building Environment Division, National Bureau of Standards, Building 226, Room B126, Washington, DC 20234
146. Peter Domanski, Mechanical Systems Section, Building Environment Division, National Bureau of Standards, Building 266, Room B124, Washington, DC 20234
147. Charles E. Dorgan, Director, Engineering Technology Center, University of Wisconsin Extension, 825 Extension Building, 432 North Lake Street, Madison, WI 53706
148. Richard Dougall, Department of Mechanical Engineering, University of Pittsburgh, Pittsburg, PA 15261
149. Alan Drucker, Consumer Products Division, Syracuse, NY 13221
150. G. D. Duffy, Air Conditioning News, P.O. Box 2600, Troy, MI 48007
151. A. H. Elmahdy, Energy and Services Section, National Research Council, Division of Building Research, Ottawa, Canada K1A OR6
152. J. N. Eustis, Department of Energy, Office of Industrial Programs, CE-121.1, 1000 Independence Avenue SW, Washington, DC 20585
153. Scott Farley, Heating and Air-Conditioning Group, The Coleman Company, Inc., 3110 North Mead, Wichita, KS 67201

CONFIGURATION OPTIONS DATA:

CARD #18 FORMAT(8I10)

MCMPOP	Switch for adding compressor can heat loss to air across the outdoor coil, =0, compressor can loss not added to outdoor air =1, compressor can loss added to air before crossing the outdoor coil =2, compressor can loss added to air after crossing the outdoor coil	0
MFANIN	Switch for adding heat loss from the indoor fan to air stream, settings are similar to those for MCMPOP	1
MFANOU	Switch for adding heat loss from the outdoor fan to air stream, settings are similar to those for MCMPOP	2

REFRIGERANT LINES DATA:

CARD #19 FORMAT(8F10.4)

Heat Transfer in Refrigerant Lines

QSUCLN	If positive, the rate of heat gain in the compressor suction line (Btu/hr), If negative, the negative of the desired temperature rise in the suction line (F^o)	242. -3.0
QDISLN	Rate of heat loss in the compressor discharge line (Btu/hr)	1648.
QLIQLN	Rate of heat loss in the liquid line (Btu/hr)	433.

CARD #20 FORMAT(8F10.4)

Lines Between Coils and from Reversing Valve to Coils

DLL	Inside diameter of the liquid line (in.)	0.194
XLEQLL	Equivalent length of the liquid line (ft)	30.4
DLRVIC	Inside diameter of the vapor line between the reversing valve and the indoor coil (in.)	0.550

XLRVIC	Equivalent length of the vapor line between the reversing valve and the indoor coil (ft)	30.1
DLRVOC	Inside diameter of the vapor line between the reversing valve and the outdoor coil (in.)	0.686
XLRVOC	Equivalent length of the vapor line between the reversing valve and the outdoor coil (ft)	6.0

CARD #21 FORMAT(8F10.4)

Lines from the Reversing Valve to the Compressor

DSLRV	Inside diameter of the suction line from the reversing valve to the compressor inlet (in.)	0.686
XLEQLP	Equivalent length of the low pressure line from the reversing valve tot he compressor inlet (ft)	2.0
DDLRV	Inside diameter of the discharge line from the compressor outlet to the reversing valve (in.)	0.555
XLEQHP	Equivalent length of the high pressure line from the compressor outlet to the reversing valve (ft)	2.0

CARD #13 FORMAT(8F10.4)

FINTYI	Switch to specify the type of fin surface, =1.0, for smooth fins =2.0, for wavy fins =3.0, for louvered fins	2.0
FPFI	Fin pitch (fins/in.)	14.0
DELTAI	Fin thickness (in.)	0.00550
DEAI	Outside diameter of the refrigerant tubes (in.)	0.392
DERI	Inside diameter of the refrigerant tubes (in.)	0.360
XKFI	Thermal conductivity of the fin material (Btu/hr-ft-^{o}F)	128.3
XKTI	Thermal conductivity of the tube material (Btu/hr-ft-^{o}F)	225.0
HCONTI	Fraction or multiple of the default computed contact conductance between the fins and tubes	100.0

OUTDOOR COIL DATA:

CARD #14 FORMAT(8F10.4)

TAIIO	Air temperature entering the heat exchanger (^{o}F)	41.7
RHO	Relative humidity of the air entering the heat exchanger	0.50

CARD #15 FORMAT(8F10.4)

QAO	Air flow rate (ft^3/min)	2300.0
FANEFO	1.0, the specified value of the combined fan-fan motor efficiency	(0.114)
	>1.0, the specified value of the fan power (Watts)	511.0
MFANFT	Switch for using static efficiency vs. specific speed curve fit for the efficiency of the outdoor fan, =0, use the specified value of FANEFO as described above =1, use the curve fit for fan static efficiency and the fixed fan motor efficiency value given in BLOCK DATA	0

CARD #16 FORMAT(8F10.4)

AAFO	Frontal area of the coil (ft^2)	5.040
NTO	Number of refrigerant tube rows in the direction of the air flow	3.0
NSECTO	Number of equivalent, parallel refrigerant circuits in the heat exchanger	4.0
WTO	Spacing of the refrigerant tubes in the direction of the air flow (in.)	0.875
STO	Spacing of the refrigerant tube passes perpendicular to the direction of the air flow (in.)	1.00
RTBO	Total number of return bends in the heat exchanger (all circuits)	64.0

CARD #17 FORMAT(8F10.4)

FINTYO	Switch to specify the type of fin surface, =1.0, for smooth fins =2.0, for wavy fins =3.0, for louvered fins	2.0
FPO	Fin pitch (fins/in.)	14.0
DELTAO	Fin thickness (in.)	0.00550
DEAO	Outside diameter of the refrigerant tubes (in.)	0.392
DERO	Inside diameter of the refrigerant tubes (in.)	0.360
XKFO	Thermal conductivity of the fin material (Btu/hr-ft-^{o}F)	128.3
XKTO	Thermal conductivity of the tube material (Btu/hr-ft-^{o}F)	225.0
HCONTO	Fraction or multiple of the default computed contact conductance between the fins and tubes	100.0

CPOW(3)	Coefficient for the second order term in evaporating temperature for the compressor power consumption	-1.338E-04
CPOW(4)	Coefficient for the linear term in evaporating temperature for the compressor power consumption	5.860E-04
CPOW(5)	Coefficient for the cross-term in condensing and evaporating temperatures for the compressor power consumption	3.638E-04
CPOW(6)	Constant term in the fit to compressor power consumption as a function of condensing and evaporating temperatures (kW)	9.759E-05
DISPLB	Base compressor displacement for the compressor map (in^3)	4.520E+00
SUPERB	Base 'superheat' value for the compressor map if positive, the base superheat entering the compressor (F^o)	20.00E+00
	if negative, the negative of the return gas temperature into the compressor (F^o)	(-95.00E+00)

CARD #9 FORMAT(8E10.3)

CXMR(1)	Coefficient for the second order term in condensing temperature for the refrigerant mass rate	-2.675E-02
CXMR(2)	Coefficient for the linear term in condensing temperature for the refrigerant mass flow rate	4.633E-00
CXMR(3)	Coefficient for the second order term in evaporating temperature for the refrigerant mass flow rate	4.703E-02
CXMR(4)	Coefficient for the linear term in evaporating temperature for the refrigerant mass flow rate	9.640E-00
CXMR(5)	Coefficient for the cross-term in condensing and evaporating temperatures for the refrigerant mass flow rate	-1.868E-02
CXMR(6)	Constant term in the fit to refrigerant mass flow rate as a function of condensing and evaporating temperatures (lbm/hr)	1.207E-04

INDOOR COIL DATA:

CARD #10 FORMAT(8F10.4)

TAIII	Air temperature entering the heat exchanger (^oF)	70.0
RHI	Relative humidity of the air entering the heat exchanger	0.50

CARD #11 FORMAT(8F10.4)

QAI	Air flow rate (ft^3/min)	1230.0
FANEFI	1.0, the specified value of the combined fan - fan motor efficiency	(0.153)
	>1.0, the specified value of the fan power (Watts)	608.0
DDUCT	Diameter of each of six identical air ducts with equivalent lengths of 100 ft. (in.)	8.00
FIXCAP	House heating load (Btu/hr), optional, used to calculate the necessary backup resistance heat in heating mode	15000.

CARD #12 FORMAT(8F10.4)

AAFI	Frontal area of the coil (ft^2)	3.1667
NTI	Number of refrigerant tube rows in the direction of the air flow	3.0
NSECTI	Number of equivalent, parallel refrigerant circuits in the heat exchanger	3.0
WTI	Spacing of the refrigerant tubes in the direction of the air flow (in.)	0.875
STI	Spacing of the refrigerant tube passes perpendicular to the direction of the air flow (in.)	1.00
RTBI	Total number of return bends in the heat exchanger (all circuits)	72.0